Design and Evaluation of iCalm:
A Novel, Wrist-Worn, Low-Power, Low-Cost,
Wireless Physiological Sensor Module

by

Hoda Eydgahi

B.S., Biomedical Engineering
Virginia Commonwealth University, 2006

SUBMITTED TO THE DEPARTMENT OF ELECTRICAL ENGINEERING AND
COMPUTER SCIENCE IN PARTIAL FULFILLMENT OF THE REQUIREMENTS
FOR THE DEGREE OF

MASTER OF SCIENCE IN ELECTRIAL ENGINEERING
AT THE
MASSACHUSETTS INSTITUTE OF TECHNOLOGY

JUNE 2008

Signature of Author: ....　　　...
Department of Electrical Engineering and Computer Science
May 23, 2008

Certified by: ....
Rosalind W. Picard
Professor of Media Arts and Sciences
Thesis Supervisor

Certified by......................................
Richard Fletcher
Research Scientist, Media Laboratory
Thesis Reader

Accepted by: ....
Terry P. Orlando
Professor of Electrical Engineering
Chairman, Committee for Graduate Students
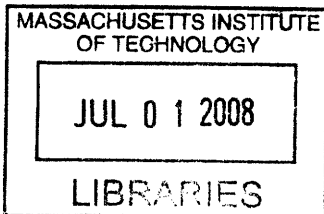
Design and Evaluation of iCalm:
A Novel, Wrist-Worn, Low-Power, Low-Cost, Wireless Physiological Sensor Module

by

Hoda Eydgahi

Submitted to the Department of Electrical Engineering and Computer Science
on May 23, 2008, in partial fulfillment of the
requirements for the degree of
Masters of Science in Electrical Engineering and Computer Science

Abstract

The impracticality of the ambulatory electrocardiogram for long-term physiological monitoring has lead to the development of many new, compact sensors that have been designed with form factor and user comfort in mind. Nevertheless, there currently is no single sensor module that would be ideal to use for continuous, long-term monitoring. The sensors tend to either lack wireless capabilities, have a short battery life, or are financially unfeasible.

After conducting a quick survey of recently developed sensors, we propose the design of iCalm: a novel, wrist-worn, low-power, low-cost, and wireless physiological sensor module. Its performance is compared against an FDA-approved platform through numerous experiments, including a few user studies. The iCalm skin conductance sensor greatly reduced noise due to motion and pressure artifacts; the iCalm heart rate sensor performed similar to the FDA-approved sensor. In addition, all of the participants in the experiments preferred the iCalm to the FDA-approved comparison sensors we tested. With iCalm, we hope to enable comfortable, long-term monitoring of the autonomic nervous system physiology and improve upon the current commercial sensors on the market.

Thesis Supervisor: Rosalind W. Picard
Title: Professor of Media Arts and Sciences

Acknowledgements

First and foremost, I would like to thank my advisor, Prof. Rosalind Picard, for her constant energy, curiosity, kindness, optimism, and support. Every time a new design of the sensors was built, Roz would enthusiastically volunteer to be the first to wear them with probability one. She even wore the sensors while on a gurney in the hospital; anything in the name of science! Her constructive feedback and unique ideas contributed to my intellectual growth and to the completion of this thesis. Most importantly though, her sincere and caring nature created a unique dynamic in our research group such that Roz was more than just an advisor—she was also a friend and, at times, even a mom away from home.

I would particularly like to thank my labmates Shani Daily and Clay Williams for helping me through this process even when they did not have to. Misery loves company: it was amazing to have you next to me through the late nights and the frustrating debugging sessions. Specifically, thank you Shani for your wise advice, patience, and organization, particularly with the group experiments; thank you Clay for your incredible contributions to the software, you have been amazingly generous with your time.

Whether it was playing squash, drinking the free hot chocolate in the third floor kitchen, teaching me how to speak Greek, or teasing me with the answers to magic tricks, the companionship (and the data!) of my other labmates was greatly appreciated: Hyungil Ahn, Rana El Kaliouby, Kyunghee Kim, Jackie Lee, Nikolaos Mavridis, Rob Morris, Selene Mota, Ming-Zher Poh, Seth Raphael, and Alea Teeters.

Thanks to Rich Fletcher for reading my thesis, for his contributions to the sensor's firmware, and for making time for me—even at 4:30 am, to Kelly Dobson for her creativity and contributions to the form factor, to Fahd Albinali for his kindness and willingness to help with the MITes, to Thought Technology's Hal Myers for kindly donating the FlexComp Infiniti, and to the Media Laboratory's Things That Think Consortium and the National Science Foundation for funding my research.

I do not believe that I could have successfully made it through the past two years without the support of the many people I have come to call my friends. One of the first people I

met at MIT was Jose Bohorquez; and I absolutely can not wait until I have the opportunity to meet Baby Bohorquez this July.

It has also been a pleasure to pass time in the company of Kostas Bimpikis, Filippos Chasparis, Alex Edmans, Adam Eisenman, Fergus Hurley, Yola Katsargyri, Ke Lu, Kaveh Milaninia, Rory Monaghan, Uzoma Orji, Annalisa Pawlosky, Nikolas Pyrgiotis, Jamal Rahi, Leslie Rogers, Michael Schnall-Levin, Premal Shah, David Tax, and the remainder of the John Gormley ski group. Furthermore, thanks to Ruben Lobel for the late night entertainment and to Ioannis Simaiakis for his unique point of view that instigated many thought-provoking conversations.

MIT is notorious for its lack of women graduate students and rightly so. I was never particularly appreciative of having female friends until I realized that not a single person in my department here at MIT would even notice a cute pair of shoes, let alone truly appreciate them. The women in my life keep me sane: Shima Daneshpour, Natalia De La Rosa, Samantha Green-Atchley, Stephanie Gil, Lacey Kymmell, Candace Mainor, Miriam Makhlouf, Golbarg Mehraei, Elnaz Naseri, Sandra Perez, Pallavi Ramnarain, Tara Sainath, and Stephanie Upson. Thank you so much for your patience, your understanding, your honesty, your sense of fashion, and your gossip. I could not have asked for a more supportive and entertaining entourage.

Even though as an older child I am supposed to be a role model for my younger brother, he has actually been a role model for me. Mahdi, you have an incredible heart; thank you for teaching me to never settle for anything less than the very best.

Finally, I'm notorious for eating dessert before dinner; but in this case, I've decided to practice some self-control and save the best for last: I would like to express my sincere gratitude towards my parents, Maryam Taabodi and Ali Eydgahi, who have raised me to be the person I am today. While I was growing up, my father would mentally challenge me with riddles and encourage me to explore the fields of mathematics and the sciences. To say that my father was more excited than I the day I received my acceptance letter to MIT is a blatant understatement; sometimes I feel as though he is living vicariously through me. My mother, on the other hand, spent time teaching me about culture and history, respect and morals, determination and perseverance. She is also my role model in that she decided to return to school to obtain both her Bachelor's and Master's Degrees all while raising me and my brother. In fact, she's currently pursuing her dream of obtaining a Ph.D.; yet she still makes the time to occasionally send me some homemade pumpkin jam. Both of my parents have fully supported me in all of my endeavors throughout my life and, as such, I will forever be grateful to them. Thank you so much.

<div align="right">

— Hoda Eydgahi
May 23, 2008

</div>

This thesis is dedicated to
G. H. Taabodi and
the memory of M. T. M. Eydgahi,
my beloved grandfathers
who always encouraged me to learn
and expand my horizons
in every manner
possible.

Contents

List of Figures

Chapter 1

Introduction

One of the most commonly accepted ambulatory electrocardiography (ECG) devices was first invented by Holter and is used for continuously monitoring the electrical activity of the heart for periods of 24 hours or more. The ambulatory ECG, however, is not suitable for long term monitoring; it is bulky and heavy, and the wires and chest leads certainly do not contribute to the user's comfort level. The impracticality of the ambulatory ECG has lead to the development of many new, compact sensors that have been designed with form factor and user comfort in mind.

Despite the fact that modern day sensors undoubtedly have improved upon the original ambulatory ECG, there still exists plenty of room for further developments. In addition to the ECG, a variety of other types of sensors have been developed for monitoring physiological signals. A succinct analysis of sensors that have been recently developed in academia and commercially will be conducted to demonstrate the lack of any one sensor that would be ideal to use for continuous, long-term physiological

monitoring. The sensors tend to either lack wireless capabilities, have a short battery life, or are financially unfeasible.

In this thesis, we propose the development of iCalm, a novel physiological sensor platform designed for continuous, long-term data collection. Factors such as cost and power will certainly play a role in the design and production of the platform.

1.1 Background

In recent years, an assortment of sensors has been developed to increase the usability and practicality of physiological monitors, such as the ambulatory ECG monitor. As means of minimizing the sensor size and eliminating the long wires, many sensors have incorporated photoplethysmography (PPG) instead of ECG to monitor heart rate as well as other physiological metrics. PPG basically involves emitting light onto the human skin using LEDs. Since the absorption of light in blood is a function of the light wavelength and hemoglobin oxygenation, this measurement is also often used to determine relative blood oxygenation. Although the absorption of light as a function of wavelength is not monotonic, there exist several wavelengths, such as 540nm and 800nm, where the oxygenated and deoxygenated blood have similar absorption levels. These wavelengths are referred to as the isosbestic points. The longer wavelength is typically implemented into sensors because there is less absorption from the surrounding tissues. Thus, by obtaining a measurement at the isosbestic point and an additional one at a different wavelength, both the heart rate and the relative blood oxygen level can be ascertained. In this thesis, however, we will focus on obtained the heart rate only.

Skin conductance, which is one method for measuring electrodermal activity (EDA)—also sometimes referred to as galvanic skin response (GSR)—measures the readiness with which the skin transmits a small electric current [1]. There exists a relationship between the sympathetic nervous system's activity and emotional arousal. When external or internal stimuli that are physiologically arousing occur, sympathetic activity increases. The skin, in turn, momentarily becomes a better conductor of electricity. Interestingly, the skin is the also only organ in the body that responds purely to sympathetic signals.

Even though arousal is widely considered to be one of the two major elements of an emotional response, it is important to remember that measuring arousal is certainly not equivalent to measuring emotion. Furthermore, although the skin conductance sensor will provide information about a person's arousal level, provided that other triggers of increased perspiration have been held constant, it will not provide any information as to the specific emotion that is being elicited. A plethora of events could cause a change in one's skin conductance levels. Events that tend to cause a sudden change in skin conductance tend to be of a novel, significant, intense, or personal nature. Arousal levels also tend to be high when a person is exercising, angry, scared, startled, or engaging in interesting mental work.

It should be noted that studying the EDA signal is certainly not a novel idea. Experimental studies focusing on changes in the skin's electrical resistance were published over a century ago by Vigouroux [2,3]. Since then, the EDA signal has been the focus of numerous psychophysiology research experiments, particularly in the 1960s-

1970s. It has also been used in research experiments focusing on stress and anxiety [4] and lie detection [5].

1.2 Overview

The remainder of this thesis is organized in the following manner: chapter two includes an analysis of recently developed sensors on the market; chapter three discusses the sensor design and specifications; chapter four describes the experimental protocols implemented and analyzes the data obtained; chapter five presents the numerous applications in which the iCalm module could be used; finally, chapter six concludes the work of this thesis and includes suggestions for future work. Participant data obtained from the experimental protocols described in chapter four are included in Appendices B-D.

Chapter 2

Modern Day Sensors

A more thorough understanding of sensors currently available on the market is certainly necessary before designing iCalm. In Sections 1.1.1 and 1.1.2, a brief survey of sensors recently developed in the commercial and academic worlds, respectively, is conducted.

2.1.1 Sensors Developed Commercially

Our research group has previously developed skin conductance sensors, including the Galvactivator [6] and the Handwave [7]. In addition, a variety of commercial heart rate and skin conductance sensors (Table 2-1) are currently available for applications such as medical research, stress therapy, or law enforcement.

Product	HR	SC	A	ECG	Wireless Protocol	Battery Life	Location on Body
BodyMedia [8,9]	No	Yes	Yes	No	Customized version of ZigBee	12 days	Arm
Brainquiry [10]	Yes	Yes	No	Yes	Bluetooth	—	Chest
FitSense [11]	Yes	No	Yes	No	Nordic	Months	Chest
HeartMath [12]	Yes	No	No	Yes	None	—	Ear/Finger
PulseTracer [13]	Yes	No	No	No	None, USB	1-2 Months	Wrist
Thought Technologies [14]	Yes	Yes	No	Yes	None	10 hr	Chest/Head
Vitaport [15]	Yes	Yes	No	Yes	None, USB	—	Chest
Vivometrics [16]	Yes	Yes	Yes	Yes	None, USB	24 hrs	Chest

Table 2-1: Current commercial products; HR refers to heart rate sensor, SC to skin conductance sensor, and A to accelerometer.

BodyMedia has developed two SenseWear® platforms, one of which is targeted towards body monitoring, the other towards weight management. Both platforms comprise four sensor modules designed for those who suffer from diabetes, obesity, and other metabolic disorders. The four sensors consist of a skin temperature sensor, GSR sensor, heat flux sensor, and 2-axis accelerometer. They provide the user with information about total energy expenditure, which is essentially the amount of calories burned, active energy expenditure, physical activity duration and levels, sleep duration, and sleep efficiency [9].

Figure 2-1: BodyMedia's SenseWear Platform

As demonstrated in Figure 2-1, the sensors are implemented into an arm band, which the user wears for continuous real-time data collection. After approximately a week, the physician uploads the data in a computer and analyzes the user's calorie burn, physical activity, and sleep behaviors. Essentially, the sensors enable the physician to gain insight into the user's key activity points and devise a behavioral modification program. The user then wears the armband along with a watch for another one to two weeks before returning to the physician. As data is collected, the sensors provide personal feedback to the user via a watch. The watch also displays daily metabolic targets set by the user's physician. In a sense, the sensor holds the patient accountable for adhering to the physician's plan, which, when combined with the real-time feedback provided by the watch, can aid users in changing their daily habits.

Whereas the SenseWear Weight Management Solution (WMS) is a long-term behavioral training tool, the SenseWear Body Monitoring System (BMS) is utilized as more of an assessment tool to help the user set a metabolic benchmark after a one-week monitoring period [9].

Brainquiry's QPET (Figure 2-2) can measure up to seven channels of unipolar electroencephalographs (EEG), electromyographs (EMG), or ECG or four channels of bipolar EEG, EMG, and ECG. In addition, it includes a GSR sensor with a range of 0-5 Mohm. It uses a Class 1 Bluetooth wireless module that has a range of 300 ft. The
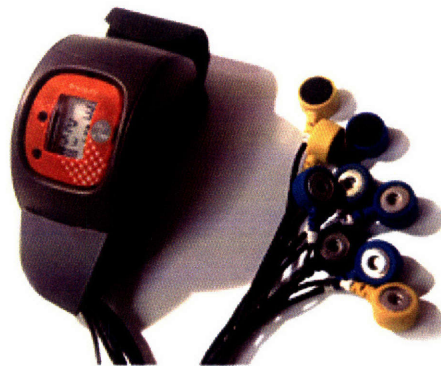
Figure 2-2: Brainquiry's QPET

sensor is accompanied by QView, which is software that provides the user with neurofeedback and biofeedback. The product is available in two different packages: the 5-lead QPET and the 9-lead QPET. The 5-lead QPET corresponds to three channels of EEG, EMG, or EKG, along with one lead for the ground connection and another for the reference connection. The 9-lead QPET is set up similarly except that it has seven leads dedicated for the EEG, EMG, or EKG signal. As evident by the sensor's form factor, it is certainly not designed for everyday use. The QPET is placed on the head to obtain an EEG signal and on the chest to obtain an EKG signal. Unfortunately, the QPET is available at a substantial cost to the user: $2,170.00 for the 5-lead and $3,018.00 for the 9-lead. The GSR sensor, which is sold separately, will cost the consumer an additional $150.00 [10].

FitSense's ActiHealth sensors monitor physical activity, heart rate, calorie burn, weight, body fat, blood pressure, blood glucose, core body temperature, and peak flow. As demonstrated in Figure 2-3, the main sensor, which measures average heart rate, is in the form of a chest strap. Other sensors are worn on the arm, the finger, and foot. The Nordic wireless protocol enables users to securely upload
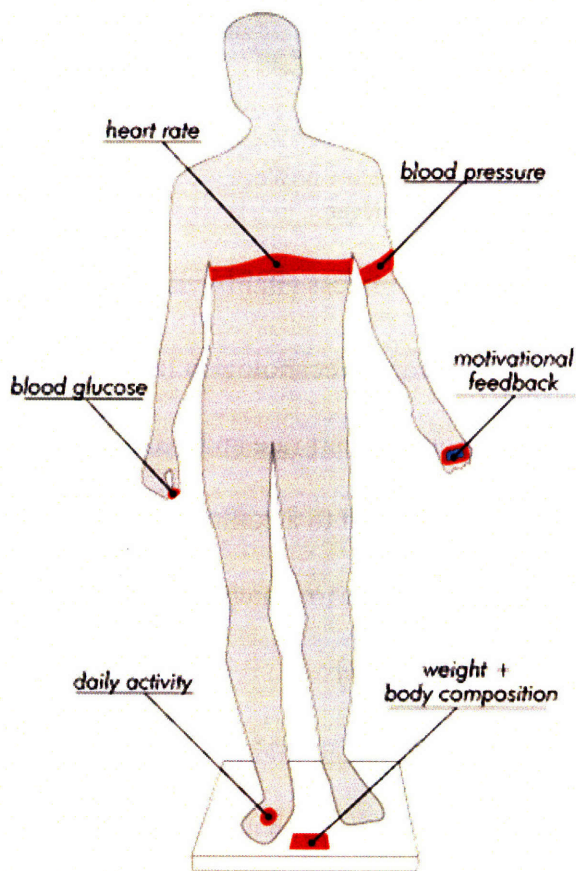
Figure 2-3: FitSense's ActiHealth Sensors

their physiological data whenever they are within a 30-100 ft range of a computer. Furthermore, the wireless protocol is more power efficient than BlueTooth: the ActiHealth sensors can operate on a lithium ion coin cell for months and even years, depending on the application. Similar to BodyMedia's SenseWear platforms, FitSense's platform is mainly targeted towards weight management, disease management, and general health and wellness [11].

Figure 2-4: HeartMath's emWave Personal Stress Reliever

HeartMath has developed the emWave Personal Stress Reliever (Figure 2-4) that is available at a price of $200. It measures heart rate and heart rate variability via the thumb or ear. The sensor then uses an LED light bar to inform users about their stress levels. It is also accompanied by software that aims to reduce stress levels and boost vitality via interactive games [12].

PulseTracer Technologies Inc. have developed the wrist-worn PT100 sensor that detects data about heart rate and pedometer activity. The battery lasts a month and the data can be uploaded to a computer via a USB drive. In addition, users have access to a personalized website to which they can refer for graphical interpretation of over 25 body health indicators [13].

Thought Technologies Ltd. has developed the FlexComp Infiniti which consists of ten channels that are compatible with sensors such as EEG, EMG, EKG, blood volume pulse, respiration, temperature, force, bend, foot switch, voltage isolator, force adapter, torsiometer adapter, and hemoencephalography. It connects to a computer through a fiber

optic cable that connects into the USB drive. Not only does the lack of wireless capabilities restrain one into using the FlexComp only when near a computer, but it also operates on four AA batteries that typically last a mere thirty hours. On the other hand, with its ability to sample at 2048 Hz on two of its channels and at 256 HZ on its other channels, it is a practical tool for real-time, computerized biofeedback and data acquisition in a clinical setting. Similar to all of the aforementioned sensors, the FlexComp Infiniti is also accompanied by software that enables users to analyze their physiological signals [14].

TEMEC Instruments's Vitaport 4 Cardio Pulmonary Screener (CPS) (Figure 2-5) is a 15-channel sensor that measures all signals that are linked to sleep-disordered-breathing: SPO_2 sensor, heart rate sensor, nasal pressure sensor, respiratory inductive plethysmography belts, body-position sensor, piezoelectrical snore sensor, activity sensor, and ECG or EMG/electrooculogram (EOG) sensor. The 12-channel Vitaport 4 Epilepsy/Sleep/Insomnia screener (ESIS) (Figure 2-6) can collect

Figure 2-5: Vitaport 4 CPS Form Factor

EEG, ECG, or EMG data for 12 to 24 hours; however, an external battery pack extends this time to several days. The data is initially collected onto a flash card in European Data Format. As such, even
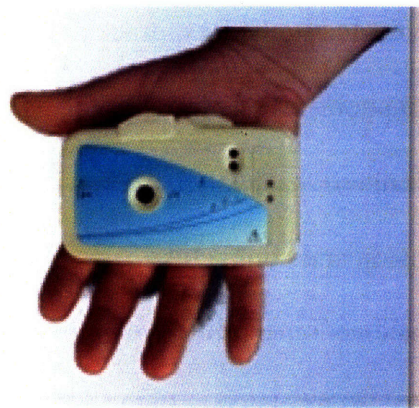
Figure 2-6: Vitaport 4 ESIS Sensor

27

though the sensors are accompanied with basic Vitascore software, users are able to

utilize their own EEG reader software for data analysis. In addition, when both an SPO_2

and ECG monitor are utilized, the ESIS sensor is able to detect not only heart rate, but

also the presence of trachycardia, bradycardia, extra systole, desaturation, and pulse

transmit time. Not surprisingly, ESIS is geared mainly towards epilepsy and sleep

studies. For instance, users can wear the sensor for a period of 24 hours in order to

determine whether they experience daytime sleepiness that could potentially be linked to

insomnia. The CPS sensor, on the other hand, predicts the occurrence of respiratory,

cardio, and pulmonary events. Furthermore, it uses data such as heart rate, pulse

transition time, continuous phase angle between the chest and abdomen, and the

harmonic distortion of the nasal pressure to

determine flow limitations [15].

VivoMetrics' Lifeshirt (Figure 2-7) is

essentially a machine washable vest which

has sensors that measure cardiopulmonary

data embedded in it [16]. It uses inductive

photoplethysmography (IP), which was first

implemented in the RespitraceTM System

[17] to unobtrusively monitor the user's

breathing. IP basically measures the

expansion and contraction of both the rib

cage and abdomen [18]. Movement in the

rib cage is correlated with the activity of the

Figure 2-7: VivoMetrics' Lifeshirt

28

intercostals muscles whereas movement in the abdomen is correlated with the activity of the diaphram. The IP sensor consists of two parallel, sinusoidal arrays of insulated wires; a high frequency, low voltage oscillating current passed through the insulated wires is used to measure the self-inductance of the two coils, which is proportional to the cross-sectional area of the region covered by the IP sensor [19]. Furthermore, the Lifeshirt single-channel ECG monitors cardiac function, heart rate, and heart rate variability [20], and a two-axis accelerometer monitors posture and physical activity. Additional peripheral sensors can be used to measure blood pressure, blood oxygen saturation, EEG, EOG, periodic leg movement, core body temperature, skin temperature, end tidal CO_2, and cough sounds. The Lifeshirt costs $10,000; this price, however, does not include the cost of peripheral sensors: the GSR sensor, for instance, will cost the consumer an additional $995. The system also includes the VivoLog Digital Diary, which is an electronic diary that enables users to record information about their mood, symptoms, and activity [16]. Data is transferred to a computer via the USB port; analysts and database specialists process the data once the user uploads it to the Internet [21]. The Lifeshirt system has been used in numerous studies related to asthma [22], chronic fatigue syndrome [23], respiratory instability [24], cardiac autonomic control [25], chronic obstructive pulmonary disease [26], and exercise [27].

2.1.2 Sensors Developed in Academia

As previously mentioned, the skin's electrical resistance is typically high and varies slowly over time. However, if someone is experiencing mental, physical, or emotional

arousal, skin resistance fluctuates rapidly. Unfortunately, motion artifacts also cause fluctuations in EDA as noted by Nakra [28]. Nakra designed the Conductor's Jacket, which consists of four EMG sensors, one respiration sensor, one heart rate monitor, one skin conductance sensor, and one temperature sensor. Using the Conductor's Jacket, Nakra observed that the vigorous motion of conducting interfered with the EDA signal. Westeyn et al. have developed ActionGSR, a wireless sensor that combines two dual-axis
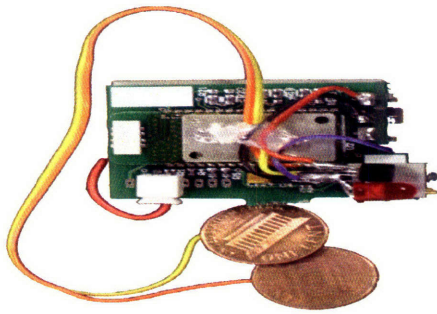
Figure 2-8: ActionGSR

accelerometers with a GSR sensor, to distinguish valid skin conductance data from noise (Figure 2-8) [29]. The skin conductance circuitry is rather simple; it uses the Darlington transistor similar to Picard and Scheirer's Galvactivator (Figure 2-9) [6]. ActionGSR uses a BlueTooth wireless radio and is able to operate for 15-20 hours on a single 3.6 V lithium ion battery. On the other hand, the Galvactivator operates on two 3 V litihium ion batteries. It is also equipped with a thumb-wheel potentiometer that allows users to easily set their individual baselines. The Galvactivator has no wireless capabilities; it maps the user's skin conductance levels to a red light emitting device (LED). As the user's skin conductance increases, the LED becomes brighter. As demonstrated in figure X, the Galvactivator collects skin conductance data from the palm, which is the standard placement for GSR sensors; on the other hand, Westeyn et al. were able

Figure 2-9: The Galvactivator

to obtain GSR data from the waist, which has a low concentration of eccrine sweat glands. Unfortunately, both ActionGSR and Galvactivator are susceptible to a drift in the skin conductance baseline when used over extended periods of time [6,29].

The HandWave, however, automatically adjusts to the aforementioned changes in baseline. It also has BlueTooth wireless capabilities; though the BlueTooth calls for using a large 9V battery that lasts for approximately three hours. It uses an automatic gain control to map the user's skin conductance to a voltage between 0-2.5 V; lower skin conductance values have greater resolution than the higher ones. The leads of the HandWave are placed on the
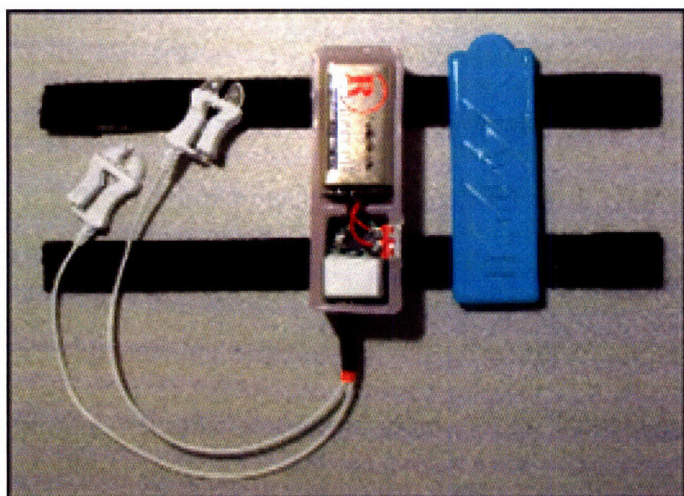
Figure 2-10: The HandWave

user's palm and the sensor itself is placed on the forearm. As demonstrated in Figure 2-10, the form factor of the HandWave is rather clunky even though it can be strapped to the wrist [7].

Hiyamizu et al have developed the Human Sensory Sensor, which measures peripheral skin temperature, pulse, and GSR to determine the level of pain or pleasure the user experiences during a massage. Unfortunately, this sensor also restrains users in that it requires them to place their finger on the sensor so that data can be collected [30].

Ryoo et al. have developed a glove that has a blood volume, heart rate variability, GSR, and heart rate detector embedded in it. It then analyzes three minute strips of the

obtained data to place the user's emotional state in one of eight categories: no emotion, anger, hate, grief, platonic love, romantic love, joy, and reverence. As demonstrated in figure 2-11, they chose to implement the sensor through a glove form factor; the sensor also has BlueTooth wireless capabilities [31].

Makikawa et al. developed a device that monitors the user's total time, distance, velocity, heart rate, and energy expenditure while jogging. The sensor's form factor consists of a belt, a headband, and a display. To determine the jogger's position, a GPS sensor is placed on the belt. The jogger's heart rate is determined through infrared PPG, which is embedded on the headband. To monitor physical activity, and, in turn, energy expenditure, an accelerometer was included in the sensor module. Unsurprisingly, motion artifacts affect the HR signal [32].

Figure 2-11: Sensor Module Developed By Ryoo et al.

David et al. have developed a low-voltage system for measuring heart rate. To determine heart rate, a piezo-microphone sensor measures the vibration of each heart beat. The information collected from the piezo-microphone is transmitted to a handheld device via an RF transmitter. The best feature of this sensor is its low minimum voltage requirement: it needs a mere 1 V for it to be functional [33].

Jacobs et al. have created the Passive Physiological Monitor, or P2M. It essentially consists of a sensor array, on which the subject lies during data collection. Each sensor element creates a voltage that is proportional to the mechanical force caused by the user's cardiac and respiratory cycles. This force, in turn, disrupts the crystalline

structure of the PolyVinyliDene Flouride (PVDF) film within each sensor element. This disturbance results in a voltage difference that is transmitted to the A/D converter via silver ink that covers each sensor element. The sensor was mainly targeted towards patients who are recently admitted into the Intensive Care Unit in hospitals [34].

Yamashita et al. were the first group to attempt to implement a simple telemetric device that utilized analog PPG on the finger for measuring heart rate [35]. The finger is now a standard location for obtaining the PPG signal, as indicated by the numerous sensors that have been developed in that region. Rhee et al [36,37] created a ring sensor that transmits data about the user's pulse to a computer via a radio-frequency transmitter. They particularly strived to minimize motion artifacts and power consumption. They achieved the former by implementing an isolating ring structure, which consists of a ring with two layers that are mechanically decoupled to each other. They achieved the latter by switching the LEDs on and off using a microcontroller. Shatlis et al. [38] have developed a low-power finger clip sensor that is designed for rapid attachment and physiological monitoring in the triage. It is capable of detecting all five major patient vital signs using a PPG, an accelerometer, and a temperature sensor.

PPG's applications are certainly not limited to determining heart rate; it is also widely utilized for measuring vascular compliance [39, 40], blood oxygen saturation levels [41], and respiratory rates [42, 43]. In some cases, the PPG signal is actually more useful than the ECG. Currently, noninvasive methods for approximating pulse wave velocity and blood pressure include measuring the time difference between features on the ECG and a peripheral PPG. [44, 45]. However, it has been shown that the aforementioned method is an inaccurate measure of blood pressure and pulse wave

velocity [46]. Rather, it has been demonstrated that a PPG is a better time reference than

the ECG signal because determining the path length between two in-line PPG signals is

easier and more accurate [47, 48].

Chapter 3

Sensor Design and Specifications

3.1 Hardware

3.1.1 Heart Rate Sensor

As previously mentioned, red and infrared light has the greatest levels of transmission through tissue. The heart rate PPG monitor basically involves a strip of four red LEDs and a matching photodiode placed under a wrist band (Figure 3-1). The LEDs were placed in a linear array as means of minimizing noise and error due to the inexact placement and slippage of the wristband over the arteries.

The heart rate sensor's circuit schematic is illustrated in Figure A-1 in Appendix A. As previously mentioned, we strived to build sensors that are pragmatic in terms of both cost and power. As such, a rail-to-rail operational amplifier with a high slew rate, a

low input bias current (I_{IB}), a low minimum operating voltage, a gain bandwidth higher than 0.9, an Iq less than 1 mA , and a low price was desired. The TLV2784 was the
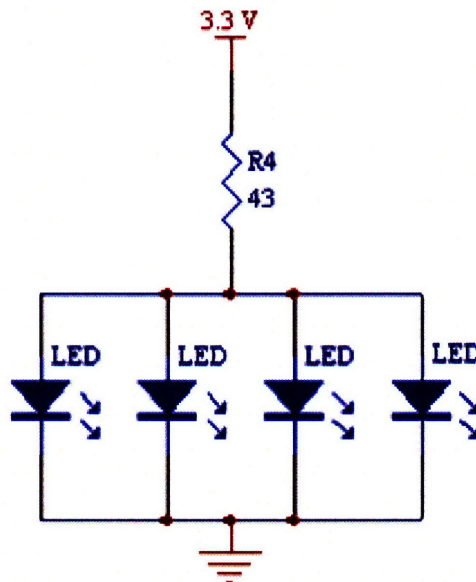
Figure 3-1: Schematic for the heart rate sensor's linear strip of LEDs. Resistor value is in Ohms.

operational amplifier implemented in all of the sensors because it meets all of the aforementioned requirements: rail-to-rail input and output, a minimum operating voltage of 1.6 V, a high slew rate of 4.3 V/uS, I_{IB} of 15 pA, Iq of 0.82 mA per channel, and a gain bandwidth of 8 MHz, and a low price of $1.20.

As previously mentioned, the PPG sensor's output signal varies with respect to blood volume and consists of two peaks. The large, periodic peaks present in a PPG signal, however, are nameless. Even though they lag behind the R wave, they peaks occur at the same frequency as R waves and can therefore be used for calculating heart rate; as such, in the remainder of this thesis, the main peak in the PPG will be referred to as R wave for simplification purposes. The smaller, secondary peaks are also nameless and correspond to venous pulsations.

As noted in Figure A-1, the first stage of the circuit diagram is a transimpedance amplifier, which converts the current produced by the photodiode into voltage. A 1 MΩ resistor was placed at the positive input of the op-amp because it doubles the value of the input signal without doubling the gain.

The second stage is a bandpass filter with corner frequencies 4.8 Hz and 10.6 Hz, a bias voltage of 1.08 V, and a gain of 45. The low cutoff value was chosen because it eliminated the DC bias and removed baseline frequencies without deforming the QRS complex of the heart beat. Since this is only a first order filter, the high cutoff value was chosen at 10 Hz to ensure the elimination of 60 Hz noise. This simple RC first order filter was implemented instead of more complicated higher order filters to minimize the noise introduced by additional stages. Since within the QRS complex, the R wave has higher amplitude than both the Q and S segments, the bias voltage was set a bit lower than 1.65 V, which is half of V_{CC}, to prevent signal saturation.

The signal obtained via PPG on the wrist has very small amplitude; therefore, a high gain is necessary in order to place the sensor's output signal within the proper range so that the microcontroller can detect the R wave peaks. The value of this gain, however, varies from user to user. For instance, a male adult with thicker skin will need a higher gain than a child with small wrists. A 50 KΩ wheel potentiometer was placed in the third stage of the heart rate sensor in order to enable users to adjust the gain so that the signal falls within the proper range. A wheel potentiometer, as opposed to a rotary potentiometer or a rheostat, was chosen so that the user would be able to easily adjust the gain without the use of a screw driver or similar tools.

The fourth stage of the heart rate sensor is merely a buffer with a bias of 3.3 V. Since the output of the third stage is an inverted heart beat signal, the sole purpose of the buffer is to invert the signal so that the output of the overall circuit properly represents a heart beat signal. It is essential that the output has the correct polarity so that the comparator in the microcontroller can properly detect the R wave peaks.

The output of the heart rate sensor is then connected to an 8-bit microcontroller, specifically the Atmel ATmega 168, which detects the R wave peaks in the signal. It operates very similarly to a comparator: when the input signal is higher than 1.5 V, it counts it as beat and ignores the signal as it decreases back to its baseline value. As the R wave reoccurs, the signal increases yet again and as it crosses the 1.5 V threshold, the microcontroller records another beat. It then subtracts the two obtained time stamps to determine the time between the two R waves. Next, the time difference values between ten consecutive R waves are averaged and used to calculate the user's heart rate. As such, when setting the gain in the third stage of the circuit, the user has to adjust to a value such that the R wave peak crosses the 1.5 V threshold level. The user also has to be cautious to not set the gain too high so that the amplitude of the input signal's other components remains below 1.5 V. For instance, if the gain is too high, the R wave could be saturated at 3.3 V while the smaller, secondary PPG waveform also crosses the 1.5 V threshold. The microcontroller, in turn, will count both waveforms in determining the user's heart rate and will produce a heart rate value that is far too high.

3.1.2 Skin Conductance Sensor

The main goal in the design of the iCalm skin conductance sensor was to improve upon both the Galvactivator and the HandWave sensors that were previously developed by my research group and to create a simple, low-cost, low-power sensor that would be comfortable to wear. As previously mentioned, the Galvactivator uses a Darlington pair which causes the skin conductance signal to have a floating baseline when the user is monitored over long periods of time. It also uses an LED to visually inform users about their relative conductance levels. Since it lacks a microcontroller, it does not digitally quantify the user's skin conductance levels. The HandWave, on the other hand, uses a microcontroller to implement an automatic gain control circuit.
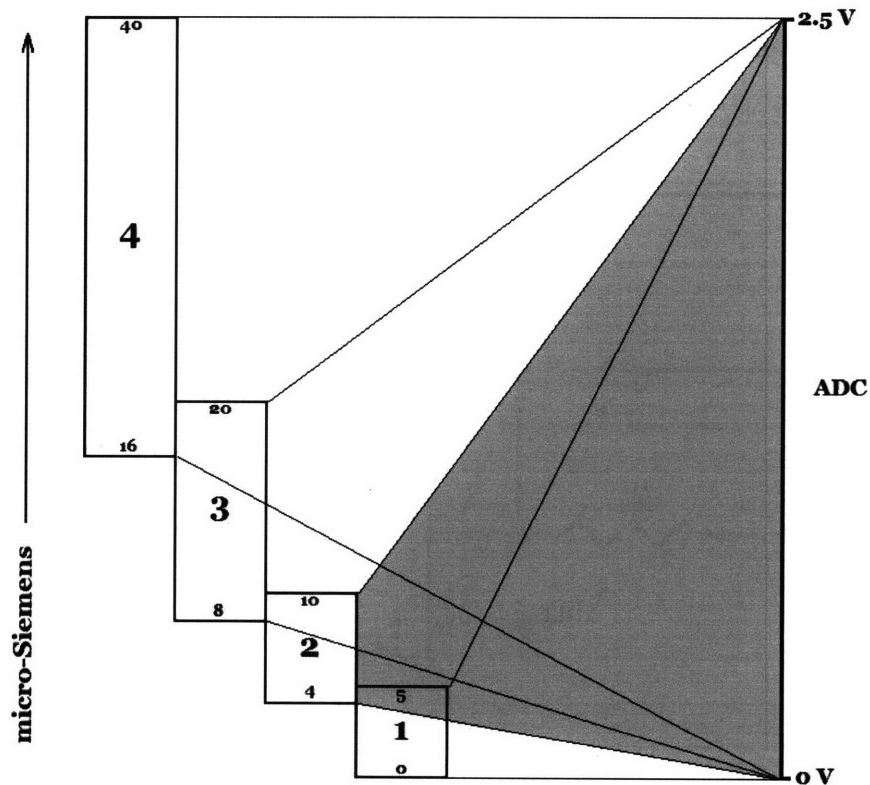

Figure 3-2: Mapping skin conductance levels via HandWave's automatic gain control

As displayed in Figure 3-2, it does so by dividing the range of skin conductance values into four distinct regions. Each region, in turn, has a fixed gain which maps the user's skin conductance values to a voltage value between 0 and 2.5 V.

An automatic gain control design was also implemented in the iCalm skin conductance sensor. Nevertheless, to maintain simplicity and minimize cost and power, the automatic gain control circuitry was developed without the use of a microcontroller. As noted in Figure A-2, merely two operational amplifiers were utilized to build the sensor. The gain of both operational amplifiers is set to one. The bias of the second operational amplifier is set to half of the V_{CC}. The second operational amplifier uses the output of the first to set the bias of the first operational amplifier. The resistor R_{skin} refers to the resistance of the user's skin, which is obtained from the leads of the skin conductance sensor that are placed on the user's wrist.
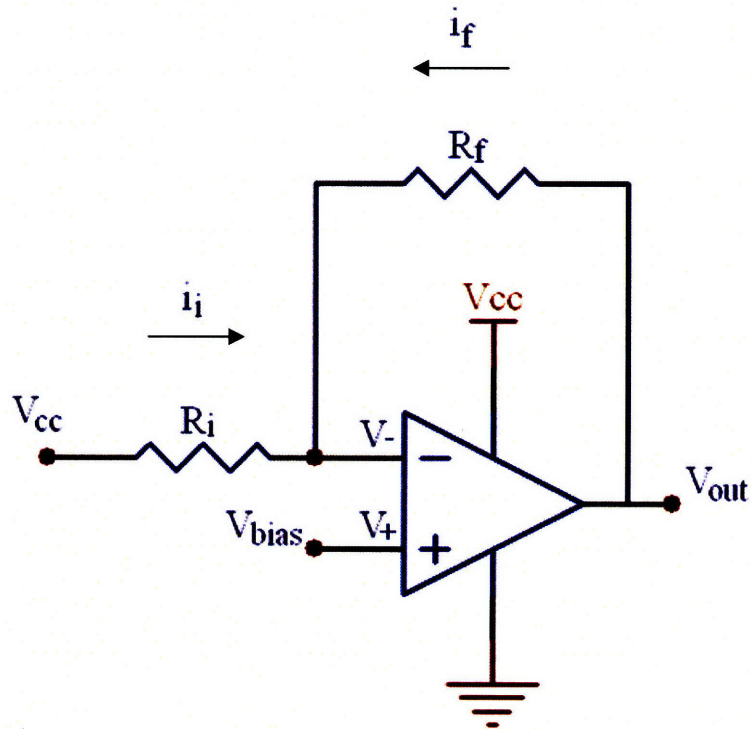

Figure 3-3: Simplified model of the first operational amplifier

Figure 3-3 is a simplified representation of the skin conductance sensor's first operational amplifier. Assuming an ideal operational amplifier,

$$V_+ = V_- = V_{bias} \qquad [1]$$

because of the presence of negative feedback. As per Ohm's Law,

$$i_f = \frac{V_{out} - V_i}{R_f} \qquad [2]$$

$$i_i = \frac{V_{CC} - V_i}{R_i} \qquad [3]$$

Using Kirchoff's Current Law:

$$i_f = -i_i \qquad [4]$$

Substituting equations 1-3 into equation 4 and rearranging terms:

$$R_{skin} = \frac{R_f (V_{CC} - V_{bias})}{V_{bias} - V_{out}} \qquad [5]$$

Using R_{skin}, the user's skin conductance value can be calculated:

$$\text{Skin Conductance} = \frac{1}{R_{skin}} \qquad [6]$$

where R_{skin} has units of $M\Omega$ and skin conductance units of microSiemens (uS). The iCalm module transmits values of V_{CC}, V_{bias}, and V_{out} wirelessly to module a laptop which utilizes the iCalm software to calculate the user's skin conductance value. EDA sensors are generally divided into two categories: constant voltage and constant current. Since voltage levels are used to determine skin conductance, it is evident that the iCalm skin conductance sensor implements constant current circuitry.

3.2 Software

The iCalm software is written in Java and essentially parses the data packets sent by the wireless chip that is connected to the output of the heart rate and skin conductance sensors. It then performs the calculations necessary to provide the user with the information of interest. For instance, it parses the packet sent by the skin conductance sensor to first attain the values of V_{CC}, V_{bias}, and V_{out} and then utilizes the obtained values to calculate the user's skin conductance level. It allows users to access and analyze their physiological data in real-time; however, they may also view it at a later point in time if desired. As illustrated in Figure 3-4, the iCalm software provides the user with a linear plot, polar plot and histogram as options for data visualization.
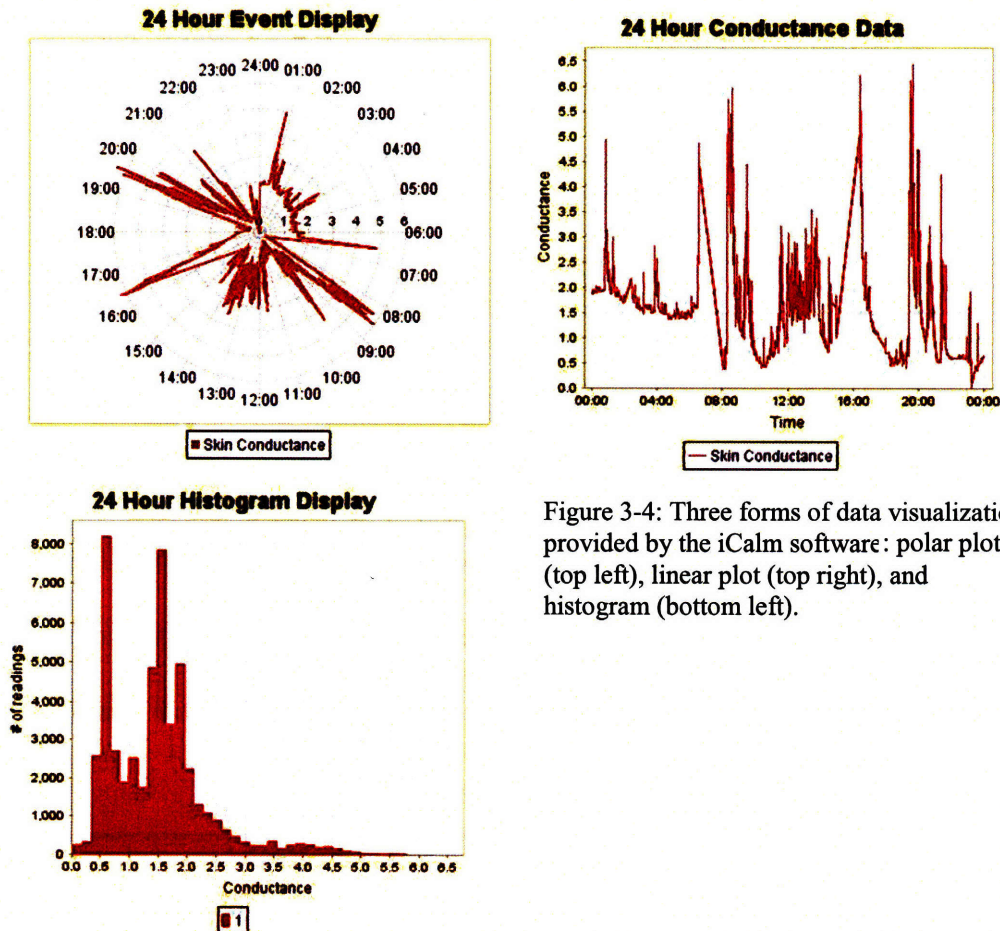

Figure 3-4: Three forms of data visualization provided by the iCalm software: polar plot (top left), linear plot (top right), and histogram (bottom left).

3.3 Firmware

A protocol based on the IEEE 802.15.4 wireless standard was chosen for the wireless connection between iCalm and the computer mainly because it is optimized for low power, low cost and portability. This wireless protocol operates at 2.4 GHz, supports frequency hopping, and is generally not affected by interference from other radio signals, such as Wi-Fi's IEEE 802.11 wireless standard, that also exist in the 2.4 GHz frequency band.

The IEEE 802.15.4 radio hardware is not only cheaper and more power efficient than BlueTooth, it can also support more sensors simultaneously. Although 802.15.4 is often used as the physical layer for building multi-hop mesh sensor networks employing ZigBee protocols, we chose not to use ZigBee because it requires a larger microcontroller to implement and is not appropriate for this application.

A packet-based transmission with Carrier Sense Multiple Access (CMSA) collision avoidance scheme was implemented by TagSense Inc. in the radio module used to enable multiple iCalm sensors to transmit data simultaneously. With a transmission rate of 1 Hz, the receiver can support twenty sensors without any noticeable degradation in performance. As the number of sensors is increased, occasional packet collisions and an effective reduction in the transmission rate, caused by the CSMA protocol, are observed. Nevertheless, if the transmission rate is decreased to 0.2 Hz, it is possible to support 100 sensors simultaneously.

Bluetooth radio devices, however, are generally used for high-bandwidth continuous streaming of data and are limited to approximately six simultaneous connections. In addition, Bluetooth devices require a significant amount of handshaking

to initialize the communication which can cause initialization delays. The wireless

protocol implemented in our system is completely ad-hoc and requires no handshaking.

3.4 Battery Life

As previously mentioned, devices that implement 802.15.4 are more power

efficient in that their battery life is measured in weeks as opposed to hours in BlueTooth

devices. The iCalm module is able to continuously collect data for over seventeen hours

on a single 3.3 V lithium coin cell battery while transmitting data at a rate of 1Hz to a

receiver with a 30 m range. The power consumption is at least a factor of ten

improvement over previous devices that have been constructed in our research group

using Bluetooth radio modules. The long lasting battery power enables users to record a

day's worth of a physiological data without the need to replace the batteries throughout

the day. It should be noted that battery life will increase as the data transmission rate is

lowered and the receiver's range is decreased.

3.5 Cost

Assuming quantities of 500, the wireless transmitter cost approximately $15; the

wireless receiver costs approximately $30; the iCalm skin conductance sensor

approximately $6; the iCalm heart rate sensor approximately $11; All of the

aforementioned costs include the components and printed circuit board (PCB) cost as

well as the assembly cost. It does not, however, include the cost of firmware, quality

control, packaging, and delivery. Given new commercially-available products, it is possible that future versions of iCalm may combine the radio module and the microcontroller into a single IC in order to further reduce cost.

3.6 Form Factor

The iCalm sensor platform is in the form of a wrist band that was designed by Dr. Kelly Dobson, an alumna of MIT's Media Laboratory. As demonstrated in Figure 3-5, the iCalm PCB fits into a pocket on top of the wrist band. iCalm's dimensions are 32 mm x 32 mm x 12 mm; this measurement includes both the wireless transmitter and the sensor itself. In addition, since the sensor circuitry detaches from the wristband at the white snaps illustrated in Figure 3-5, iCalm is washable.
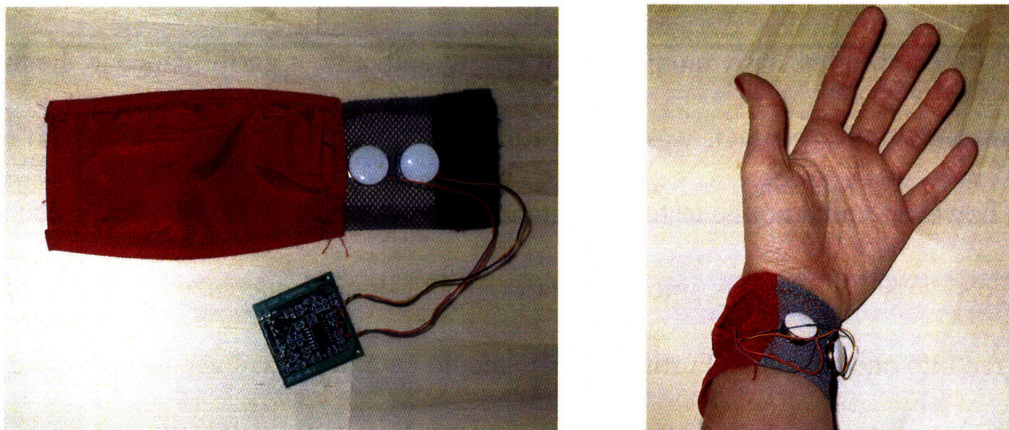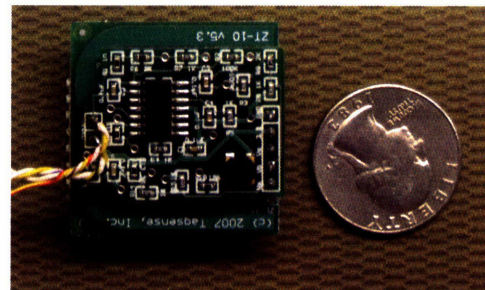

Figure 3-5: iCalm wristband form factor (top); iCalm's size in comparison to a quarter (right).

Chapter 4

Sensor Testing and Evaluation

Several experimental protocols were designed to compare the performance of the iCalm sensors with that of an FDA-approved consumer device. For the latter, we used Thought Technologies' FDA-approved FlexComp Infinity system. Since the sensors are designed for continuous, daily monitoring, it is natural that their performance in the face of pressure and motion artifacts was also evaluated. The skin conductance and heart rate sensors, however, could not be tested simultaneously due to the lack of physical space on the subjects' wrists and fingers since the heart rate and skin conductance sensors were not yet merged into one package. Furthermore, it should be noted that since the sensors are designed with usability in mind, we do not intend for them to be worn with any conductive gels. As such, all the skin conductance sensor experiments were conducted with dry electrodes.

4.1 Skin Conductance Sensor

The skin conductance tests involve users wearing four sensors: a Flexcomp GSR sensor placed on the index and middle fingers on the outermost phalanges and an iCalm skin conductance sensor placed on the wrist of each hand as illustrated in Figure 4-1. The dual placement of the two sensors will validate the presence of a slight difference in left and right hand skin conductance levels, as described by Boucsein [50].
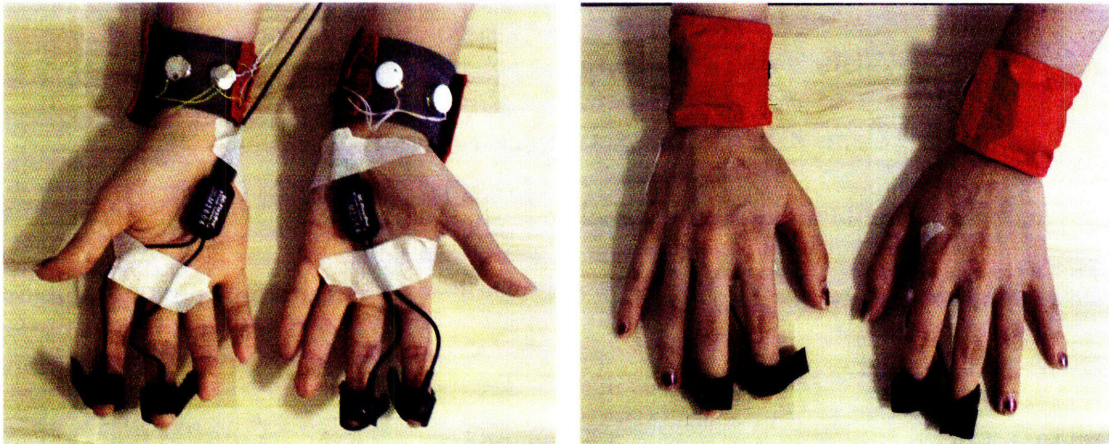

Figure 4-1: Sensor placement for the skin conductance sensor experiments.

A five minute experiment was conducted with n=12 participants during which each participant was asked to relax and not move their hands so as to prevent any motion artifacts from potentially corrupting the skin conductance signals. At every one-minute interval during the first four minutes, a loud burst of noise was released with an air horn to startle the participant. Thirty seconds after the last air horn, he or she was asked a series of three questions:

1. "What is your favorite flavor of ice cream?"

2. "What is your favorite color?"

3. "Please describe your first sexual experience."

Since the last one is a fairly sensitive and personal question, it was posed rhetorically simply to raise the user's arousal levels. The data obtained from the experiment are presented in Appendix B.

As evident in Appendix B, there indeed exists a small distinction in the conductance of the left and right hands. In addition, there exists a slight time difference between when the noise is generated and when the user's skin conductance begins to rise in response to it. This time difference, however, does not seem to depend on whether the sensor is placed on the wrist or on the finger. Further testing is required in order to make a more accurate claim. There also exists an increasing trend amongst the skin conductance data obtained from the iCalm. It should be noted that in experiments that measure skin conductance, the participant typically wears the sensor for approximately fifteen minutes between data collection begins. This time delay is implemented simply to allow some time for a moisture barrier to develop between the sensor and the participant's skin. In our experiments, however, the participant wore the sensor for one minute before initiating data collection. As such, the moisture barrier was accumulating as the measurements were taken, which resulted in an increasing upward trend amongst all the data collected with the iCalm sensors. Since the fingers have more eccrine sweat glands, not as much time is required for the moisture barrier to develop. Thus, the skin conductance data obtained with the FlexComp do not demonstrate the increasing trend. Nevertheless, the largest discrepancy evident in the figures is the difference in the magnitude of skin conductance obtained from the two methodologies. To verify that the difference is not due to the sensor itself, but its placement, two additional sets of
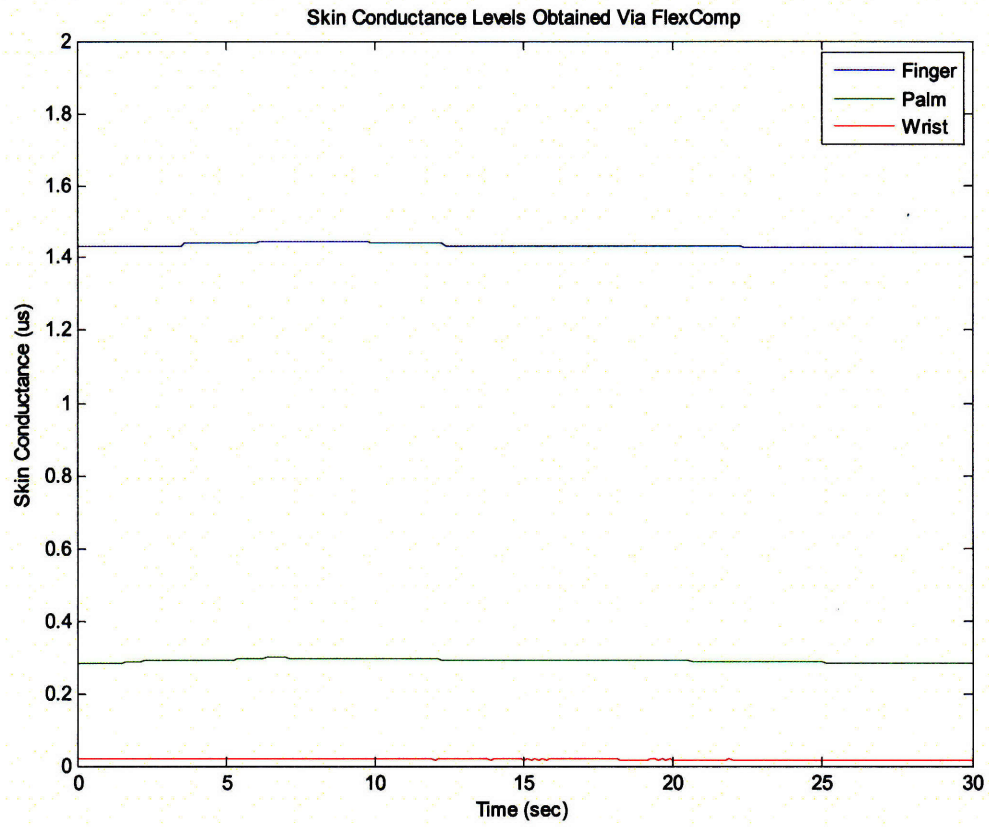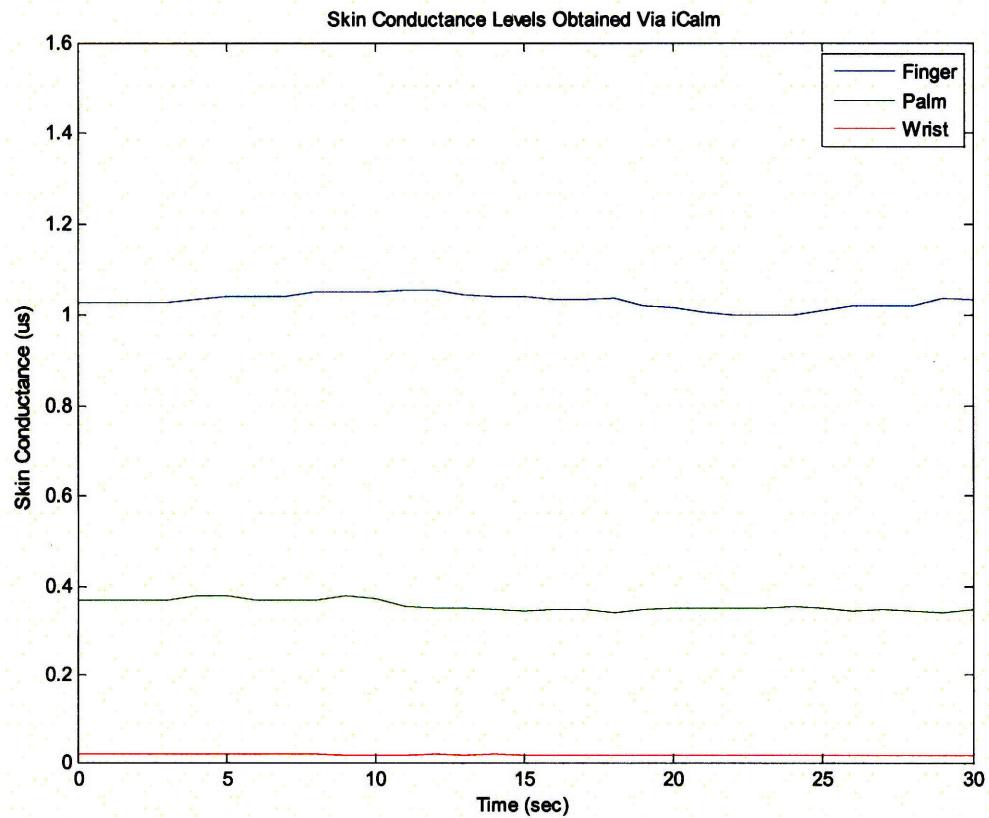
Figure 4-2: Skin conductance levels obtained from the finger, palm, and wrist via the FlexComp (above) and the iCalm (below).

49

experiments were conducted. The participant's baseline skin conductance was monitored simultaneously on three different locations on the body: tip of the index and middle fingers, middle of the palm, and the wrist of the dominant hand. This experiment was initially conducted with the FlexComp and repeated using the iCalm.

Figure 4-2 clearly illustrates the variation in skin conductance levels in the three aforementioned locations. The disparity in skin conductance levels in the three regions is due to the uneven distribution of eccrine sweat glands across the three regions. It is undeniably the high concentration of these glands on the fingers and palms that has resulted in these regions being labeled as the gold standard for EDA measurements. As verified in Figure 4-2, the fingers and palms are indeed more sensitive than the wrist to small changes in skin conductance levels. Nevertheless, skin conductance varies not only with location, but also with the amount of pressure on the skin. As such, baseline skin conductance values were initially obtained from the participant's dominant wrist with iCalm alone; next, a snug wrist band was placed on top of the sensor as means of increasing pressure.

It can be observed from Figure 4-3 that the amount of pressure applied at the site of measurement indeed changes the skin conductance levels obtained. It should be noted that the reason the magnitude of the signal peaks for Participant #7's left hand FlexComp sensor is much lower than that of the right hand's is that the sensor was loosely strapped around the finger (Figure B-19). As such, there was much less pressure and surface between the sensor and the skin. While participants' skin conductance levels vary with both sensor location and skin surface pressure, baseline skin conductance levels also vary across people—even when applied under the same conditions. Regardless, it is essential

to recognize that in monitoring users, it is the relative change in the magnitude of the EDA signal that is important, not the actual magnitude itself. This idea is clearly

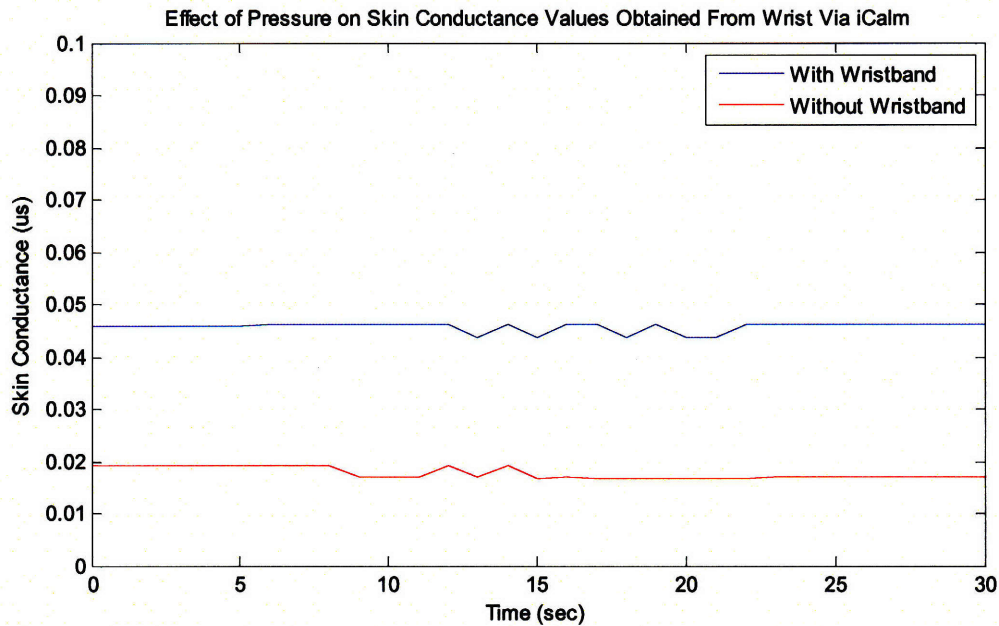**Effect of Pressure on Skin Conductance Values Obtained From Wrist Via iCalm**

Figure 4-3: Effect of pressure on skin conductance values obtained from the wrist with iCalm

presented through Participant #7's data (Figure B-19, B-20, B-21). The graph of the normalized data indicates that the left and right hand FlexComps both produced skin conductance plots with nearly the same morphology; the right hand simply has a higher sensitivity to change. This discrepancy in sensitivity is a reasonable result considering that there was a higher pressure and surface area between the sensor and the skin when compared to the left hand.

Although the participants' skin conductance data exhibit distinctive peaks at the sound of the air horn and at the questions, many of them also include smaller peaks in between the major ones. Without a doubt, skin conductance is by no means a measure of emotion; it is at best a measure of arousal level, which can be impacted by motion and pressure artifacts as well as other sources of moisture. Both laughter and anticipation

increase arousal levels. Since many participants would nervously laugh in between the air horns, their skin conductance would temporarily increase and result in the creation of the smaller peaks. Participant #7 was aware of the air horn element of the experiment; after the experiment, he mentioned that he was particularly nervous prior to the first air horn. He had heard the experimenter making some noise and assumed that the air horn was going to be blown at any second. Naturally, his anticipation caused an increase in his skin conductance before the air horn was blown for the first time as evident in Figures B-19 through B-21.

Since the iCalm sensors are designed for long-term physiological monitoring, it is necessary to evaluate their performance against the FlexComp while partaking in daily activities. An experiment, during which each of the n=12 subjects completed the following tasks in the afternoon was conducted:

1. Relaxing

2. Blowing up a balloon

3. Typing

4. Drinking a cup of water

5. Walking

6. Jumping Jacks

7. Answering Questions

The questions asked were the same three questions as previously mentioned. Since the FlexComp does not have wireless capabilities, the subject was followed around the testing area with a laptop and the sensor box during the walking and jumping jacks phase

of the experiment protocol. The FlexComp sensor wires were taped to the participant to minimize motion artifacts; the iCalm was worn comfortably on the wrist.

As evident by some of the experimental data obtained, such as those illustrated in Figures C-10, C-16, C-2, and C-24, not all people are particularly reactive on their wrists when measuring their skin conductance. Nevertheless, everyone, including those who were generally unresponsive, demonstrated some increase in skin conductance while performing jumping jacks. In addition, everyone other than participant #12, whose data is plotted in Figures C-23 and C-24, experienced an increase in skin conductance when they were asked the personal question at the end of the experimental protocol. Thus, it seems as though everyone elicits some level of change in his or her skin conductance levels on the wrist; however, the magnitude of this change varies from person to person. It would be interesting to conduct additional experiments to discover what percentage of the population is reactive on their wrists while performing daily activities that are not particularly arousing, such as typing or walking.

In order to ensure that the data collected is valid skin conductance data as opposed to noise due to pressure or motion artifacts, the typing and jumping jacks section of the experimental protocol were repeated in a slightly modified manner while the participant was relaxing. For the typing segment, the participant first mimicked the typing motion while "typing" in the air as opposed to an actual keyboard; she then typed on a keyboard for comparison. For the jumping jacks segment, the participant imitated the hand movements of the jumping jacks while sitting. In addition to the two sets of sensors, a MITes accelerometer developed by the House_n research group at the MIT Media Laboratory was placed on the participant's dominant wrist. The goal of this experiment

53

was to observe the performance of the sensors in the face of pressure and motion artifacts while maintaining a skin conductance level similar to that obtained while the subject is in a calm state.

Figures 4-4 and 4-5 illustrate the results of the first series of pressure and motion artifact test conducted. In figure 4-4, it seems as though the artifacts create an oscillation in the skin conductance signal resulting in approximately 48% and 35% variation in the values obtained via the left and right FlexComp, respectively. The morphology of the iCalm skin conductance signal, on the other hand, is essentially monotonically increasing, which results in an overall variation of approximately 25% and 22% for the data obtained from the left and right iCalm, respectively. Since there exists a slight variation in the skin
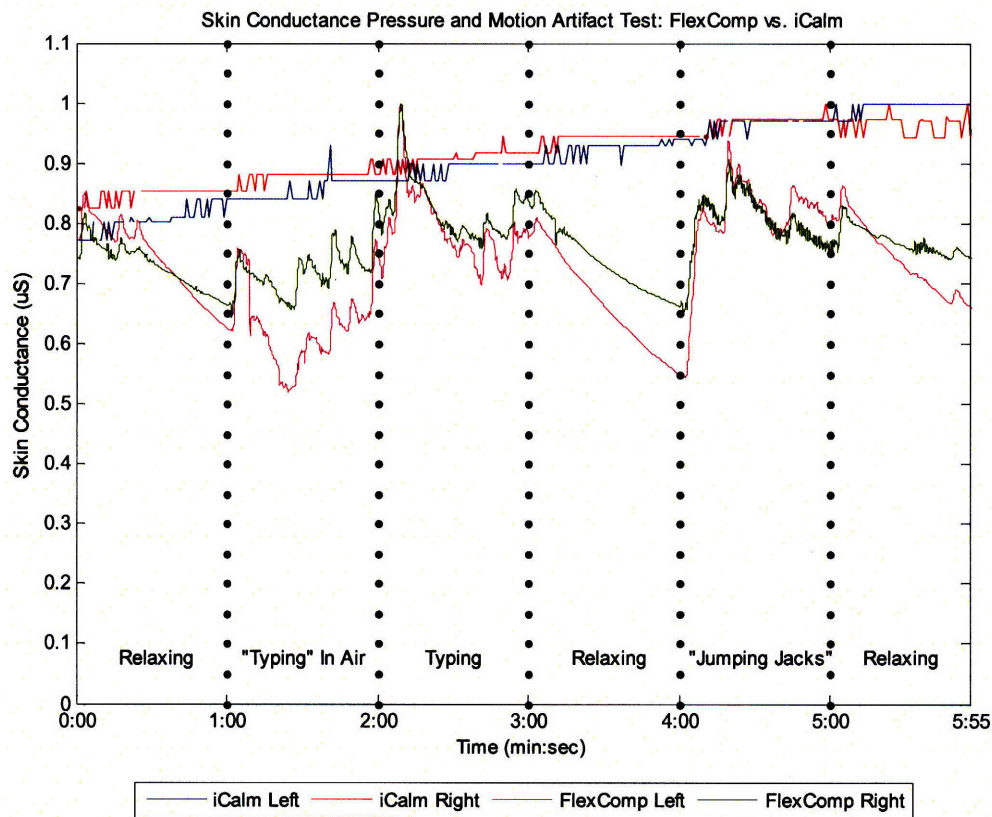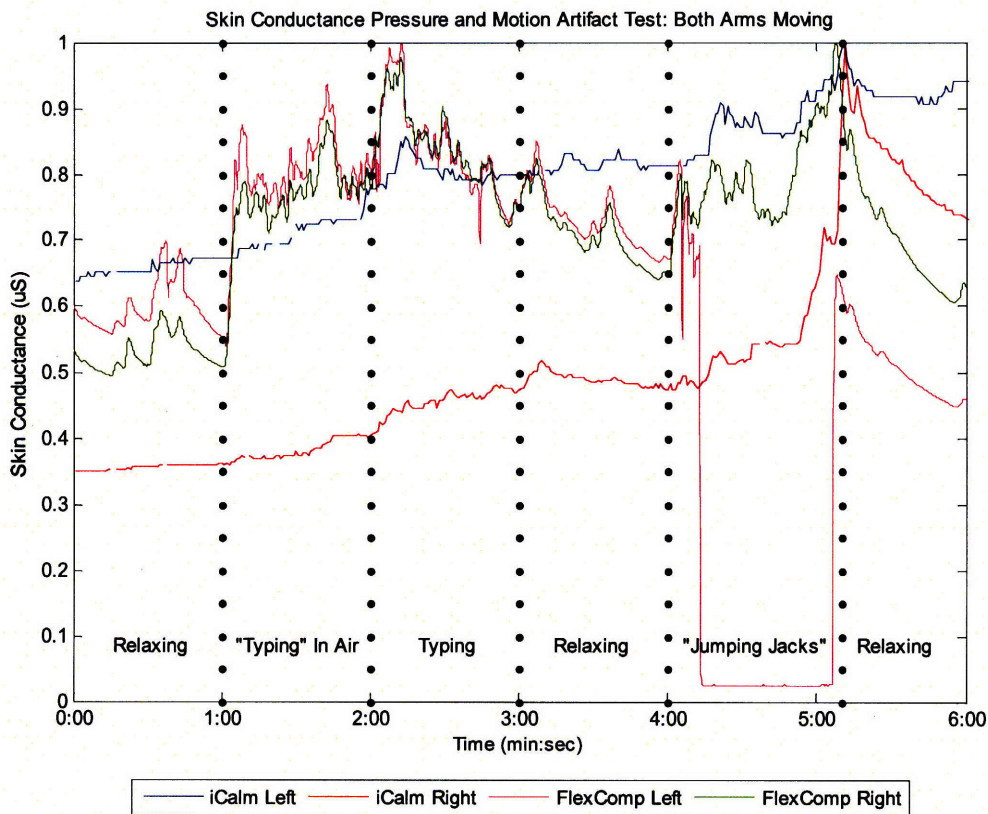

Figure 4-4: Normalized skin conductance data obtained from the pressure and motion artifact experiment
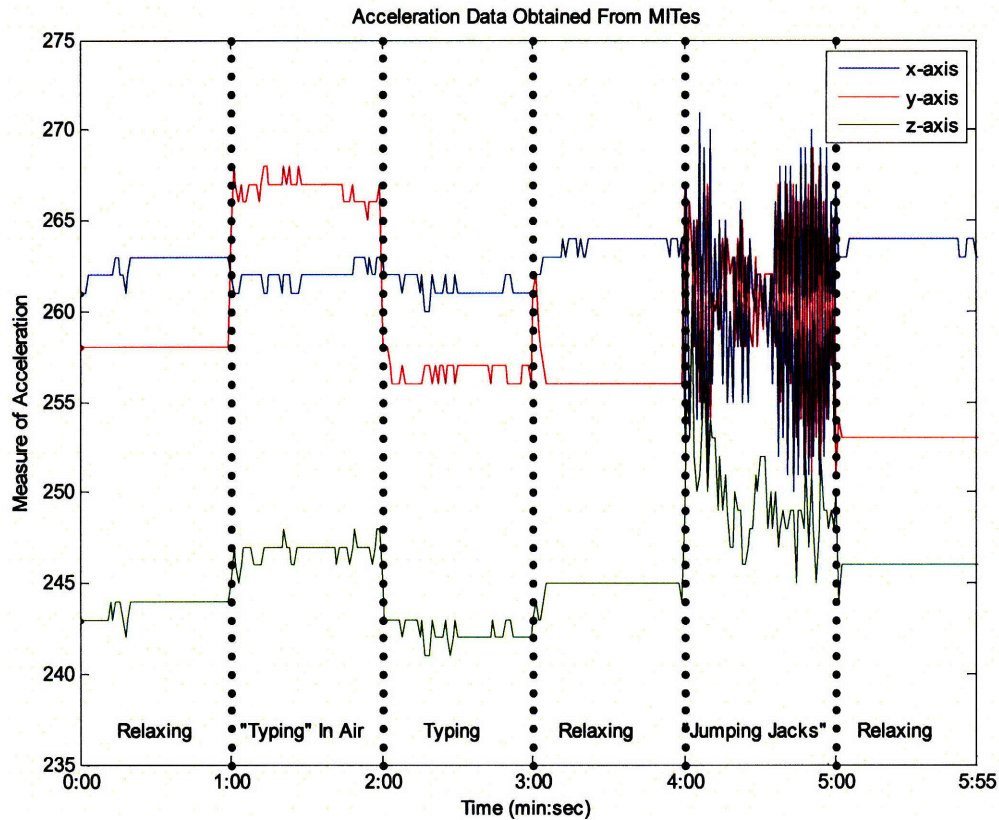
Figure 4-5: Acceleration data obtained from MITes placed on the participant's right wrist during the pressure and motion artifact experiment for skin conductance sensor

conductance data even while the user is resting, the minor increase in the iCalm data represents that of an actual increase in skin conductance as opposed to an artifact-induced increase. It should also be noted that the user is becoming accustomed to wearing the sensor; as such, a tiny moisture barrier is developing between the sensor leads and the user's skin, which leads to the slight increase in skin conductance levels.

As demonstrated in Figure 4-4, the FlexComp skin conductance data display many peaks during the typing and jumping jacks segments of the experimental protocol. In order to explore whether these peaks correspond to noise or actual skin conductance responses, the experiment was conducted once again with a slight change in protocol: the participant first repeated the experiment as before; next, she repeated the experiment

while holding her left arm still. In other words, she performed the activities using only her right arm and hand. In addition, the participant wore the sensor for five minutes before the start of the experiment as opposed to one minute as conducted in the other skin conductance experiments. The results are illustrated in Figure 4-6 and 4-7.

It should be noted that the sharp decrease in skin conductance as illustrated in Figures 4-6 and 4-7 corresponds to the FlexComp sensor slipping of the participant's fingers. This signal is also evident in participant #1, 7 and 12's data, particularly while performing jumping jacks (Figures C-1, C-2, C-13, C-14, C-23, and C-24).

As illustrated in Figure 4-6, in contrast to Figure 4-4, both the FlexComp and the iCalm have obtained similar data, particularly in the "jumping jacks" segment of the

Figure 4-6: Normalized skin conductance data obtained from the pressure and motion artifact experiment with both arms moving.
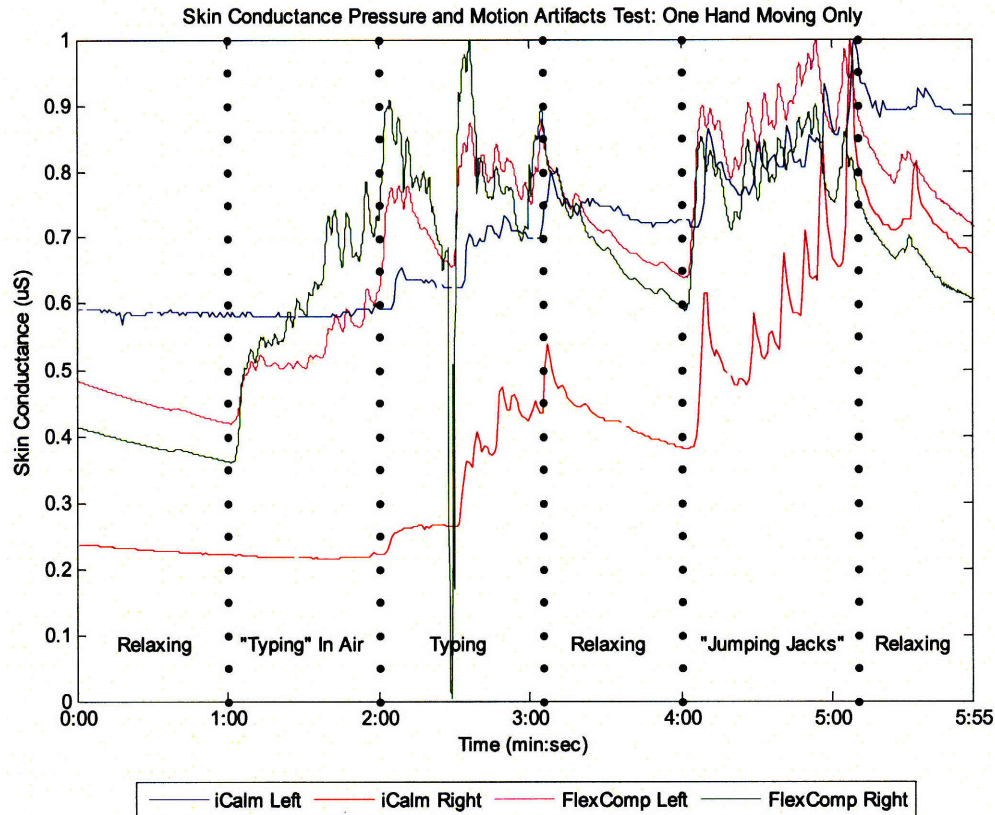
Figure 4-7: Normalized skin conductance data obtained from the pressure and motion artifact experiment with only the right hand moving.

experiment—when a slight moisture barrier has built up, causing the iCalm to be more sensitive. The effect of this moisture barrier is further observed in Figure 4-7 where the iCalm data is very similar to that obtained via the FlexComp; in addition, the participant's baseline skin conductance levels are fairly uniform during the first two minutes of the experiment. These results indicate that even though the peaks in the FlexComp signal might be slightly contaminated by noise, its magnitude is generally not large enough to blatantly affect the skin conductance signal. The FlexComp skin conductance data, however, seems to be slightly affected by motion artifacts during the typing in air segment of the experiment. Furthermore, the data illustrate that even an action as

seemingly insignificant as typing does indeed increase arousal levels. Further studies need to be conducted in order to develop an experimental protocol that can be an accurate measure of pressure and motion artifacts without increasing skin conductance. Finally, the difference in the participant's reactivity between Figure 4-4 and Figure 4-6 and 4-7 further illustrates the importance of allowing participants to wear the sensors for a longer period of time before collecting data.

Nevertheless, we learned that every participant preferred the iCalm sensor to the FlexComp; in fact, many of them asked if they could have one to keep. Some participants even felt compelled to express their frustration during the typing segment of the experiment without being prompted to do so:

"I hate typing with crap ,on my hands. It makes my life very difficult."

"I was born in Iowa... and now I am in Msschusets and Hoda is annoying me."

"It is difficult to type with sensors on, so there may be many spedllings errors."

"I really hate writing wth thyis."

"I can ype withthis as long as I look at the keys, but I'm so used to not looking it takes some concentration to do it any other way. Ah well..."

The original typed quotes are included simply to illustrate user frustration with the slow speed and the numerous typing errors that the FlexComp would cause—even after repeatedly utilizing the backspace key.

4.2 Heart Rate Sensor

Many of the experiments that were conducted for the skin conductance sensor were also repeated for the heart rate sensor. Unlike the skin conductance tests, the heart rate tests involve users wearing only two sensors: a FlexComp blood volume pulse sensor on the index finger and an iCalm heart rate sensor on the wrist of the dominant hand. The dual placement of the sensors is unnecessary since there does not appear to exist a discrepancy in the values obtained from the left and right hands.

Since the user's heart rate is obtained using photoplethysmography, the amplitude of the signal highly depends on the placement of the LED strip and diode. For instance,
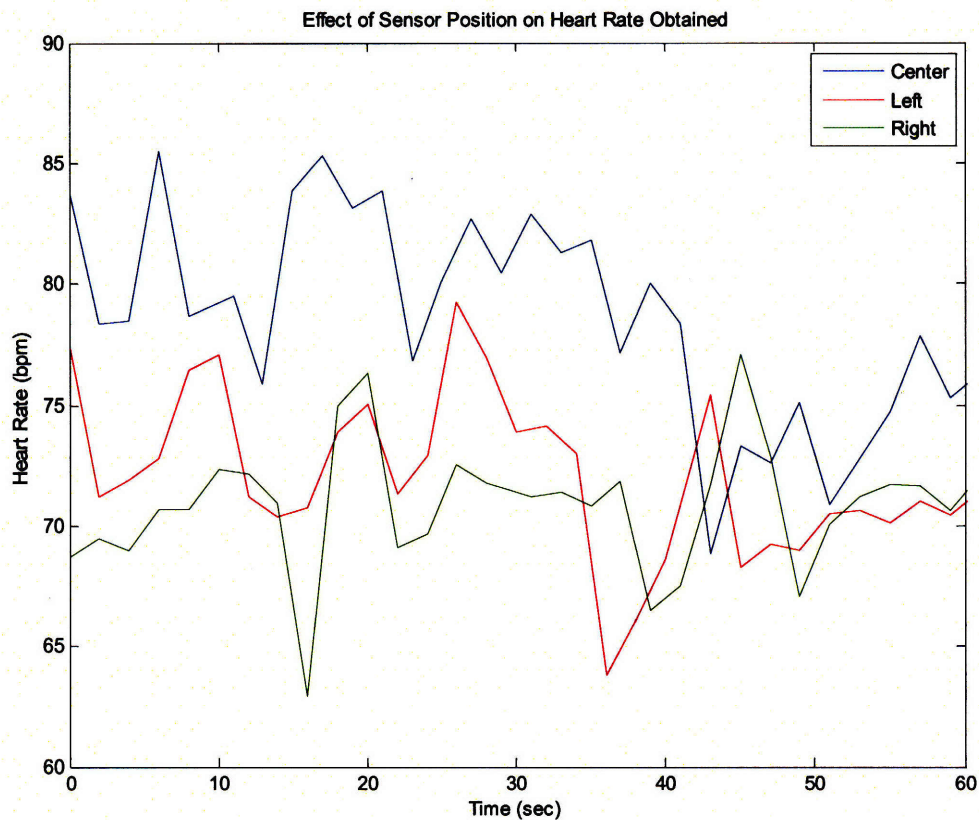
Figure 4-8: Effect of sensor position on the obtained heart rate value

59

suppose the gain of the sensor is set such that the peaks in the PPG signal barely pass the 1.5 V threshold that is used to calculate the number of beats per; and the sensor is moved such that the amplitude of the new heart rate signal obtained is lower, the number of peaks in the PPG signal that cross the threshold will decrease, which, in turn, results in a lower calculated heart rate value. To verify this concept, the sensor was used to obtain a participant's heart rate from three locations: center, slightly left of the center, and slightly right of the center of the dominant wrist.

As illustrated in Figure 4-8, the heart rate obtained when the sensor is placed on the arteries in the center of the wrist is indeed higher than that obtained when it is placed off center. It should be noted that a low data transmission rate of 0.5 Hz was used; as such the data obtained is not particularly smooth. The heart rate sensor's performance during daily activities was then tested. The protocol implemented is very similar to that used to evaluate the iCalm skin conductance sensor. N=12 subjects completed the following tasks:

1. Relaxing

2. Deep Breathing

3. Blowing up a balloon

4. Typing

5. Drinking a cup of water

6. Walking

7. Jumping Jacks

The three questions asked at the end of the analogous skin conductance experiment were removed from this experimental protocol since they no longer instigate an element of

surprise. Once again, since the FlexComp does not have wireless capabilities, the subject was followed around the testing area with a laptop and the sensor box during the walking and jumping jacks phase of the experiment protocol. The FlexComp sensor wires were also taped to the participant to minimize motion artifacts.
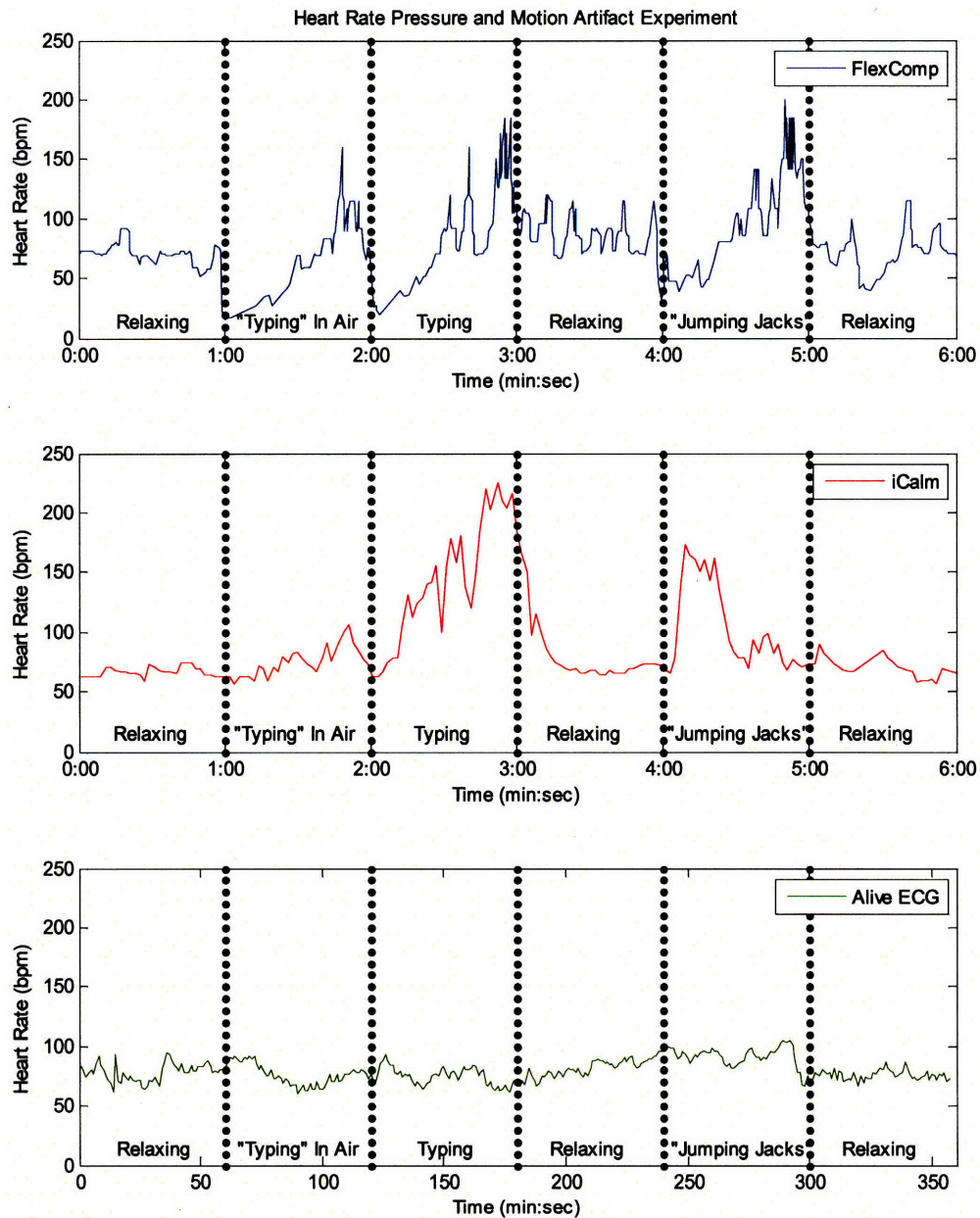
Figure 4-9: Heart rate data obtained from the pressure and motion artifact experiment
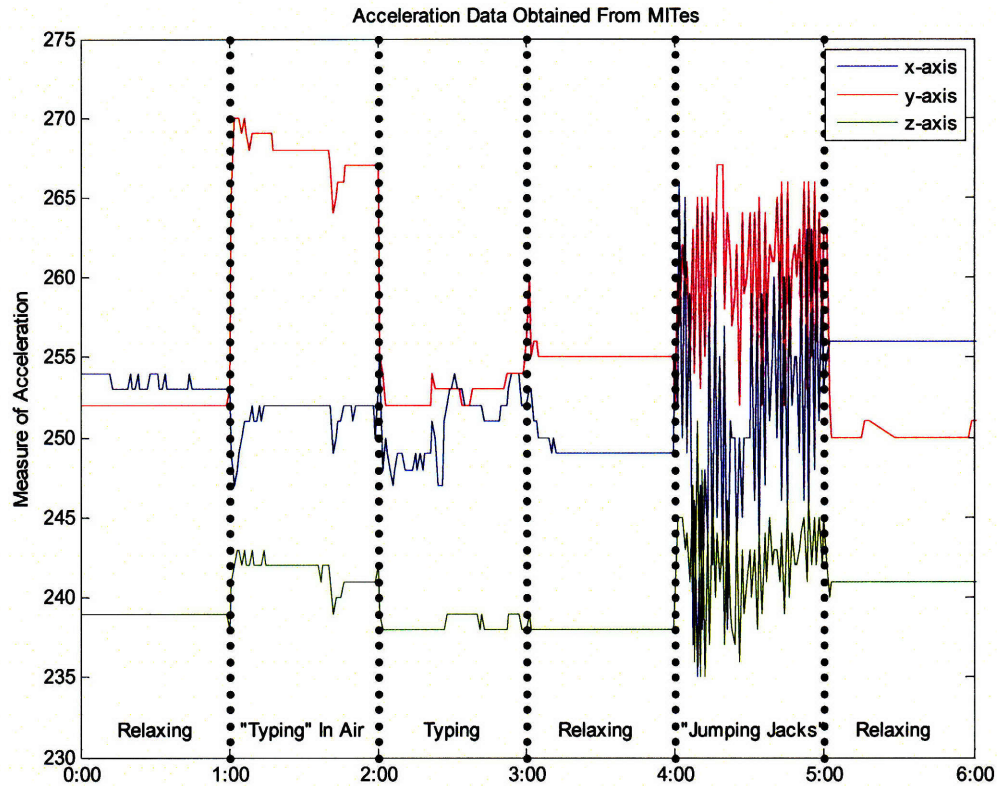
Figure 4-10: Acceleration data obtained from MITes during the pressure and motion artifact experiment for heart rate sensor

As evident by the data provided in the Appendix D, the heart rate signal obtained from both the FlexComp and iCalm is heavily affected by motion artifacts. To evaluate the extent of signal corruption, the experiment which analyzed the effects of pressure and motion artifacts on the skin conductance signal was repeated for the heart rate sensor; in this protocol, however, Alive Technologies' wireless ECG sensor was placed on the chest as a control. The remaining sensors were placed on the participant's dominant hand and the results are presented in Figures 4-9 and 4-10. In Figure 4-11, the data obtained from the Alive ECG sensor is overlaid with that obtained from the FlexComp and iCalm for an easier comparison with the control.
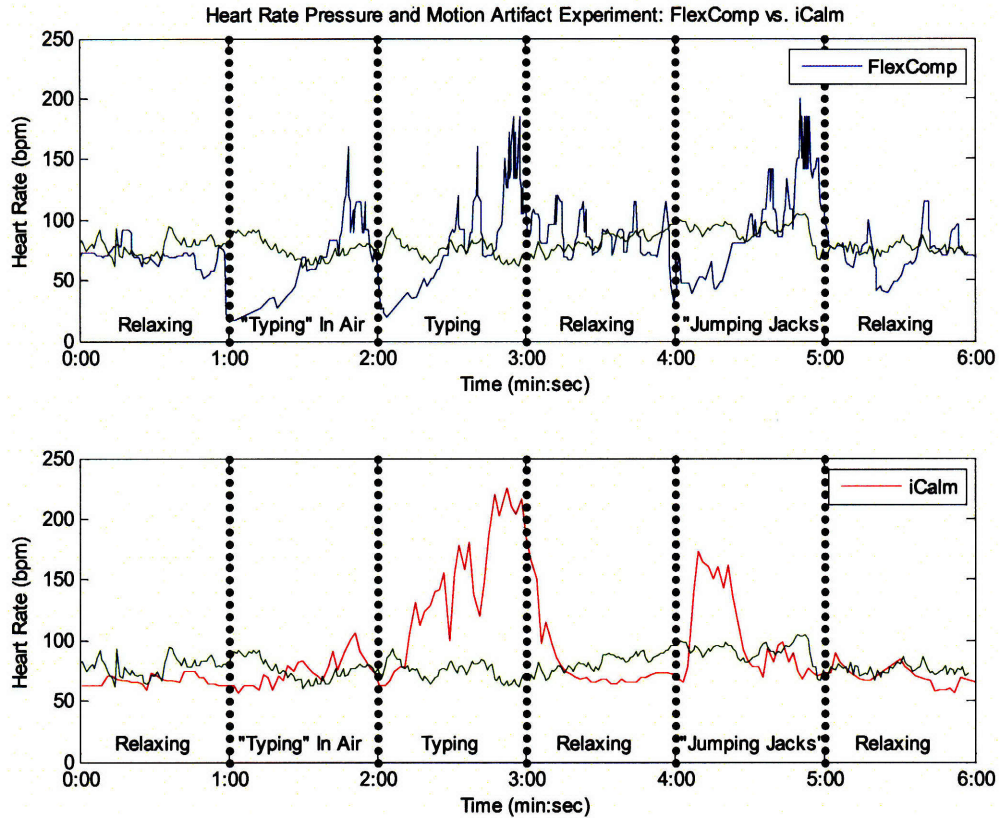
Figure 4-11: Results of the FlexComp vs. iCalm heart rate preesure and motion artifact experiment overlaid with that of the Alive ECG

Unfortunately, both signals are highly corrupted by pressure and motion artifacts. Further signal processing needs to occur before the data obtained is able to provide users with true heart rate data. It should be noted that even though motion artifacts can add noise to a PPG signal, even clean PPG signals vary from user to user. For instance, the morphology of the PPG waveform depends on factors such as the amount of pressure between the PPG sensor and the human skin [51, 52], vascular aging [53, 54] and vasoactive drugs [53], local cooling of body around the PPG sensor [55, 56], and the amount of exercise users partake in on a regular basis [57]. Nevertheless, the iCalm heart rate sensor seems to operate as well as the FlexComp while the sensor is not subjected to noise-causing artifacts. An experiment was conducted during which the participant was

asked to relax and browse through videos on youtube.com for five minutes; after 3:30 minutes, the experimenter surprised the unsuspecting participant.
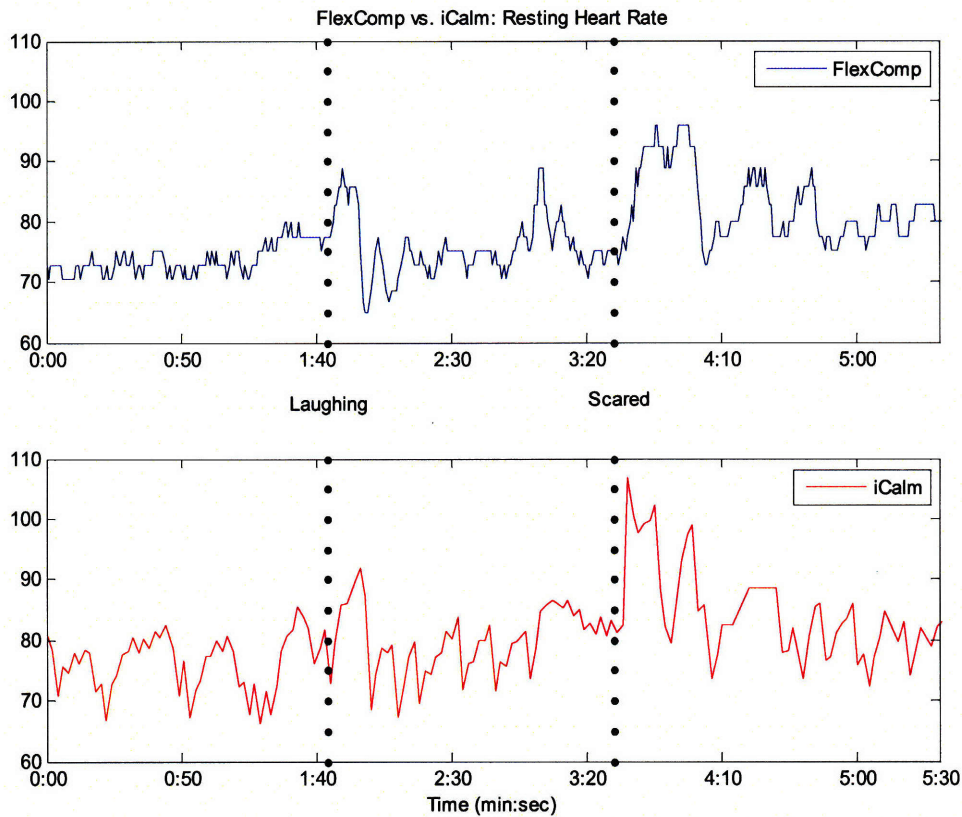
Figure 4-12: A comparison of resting heart rate values obtained with the FlexComp and the iCalm

As indicated in Figure 4-12, without the presence of motion and pressure artifacts, both sensors operate relatively similar. The iCalm heart rate values, however, seem to be more variable than the FlexComp. This discrepancy is reasonable considering that, in this experiment, iCalm had a sampling rate of 0.5 Hz, while the FlexComp's was much higher. The FlexComp input channel with a sampling rate of 2048 Hz was used; however, the software provided us with data sampled at 8 Hz.

Both systems work well under the same relatively motionless conditions. Each system, however, offers its own relative advantages. The FlexComp offers a high

sampling rate whereas the iCalm offers a comfortable form factor, cost efficiency, and

wireless capabilities.

Chapter 5

Sensor Applications

The comfortable, low-power, and wireless aspects of the iCalm module enable it to be easily utilized for a plethora of physiological monitoring applications: whether it be long-term, short-term, group, or single person monitoring. These applications range from autism to education pedagogy to weight loss.

5.1 Weight Loss and Physical Fitness

Similar to most of the aforementioned current consumer products on the market, the iCalm sensor module can be used to aid the obese in shedding extra pounds or those who are simply seeking to reach a certain level of physical fitness; the former scenario involves long-term physiological monitoring, whereas the latter involves short-term monitoring. Since current PPG heart rate sensors, including the iCalm, are sensitive to motion artifacts, they will not be useful for continuous monitoring. However, since

iCalm has a comfortable form factor, people can wear it while exercising simply to obtain a momentary heart rate value. In order to do so, they would have to hold their hand still for a few seconds before obtaining an accurate reading. For more long-term physiological monitoring, the iCalm could help people with chronic conditions, such as obesity, cardiovascular disease, and diabetes.

5.2 Self Stress Monitoring

Stress usually causes an increase in both heart rate and skin conductance. As such, iCalm can be utilized to help people control and decrease their stress levels. Similar to the physical fitness application, it can be coupled to an iPod and play soothing songs with a low tempo as means of relaxing the wearer. Users can also utilize a diary to maintain a daily record of significant events that occurred throughout the day and correlate those events with changes in their skin conductance and heart rate levels. After analyzing their data, users can identify events that trigger can increase in their stress levels. They can then learn to adapt to such events so that they can maintain their composure.

5.3 Video Games

As a fun application of the sensors, iCalm can also be coupled to video games. For instance, assume that a racing video game has been developed. The game initially measures the players' skin conductance levels for five minutes prior to the start of the game. Once the race starts, the player with a lower relative skin conductance level is able

to reach higher speeds and, in turn, have a greater chance of winning. The video game would help players to not only learn about their physiological signals, but also encourage them to maintain control over them despite the excitement of the game. As a result, players would learn to better maintain their composure even at times when they are not playing video games. This idea has already been implemented by Bersak et al.; they created Relax-To-Win, a competitive two player racing game that uses skin conductance to measure relaxation [58].

5.4 Product Feedback

Many companies are interested in users' honest feedback, particularly during the product's development phase. Although self-report measures can provide companies with some level of feedback, it is still a subjective method for obtaining data on user experience. Furthermore, if the user initially had a pleasant experience with the product but ended the trial with an unpleasant experience, they are more likely to be more dissatisfied with the product than someone who had the same feelings towards the product but in reverse order. Physiological signals, however, are an objective method of determining some aspects of users' feelings while experiencing a product. As such, companies will have a more complete comprehension of the overall user experience by coupling self-report measures with data obtained a platform, such as iCalm.

5.5 Drug and Smoking Cessation

A better comprehension of the environmental and behavioral triggers that cause addicts to relapse is certainly necessary. Psychosocial and pharmacological treatment for addiction can hardly be deemed as successful: an astonishing 70% of cocaine addicts who are treated resume heavy cocaine use within a year; similar rates prevail for other addictions. A combination of neurobiological, behavioral, individual, cultural, and environmental factors contribute to the occurrence of relapse. An improved understanding of the aforementioned factors requires the simultaneous measurement of co-occurring behavioral and biological variables that is continuous, unobtrusive, and objective. The iCalm sensor module should be coupled with a cell phone, and possibly also a global positioning system, and an event marker or electronic diary. It may then be able to detect physiologic changes associated with craving by using the sensors; learn about the social and environmental contexts that occur at the time of the physiologic change by using the event marker or electronic diary; deliver empathetic interventions in the form of text messages; and utilize machine learning to anticipate when users might be susceptible to another craving. This scenario is very similar to that described by Picard [59].

Furthermore, since iCalm will be coupled to a cell phone, it will be able to provide real-time interventions delivered to addicts at their moment of greatest need: when they are experiencing a craving. By approaching the situation through active intervention instead of passive observation iCalm can essentially be utilized to change the addict's ability to make better decisions when experiencing a craving. In addition to cocaine

addicts, iCalm can be utilized to deliver the same real-time intervention to those who are attempting to quit smoking and other drug use.

5.6 Autism Spectrum Disorder

Quite often in the classroom, a student with autism may appear calm on the outside, when they are actually feeling over stimulated on the inside. If the teacher is not aware of the student's true state, they may be caught by surprise if the student begins an outward rage or a self-injurious behavior, such as biting or hitting himself. Technology such as iCalm, however, would enable the student to communicate increases in inner arousal levels to the teacher before they escalate out of control. Since at a data transmission rate of 1 Hz, iCalm is capable of simultaneously supporting up to twenty sensors, teachers could have access to both each student's individual data as well as aggregated group data on the entire classroom. We suggest teachers should also wear the sensor for symmetry so that both students and teachers can learn about how their signals behave and reflect on which types of interactions change them. The idea is that by enabling physiological data to be communicated and associated with productive learning interactions, iCalm module essentially would enable teachers to maintain a classroom environment that allows autistic students to remain in a productive state for learning [60, 61].

5.7 Educational Pedagogy

Educational researchers are consistently looking for engaging pedagogy that will enable students to both remember and apply what they have learned. Similar to the product feedback scenario, testing and self-report measures can give insight into the effectiveness of teaching strategies. On the other hand, the iCalm platform, particularly the skin conductance sensor, would provide researchers with affective data relating to arousal, which correlates with memory and attention. This information could essentially change how teachers evaluate their pedagogy. Similar to the use of the platform described in the case of the autistic student, iCalm provides teachers with real-time insight into how engaging their pedagogy is and enables them to adapt appropriately. In addition, if the lesson is video taped, teachers or researchers could revisit the lesson and correlate high arousal points with moments in their teaching. This research is currently being pursued by Shaundra B. Daily, who is a Ph.D. candidate in our Affective Computing research group.

It is important to note that the purpose of iCalm is not to monitor a group of people as it is to enable them to learn, self-reflect, and communicate if they choose to do so. iCalm's wrist-worn form factor can be easily removed by users when they choose to not share their data with others. As such, the privacy of the participant is respected at all times.

Chapter 6

Conclusions and Future Work

6.1 Summary

In this thesis, we attempted to enable comfortable, long-term monitoring of the autonomic nervous system physiology and improve upon the current commercial sensors on the market by presenting the design and evaluation of iCalm, a novel, wrist-worn, low-power, low-cost, and wireless physiological sensor module. iCalm's unique wrist-worn form factor enables users to comfortably wear it for continuous, around-the-clock physiological monitoring. Since many people already wear wrist accessories, such as watches and bracelets, they do not need a long time to get accustomed to wearing iCalm; in other words, the sensor does not seem like a foreign object to most people. In fact, all of the participants in the experiments preferred the iCalm to the FDA-approved comparison sensors we tested. Its wireless capabilities enable users to monitor their physiological signals without hassling with tangling wires; physiological data is still

72

transmitted as long as they are in a 50 meter radius vicinity of a wireless receiver. Its power efficiency enables them to go through the day without having to deal with the annoyance of changing batteries more than once a day. It also enables both individual and group monitoring for participants who are willing to wear the sensor and share their data.

From a hardware aspect, the iCalm skin conductance sensor is ready for 24/7 wear; in particular, further experiments should be conducted to determine the effect of pressure and motion artifacts on the sensor. It would also be quite interesting to receive feedback from future users about the data they obtained to determine the general population's level of reactivity on the wrist. The iCalm heart rate sensor, on the hand, is sensitive to both pressure and motion artifacts. As such, further developments, which will be discussed in Section 6.2.2, need to be completed before it is ready for mass distribution.

6.2 Suggested Future Work

6.2.1 Hardware Improvements

A 3-axis accelerometer should be implemented in the next version of the iCalm. Since data transmission consumes the most amount of power, if there exists too much motion, such as when the user is running, iCalm could stop transmitting data as means of saving battery power. Data obtained from the accelerometer could also result in a better analysis of the two signals obtained from the other two sensors. In addition, other

methods for further increasing the power efficiency of the sensor and reducing its size should be explored.

The iCalm skin conductance and heart rate sensors are currently placed in two separate packages. Combining these two sensors into one compact package will prevent the user from wearing two separate sensors when measuring skin conductance and heart rate simultaneously. Undoubtedly, a more miniature version of the sensor will certainly lead to the design of more intriguing form factors. The placement of the sensor on other body parts, such as the ear—in the form of an earring—or the ankle, could be further investigated. It should be noted that as the sensor design becomes more aesthetically pleasing and comfortable, peoples' willingness to continuously wear it will also increase.

6.2.2 Software Improvements

It would be interesting to develop advanced filtering algorithms and apply them to the heart rate signal obtained via iCalm in order to remove motion and pressure artifacts. One suggestion would be to use two or three diodes instead of the one used in the design of iCalm and utilize the obtained signals to determine the noise contribution. A blind source separation algorithm, such as independent component analysis, could be implemented to separate the heart rate signal from noise.

In addition, the development of an electronic diary, in which the user could mark major events throughout the day, would be a practical tool for understanding the causes of data fluctuation. Users could then analyze their physiological signals and correlate

them to the information provided in the diary. Such self-reflection is a major component of many of the aforementioned sensor applications.

6.2.3 Wireless Improvements

From a wireless viewpoint, many improvements could be implemented in the system's design. As evident in many of the obtained experimental data, quite often, the sensor would briefly stop transmitting data to the wireless receiver. The pause in transmission is most apparent in Figures C-15, C-16, C-19 and C-20, during which the sensor stops transmitting data for 106 and 85 seconds, respectively. After some investigation, this pause in data was caused by the receiver locking up periodically due to wireless noise in the environment that was interpreted by the microcontroller as a valid command packet. TagSense is currently fixing the radio receiver buffer firmware in order to prevent ambient noise from causing this behavior.

Increasing the transmission distance would enable the user to wander further away from the receiver without losing data. On the other hand, since most people carry a cell phone with them at most times, iCalm could send data to a cell phone instead of a laptop. In this situation, increasing the range of wireless receiver would not be as much of a concern and could save battery life. It would also be interesting to create a hub of wireless receivers, such as those currently available through TagSense Inc., in an area in which the user spends a lot of time, such as the work place building, so that the user would always be in the range of a receiver as long as they are in that area.

6.2.4 Application Explorations

As previously discussed, not everyone generates a notable change in skin conductance on his or her wrist while performing daily activities. It would be interesting to obtain further information about the experiment participants to ensure that they are not consuming any medication that would interfere with their sympathetic nervous system or their eccrine sweat glands. Furthermore, the reactivity on the wrist could be correlated with the personalities of the participants. For instance, do introverted people exhibit higher skin conductance reactivity?

Some experiments have been conducted with the iCalm during which the user wore the sensors while sleeping. Throughout the night, the user's skin conductance had several peaks. If the iCalm is coupled to an EEG, it could be determined whether or not these peaks correspond to rapid eye movement (REM) sleep or other sleep stages. If so, the iCalm sensors could be implemented as part of an alarm clock that wakes people up at a time when they are less likely to be groggy and more likely to feel refreshed. Thus, the alarm clock could be used to increase users' energy levels and boost their mood throughout the day.

Appendix A: Circuit Schematics
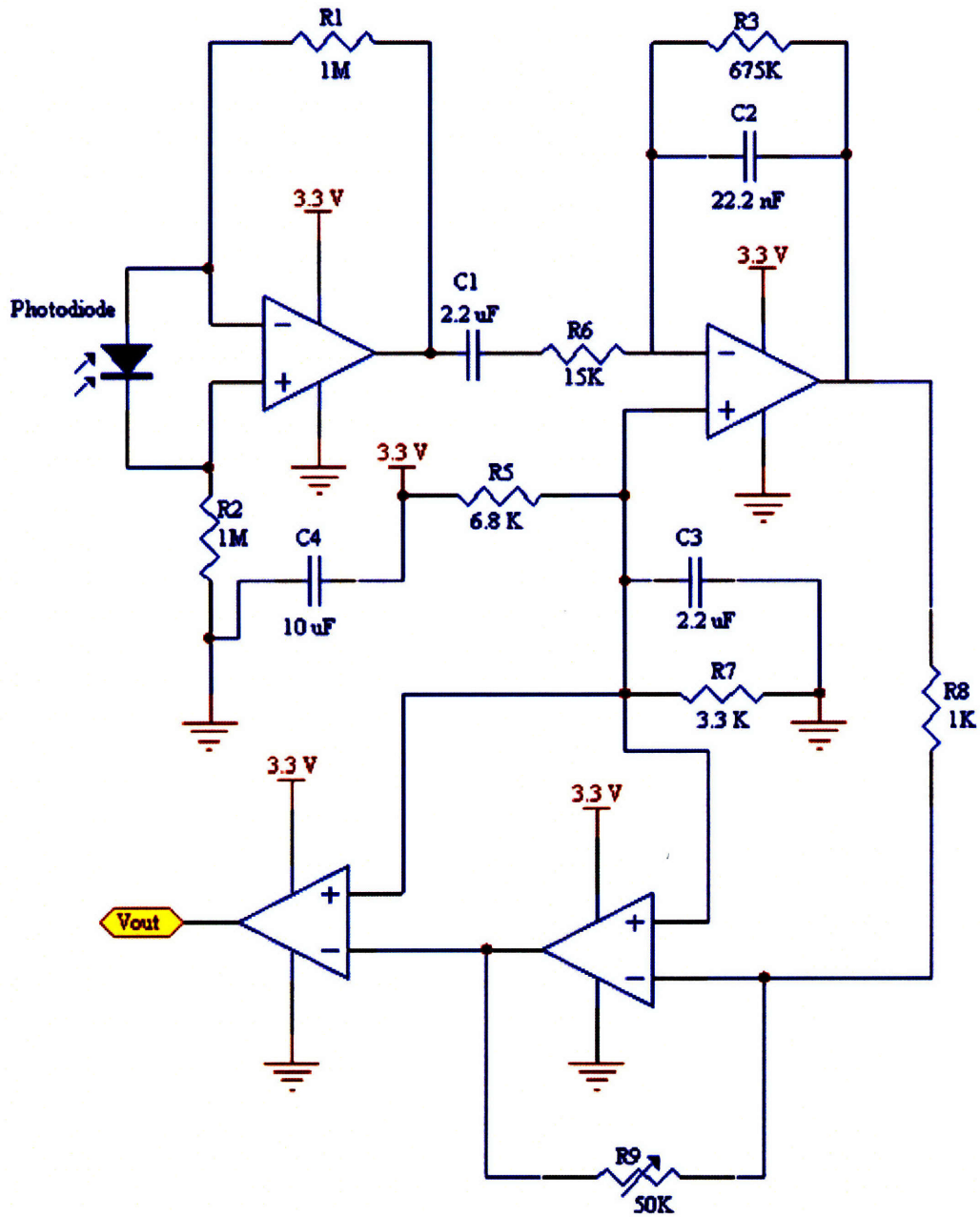
Figure A-1: Heart rate sensor schematic. All resistor values are in units of Ohms.
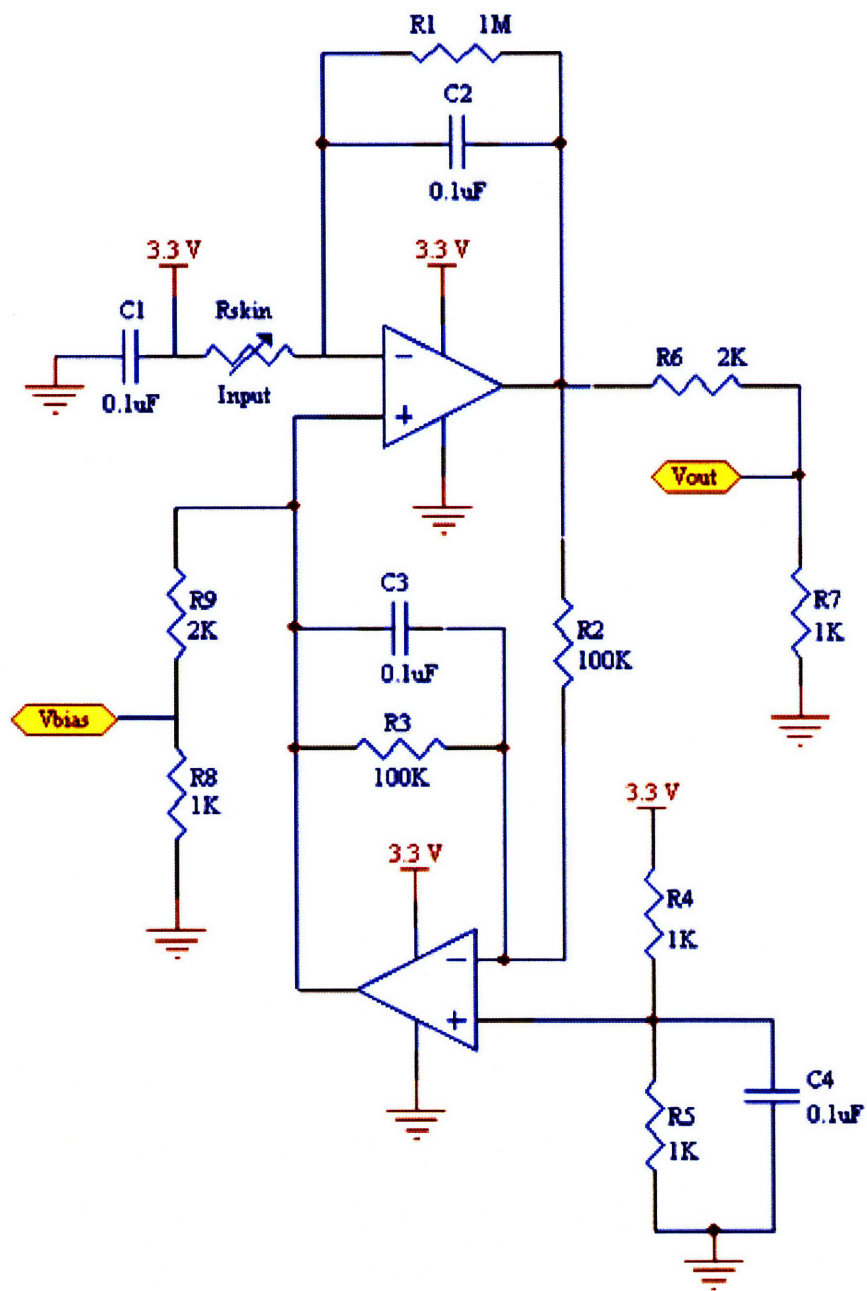
Figure A-2: Skin conductance sensor schematic. All resistor values are in units of Ohms.

Appendix B: Air Horn Experiment

B.1 Participant #1
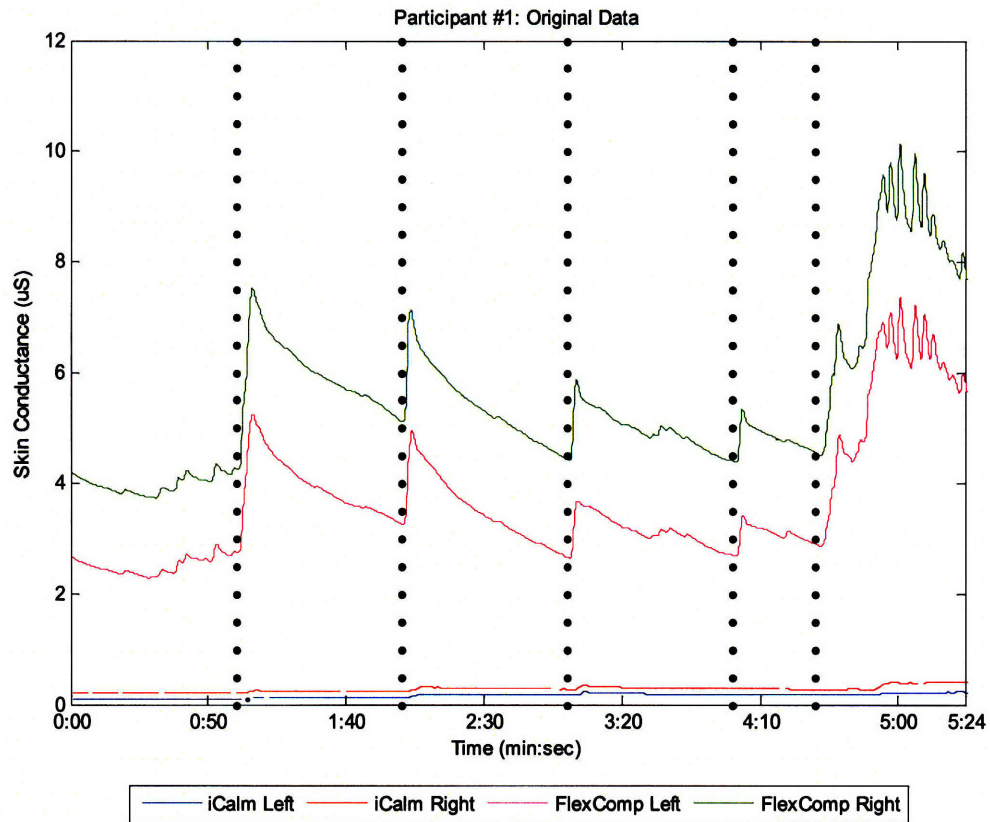
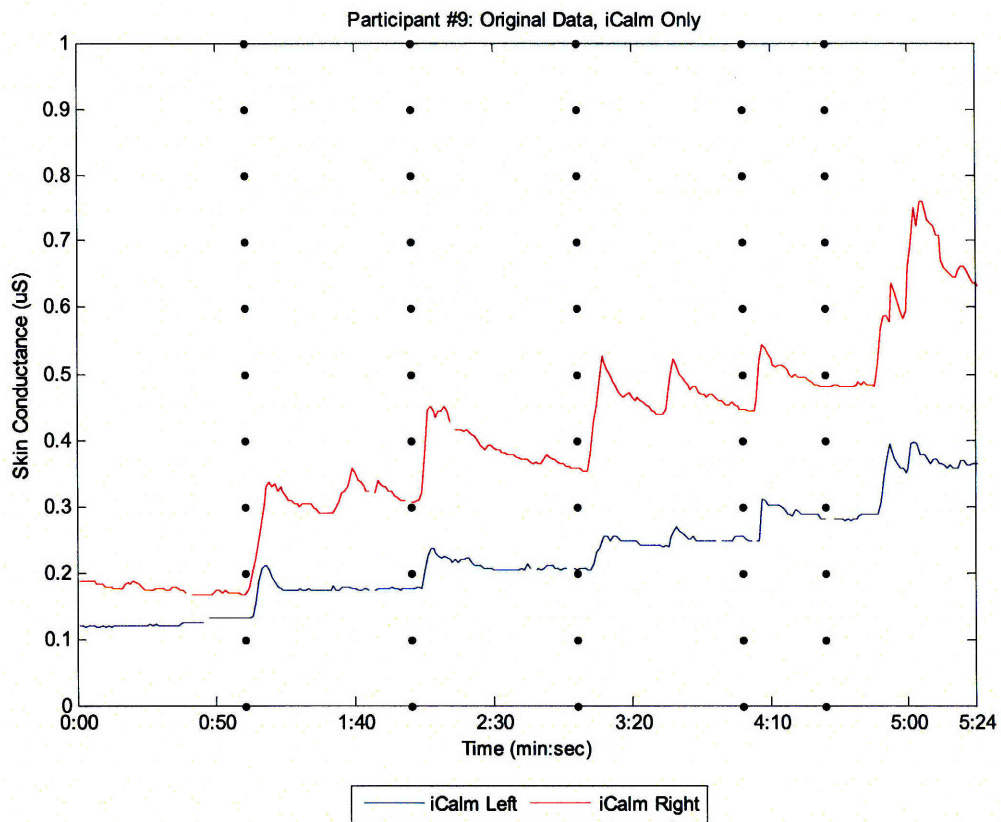Figure B-1: Participant #1's original skin conductance data
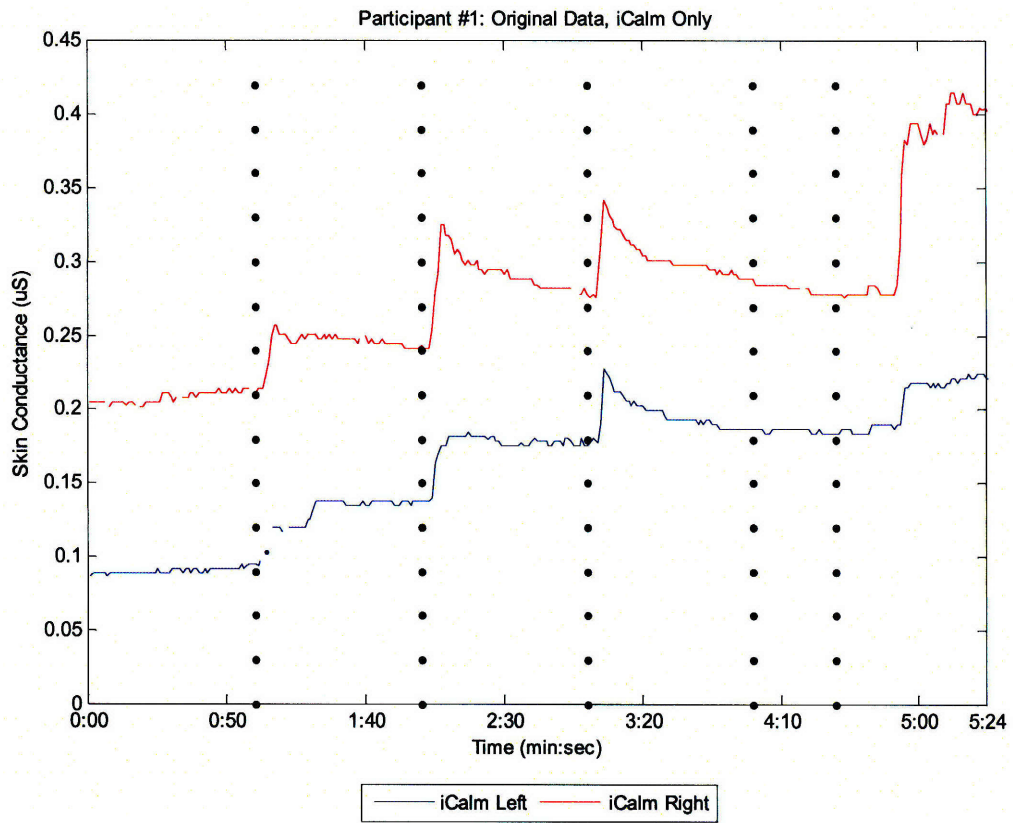
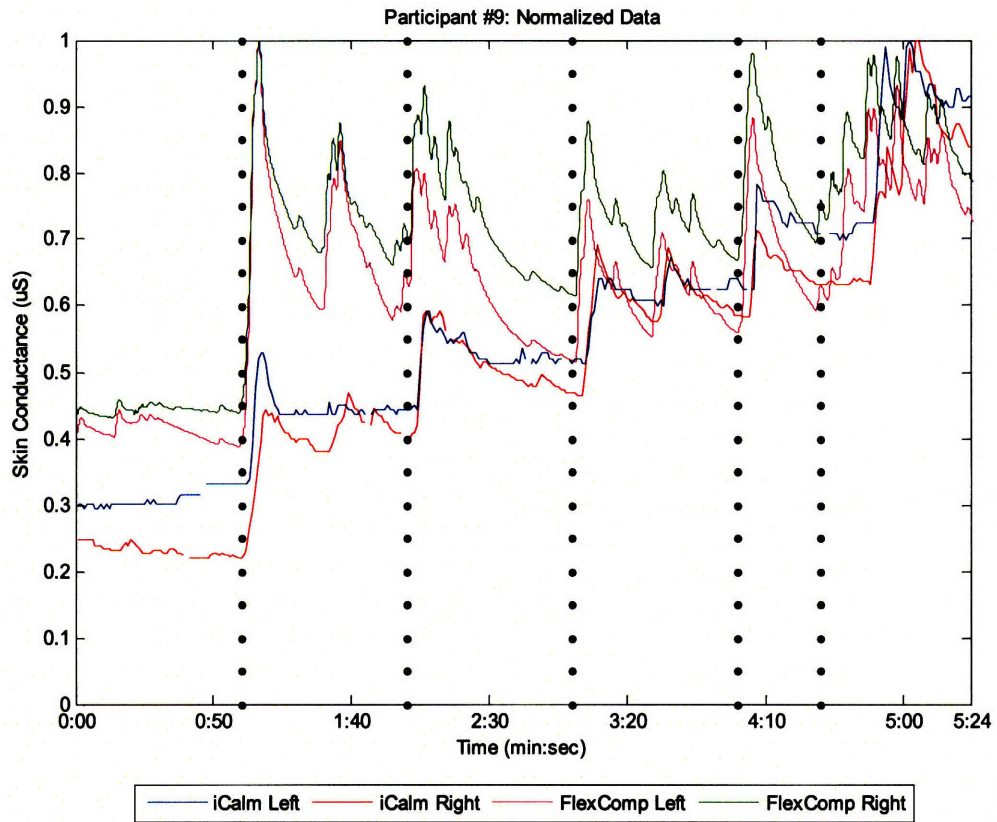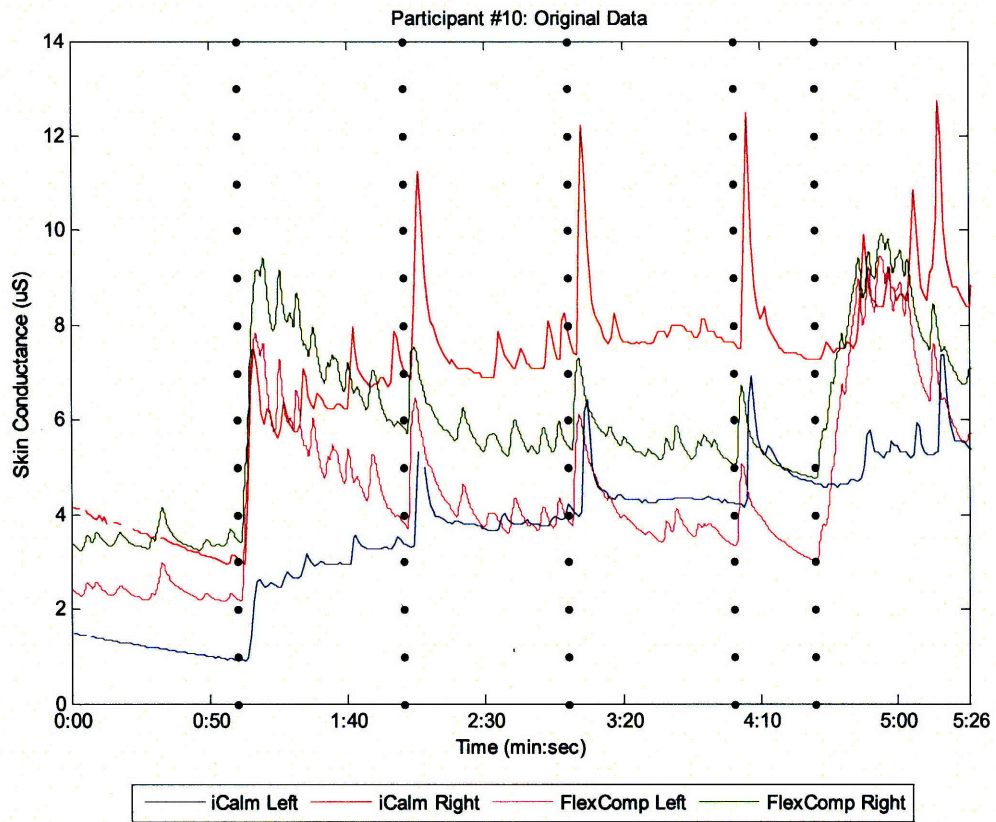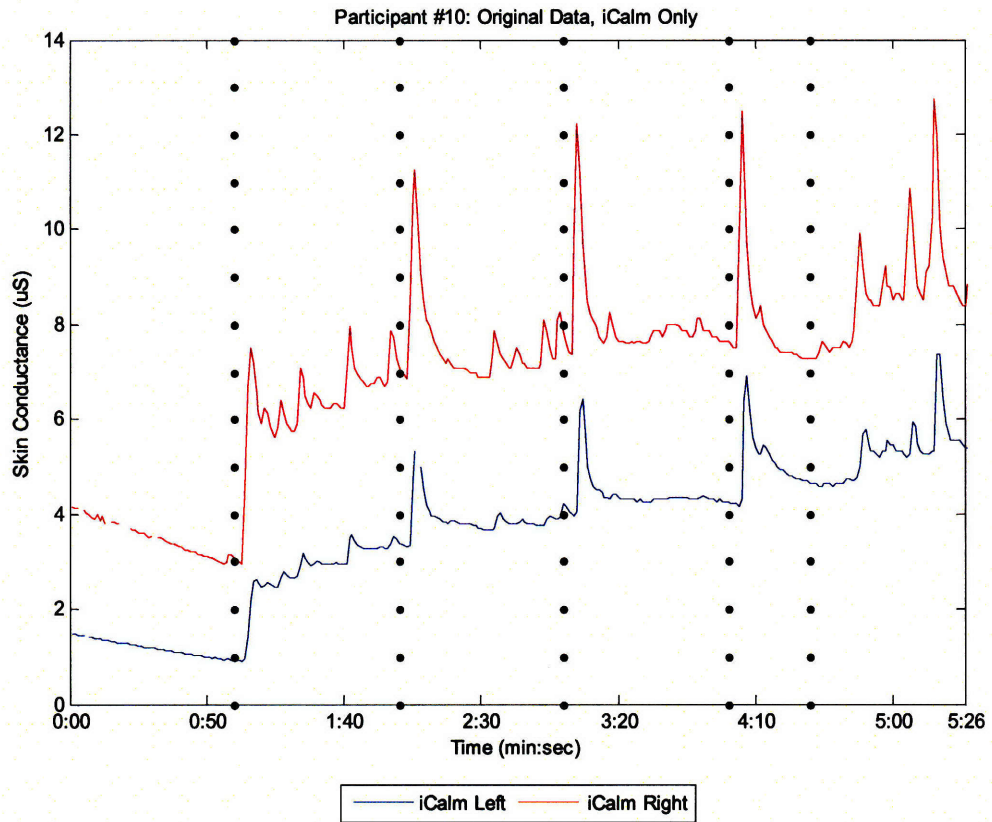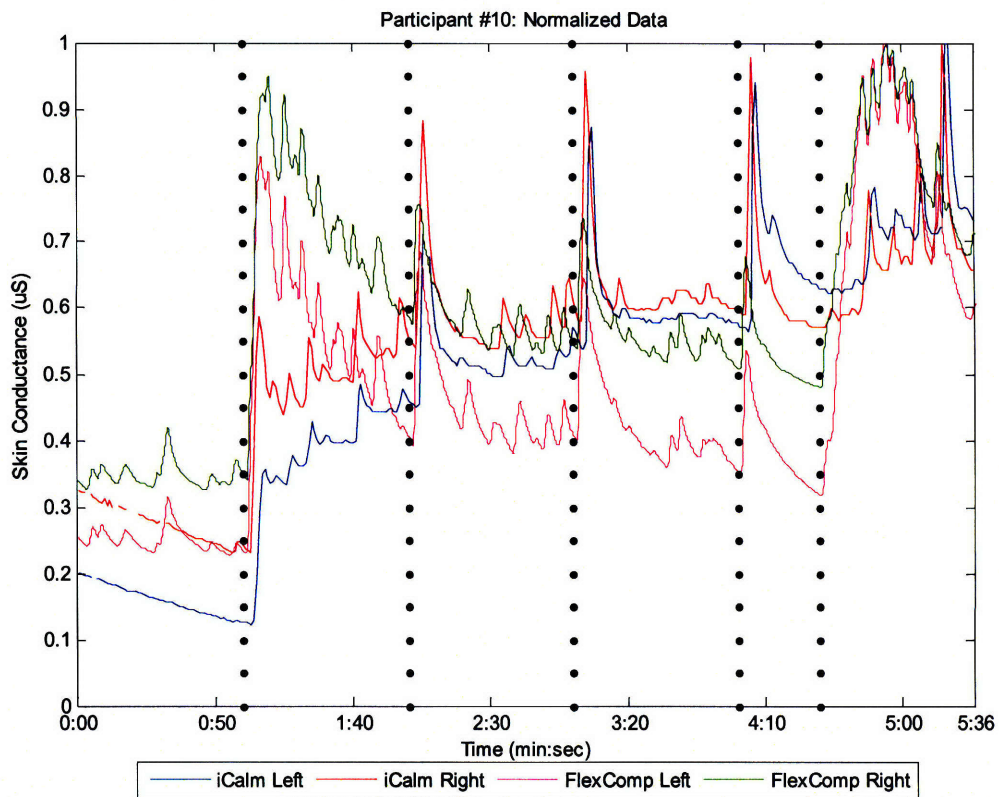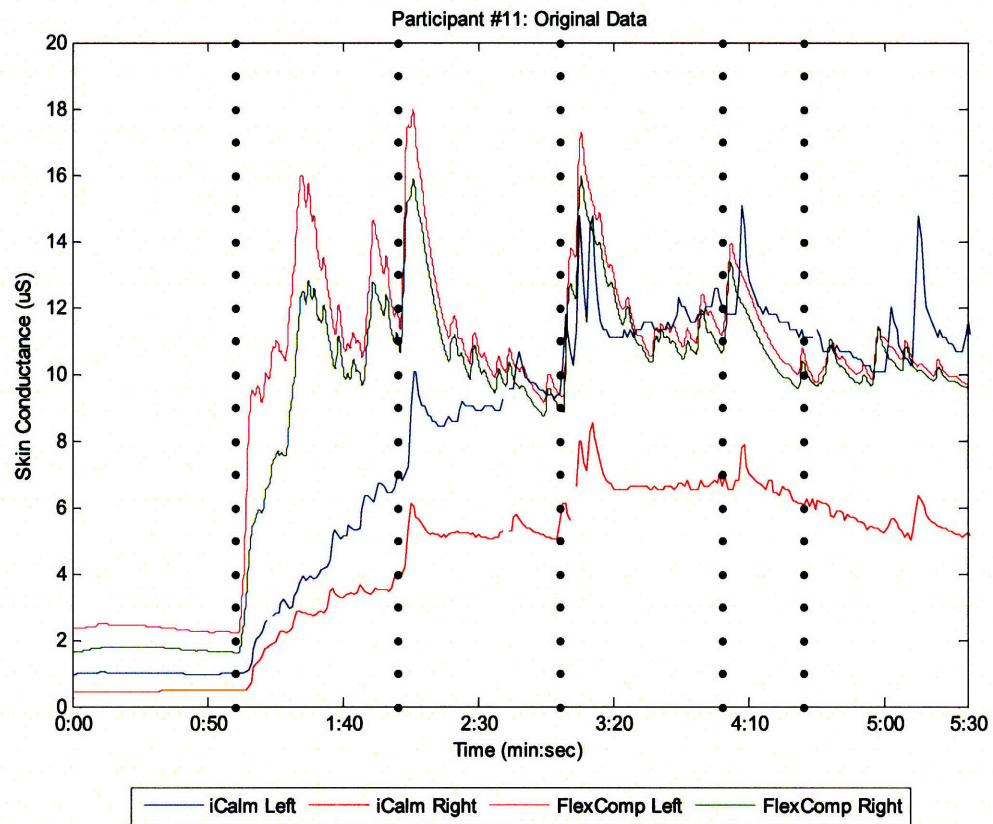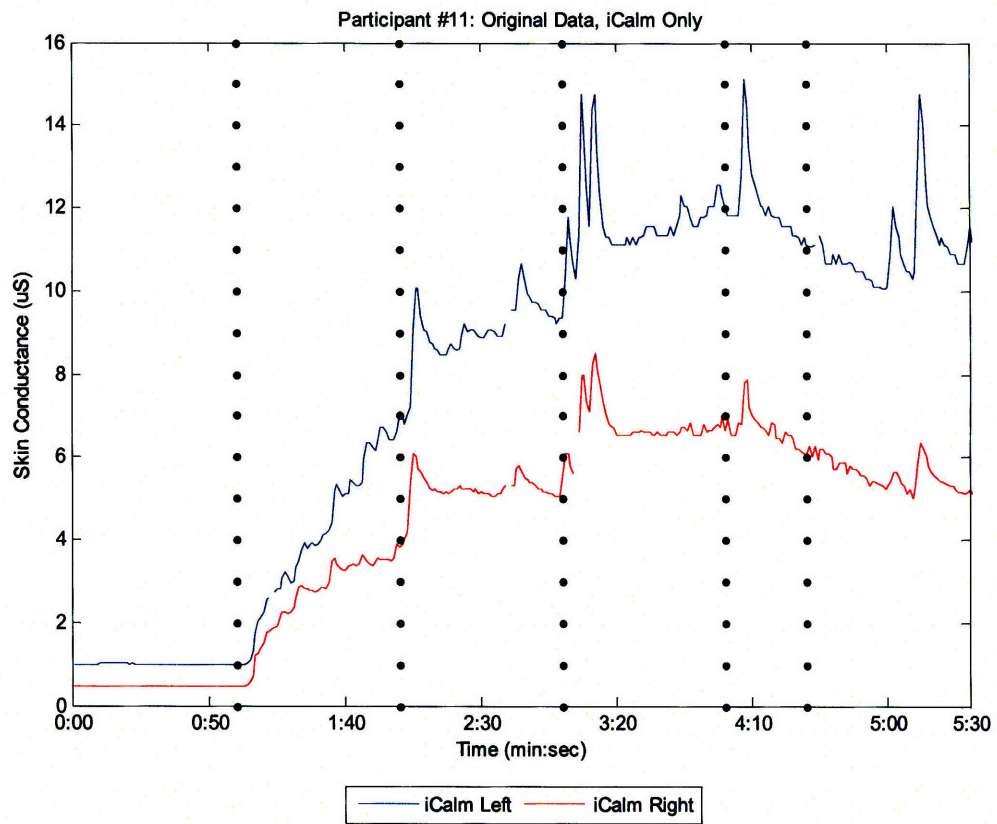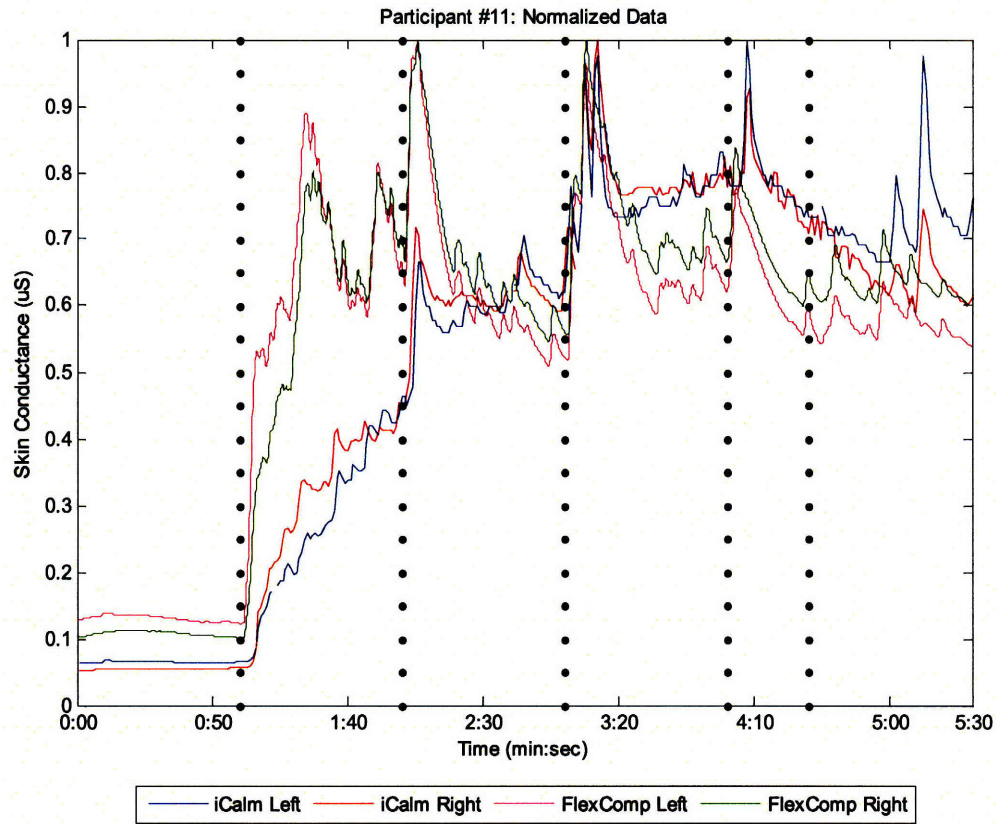Figure B-2: Participant #1's original skin conductance data obtained with iCalm
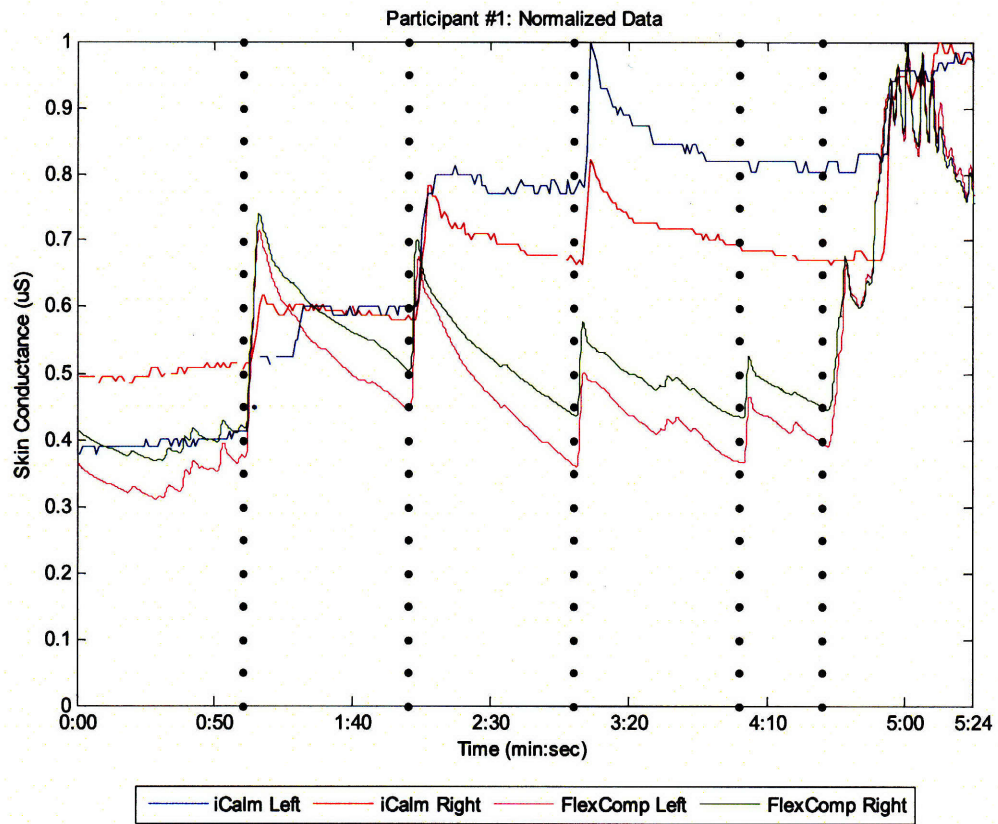
Figure B-3: Participant #1's normalized skin conductance data

B.2 Participant #2
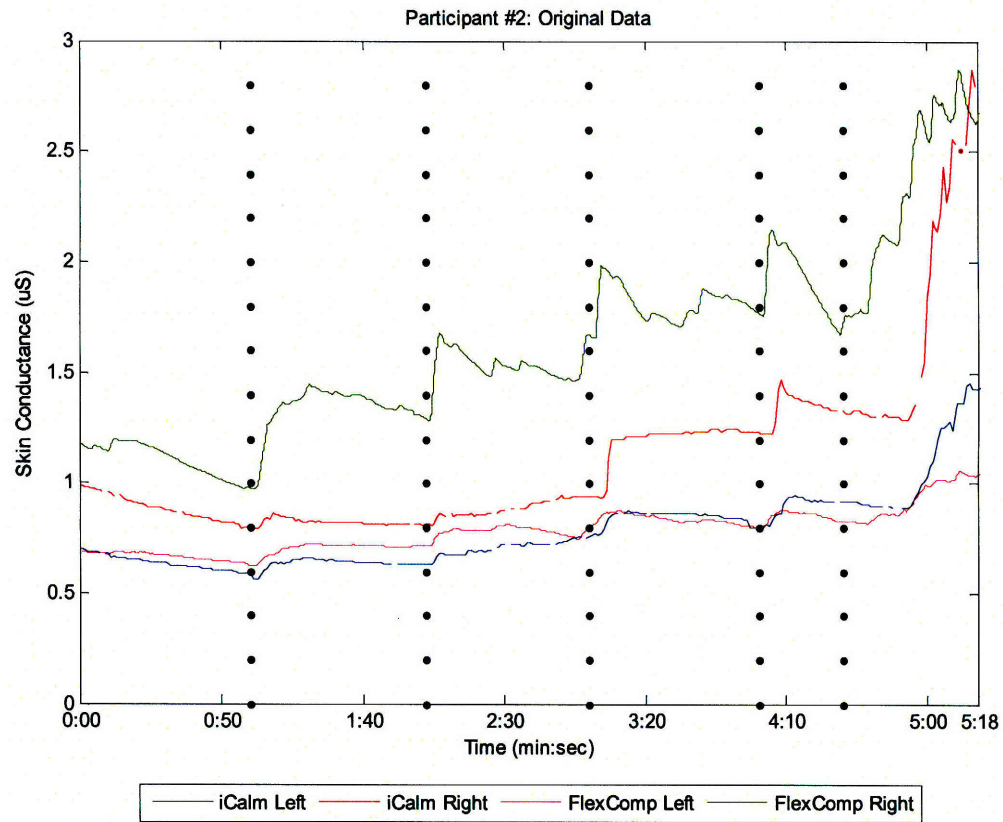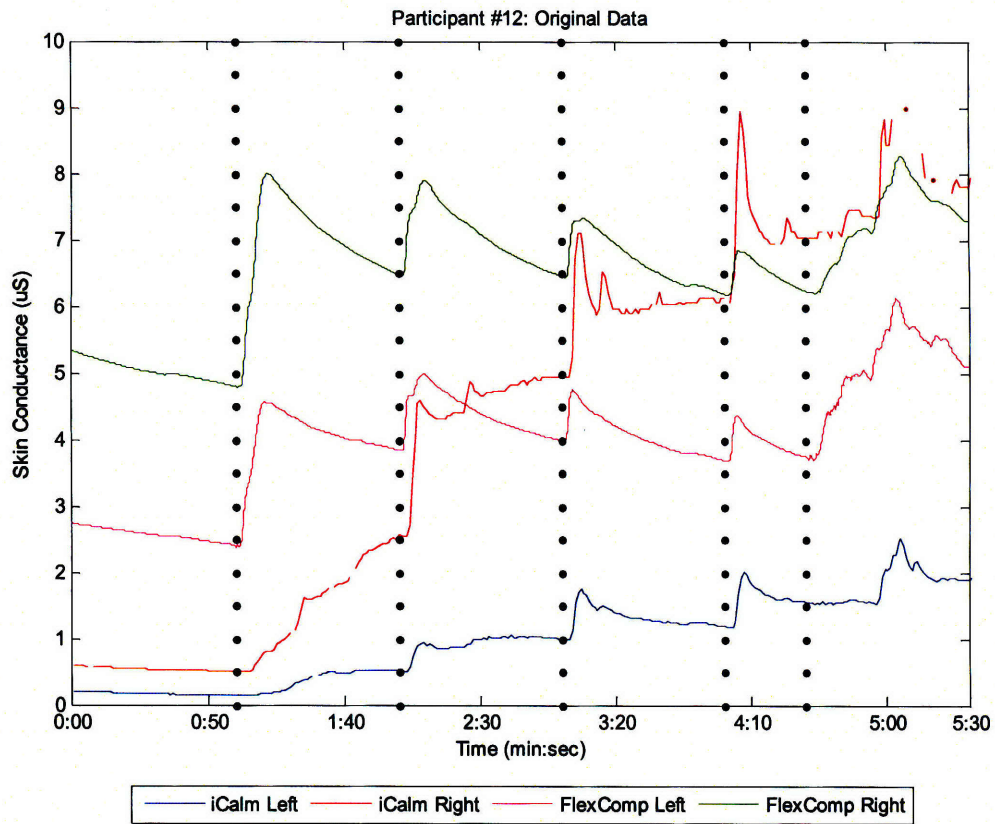

Figure B-4: Participant #2's original skin conductance data
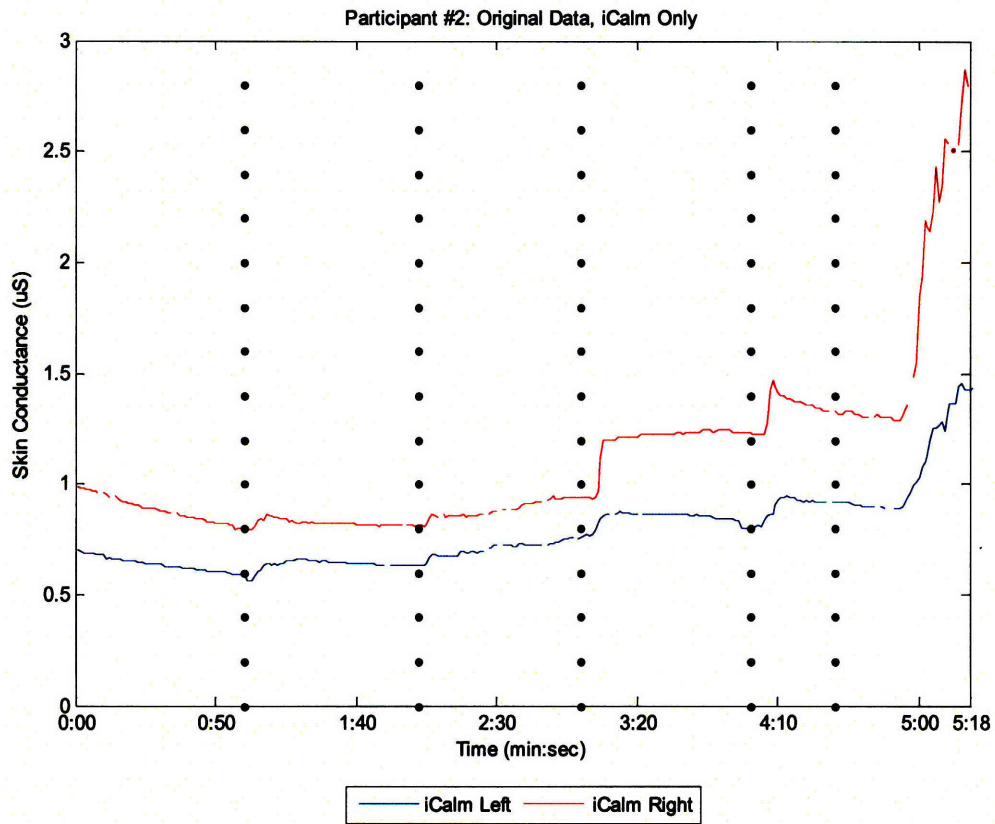
Figure B-5: Participant #2's original skin conductance data obtained with iCalm
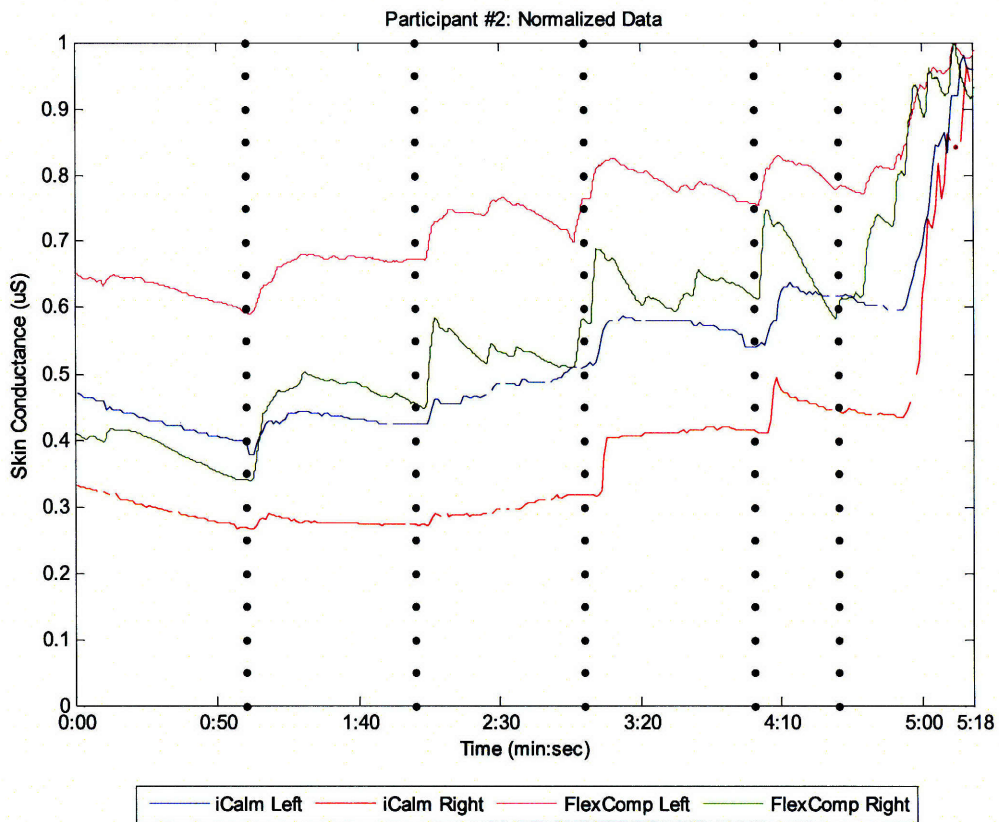
Figure B-6: Participant #2's normalized skin conductance data

B.3 Participant #3
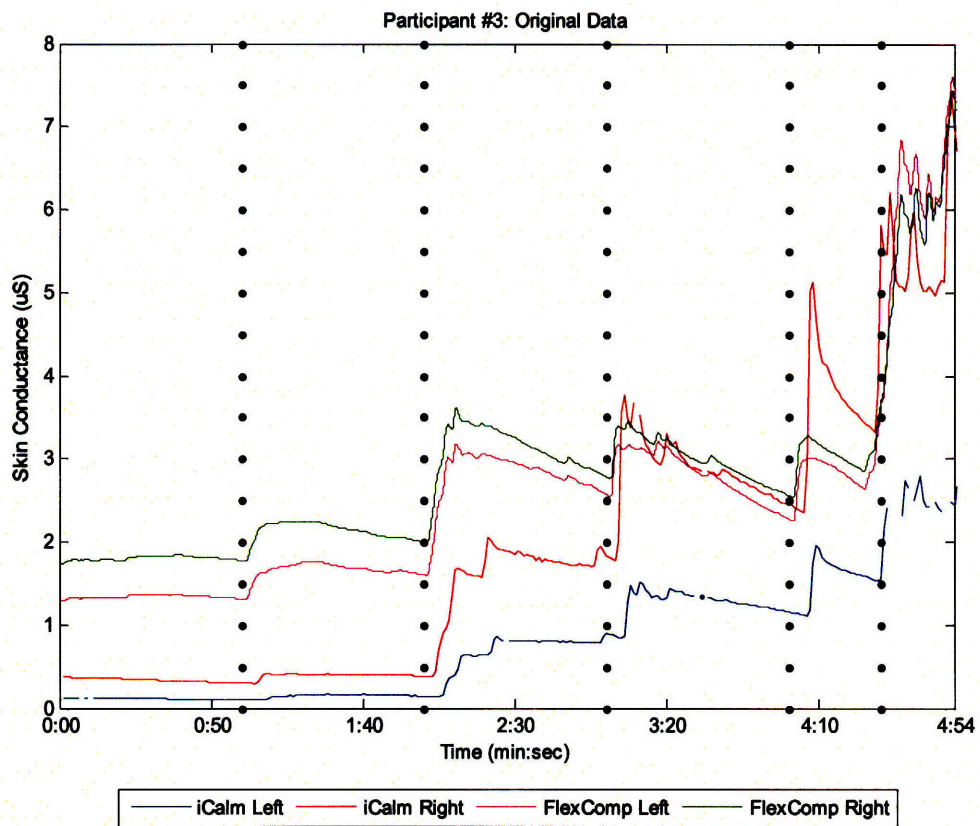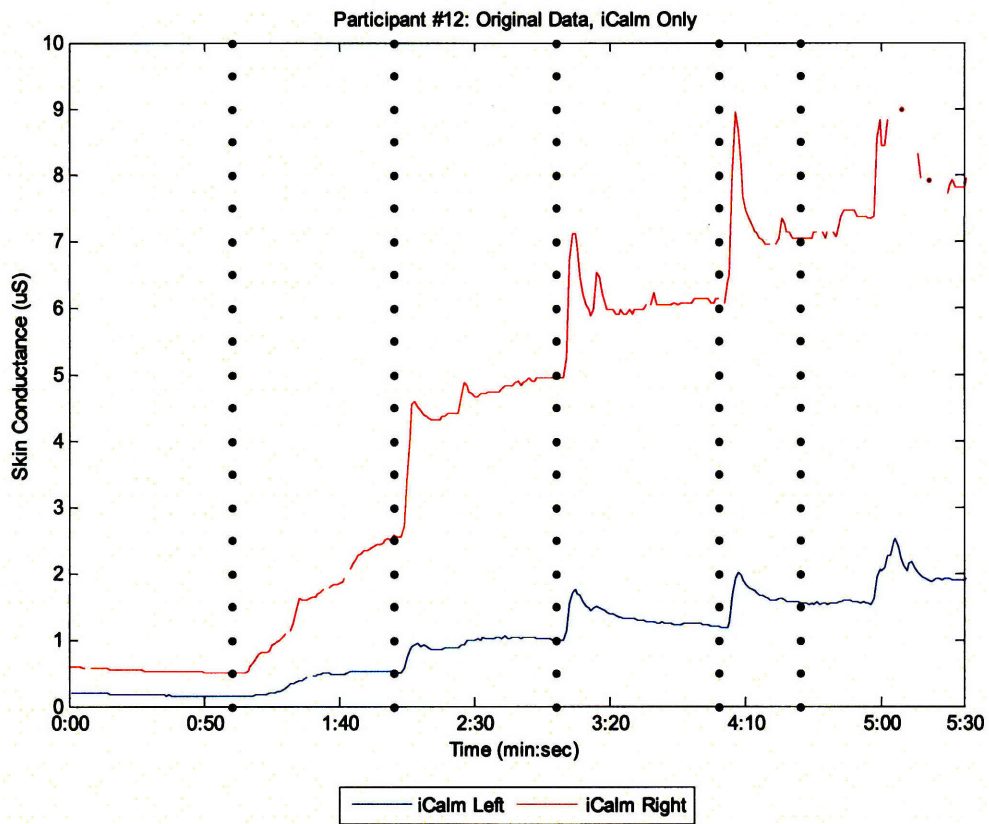

Figure B-7: Participant #3's original skin conductance data
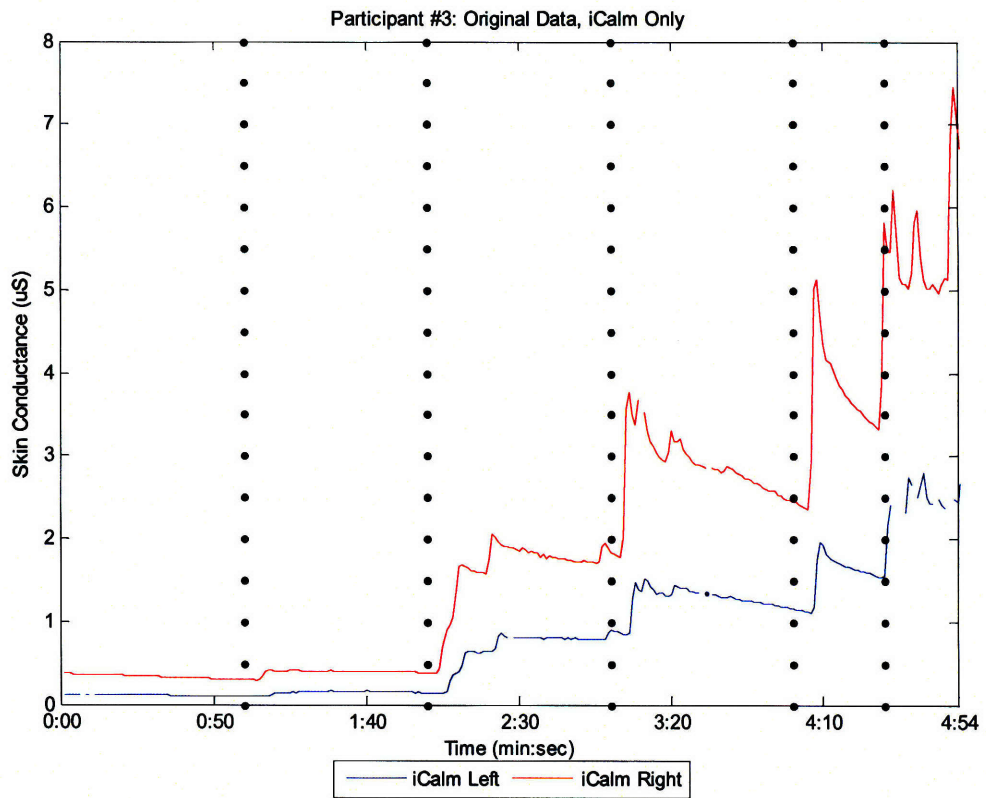
Figure B-8: Participant #3's original skin conductance data obtained with iCalm
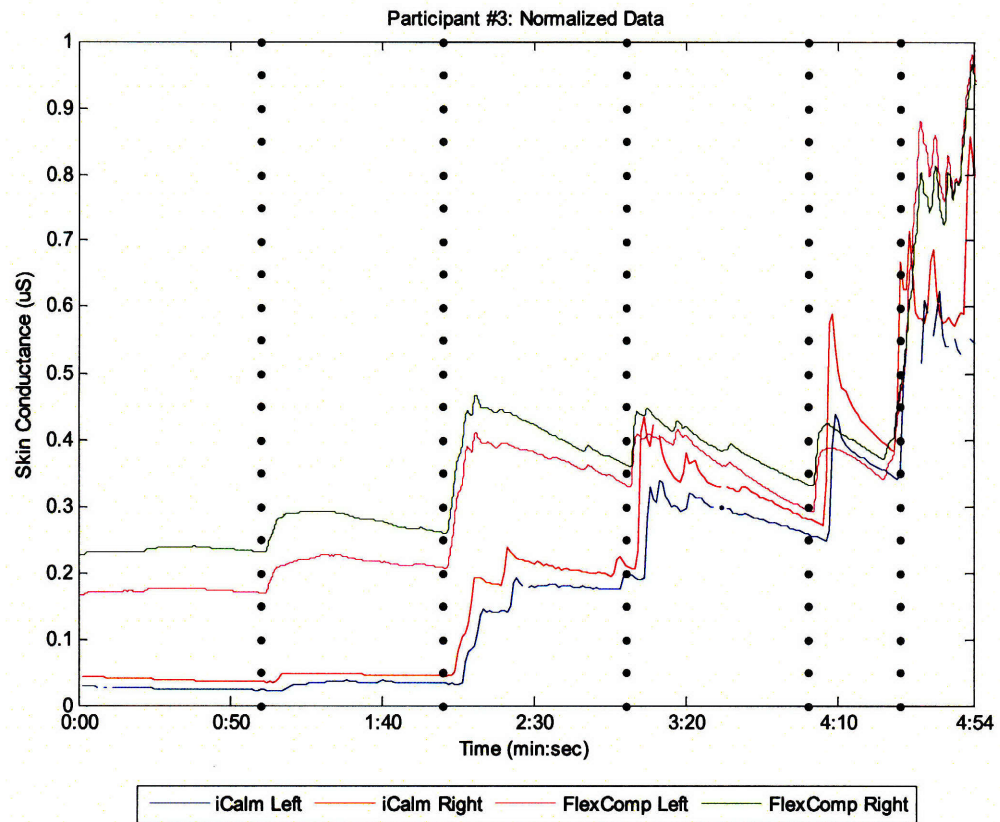
Figure B-9: Participant #3's normalized skin conductance data

B.4 Participant #4
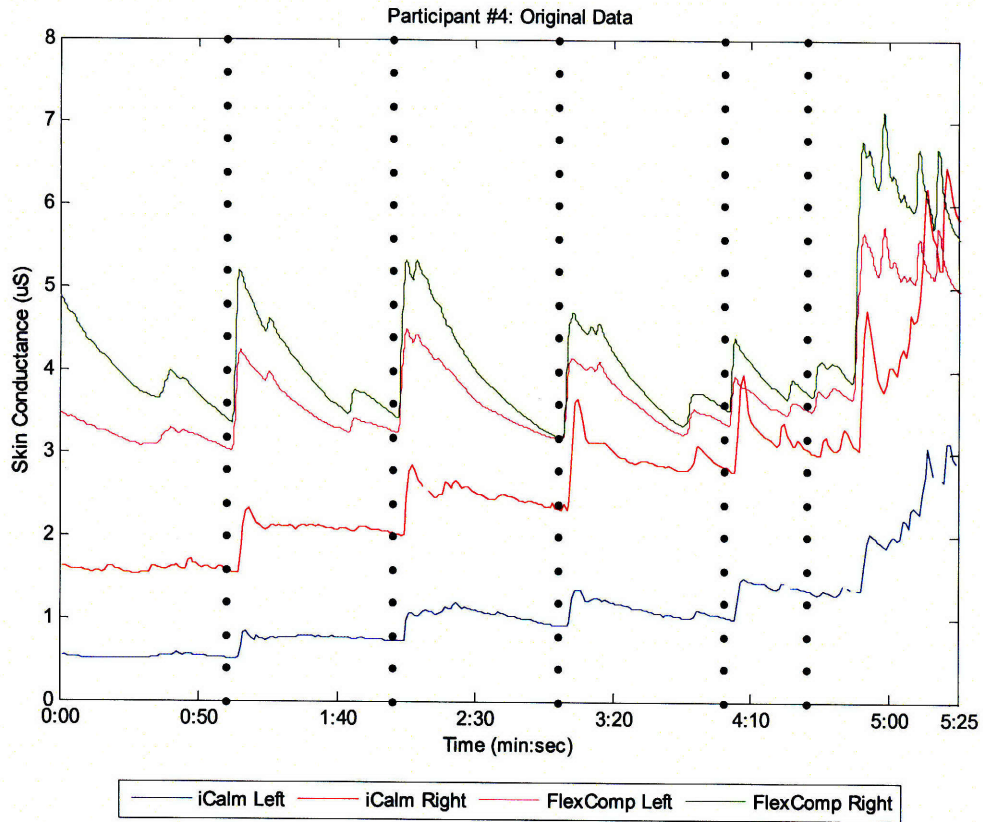
Figure B-10: Participant #4's original skin conductance data
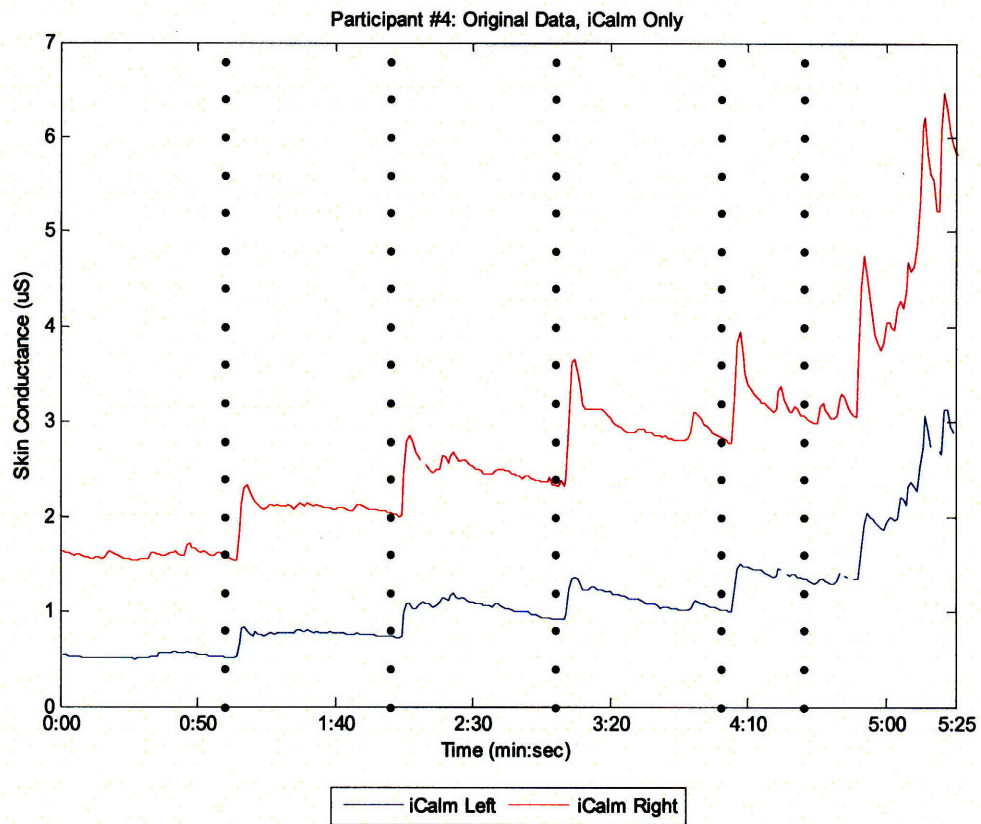
Figure B-11: Participant #4's original skin conductance data obtained with iCalm
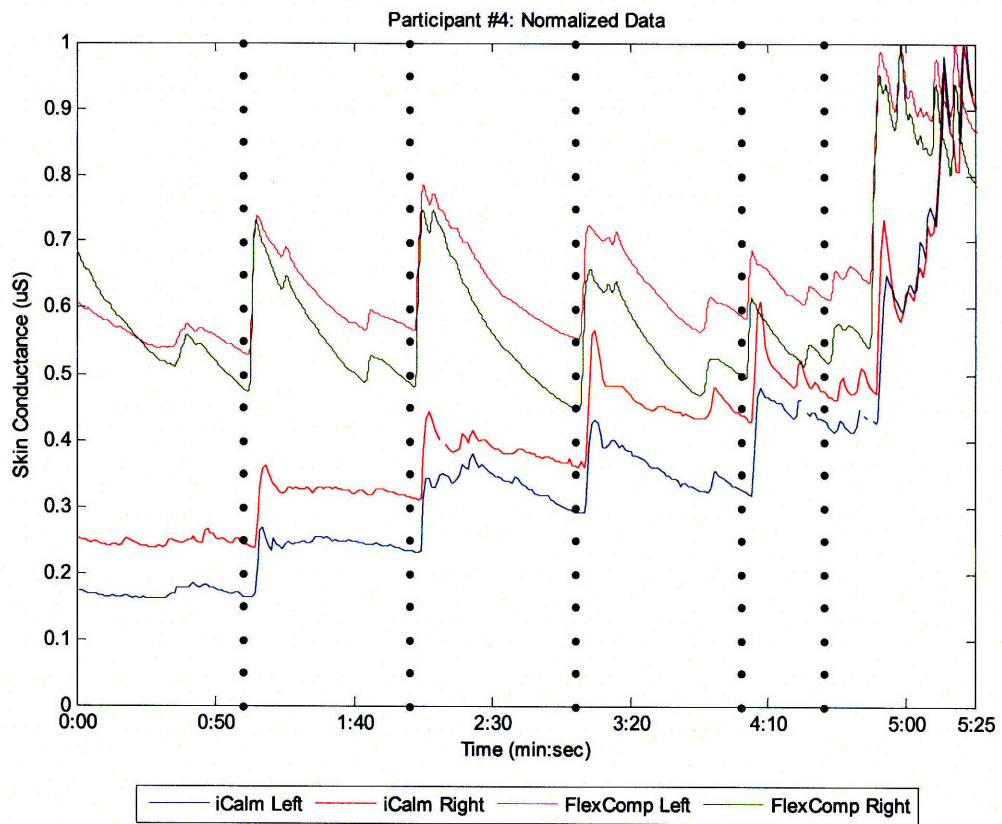
Figure B-12: Participant #4's normalized skin conductance data

B.5 Participant #5
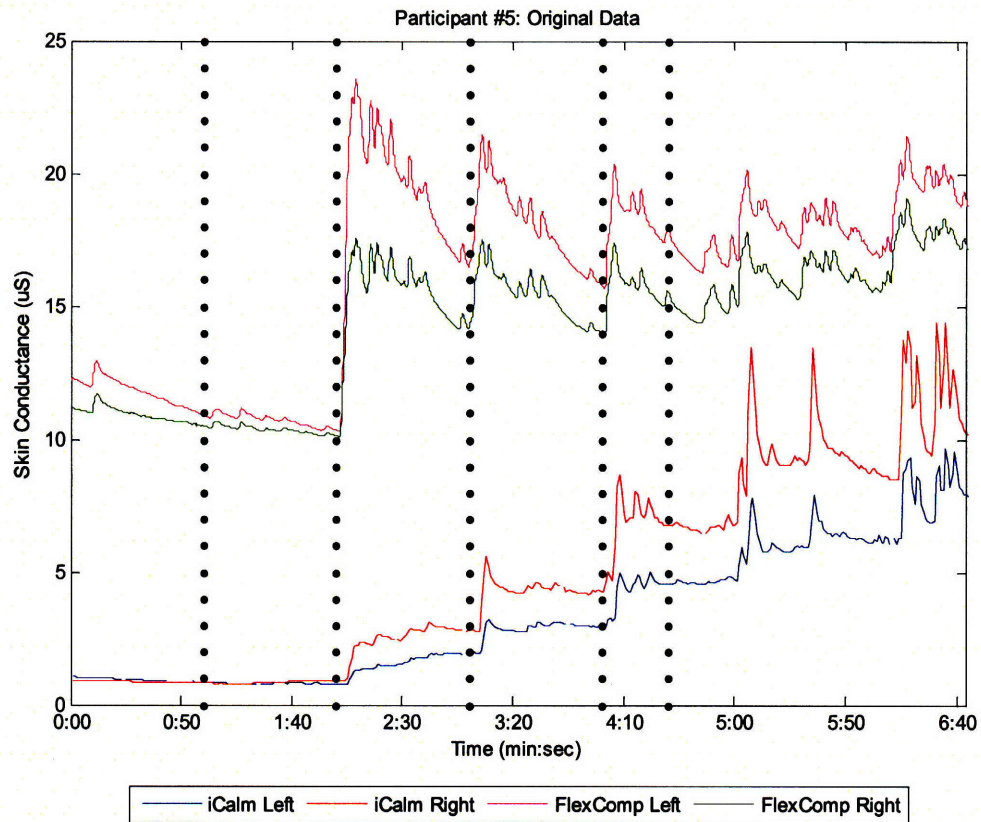
Figure B-13: Participant #5's original skin conductance data
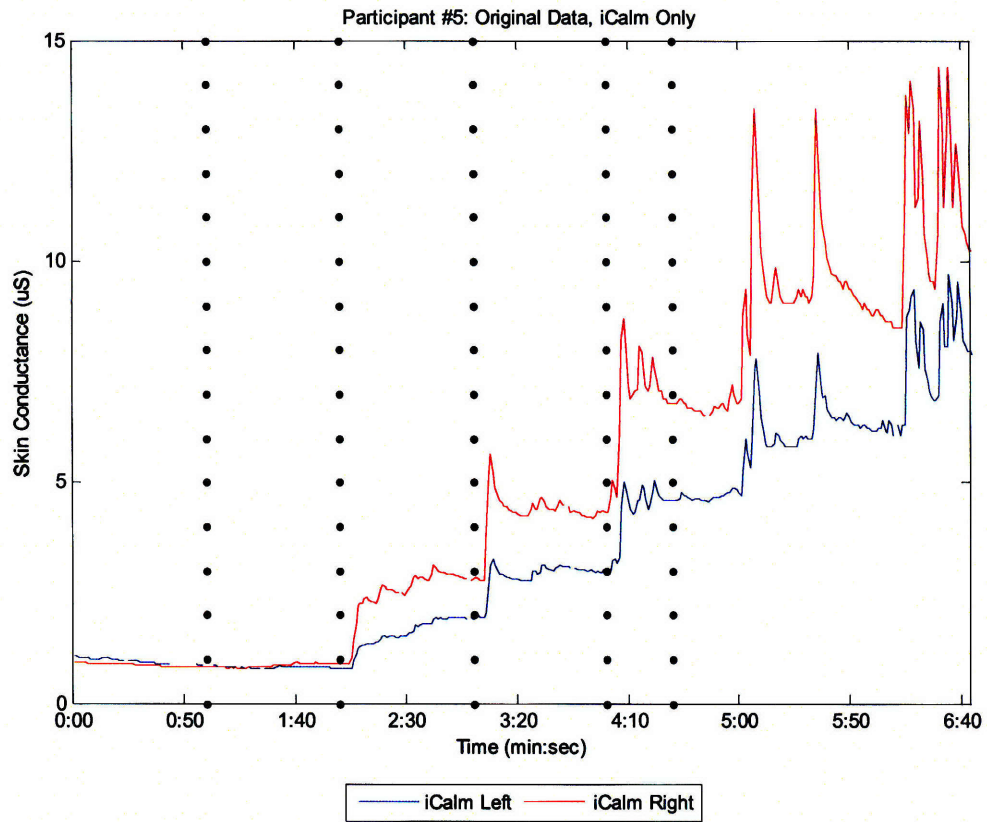
Figure B-14: Participant #5's original skin conductance data obtained with iCalm
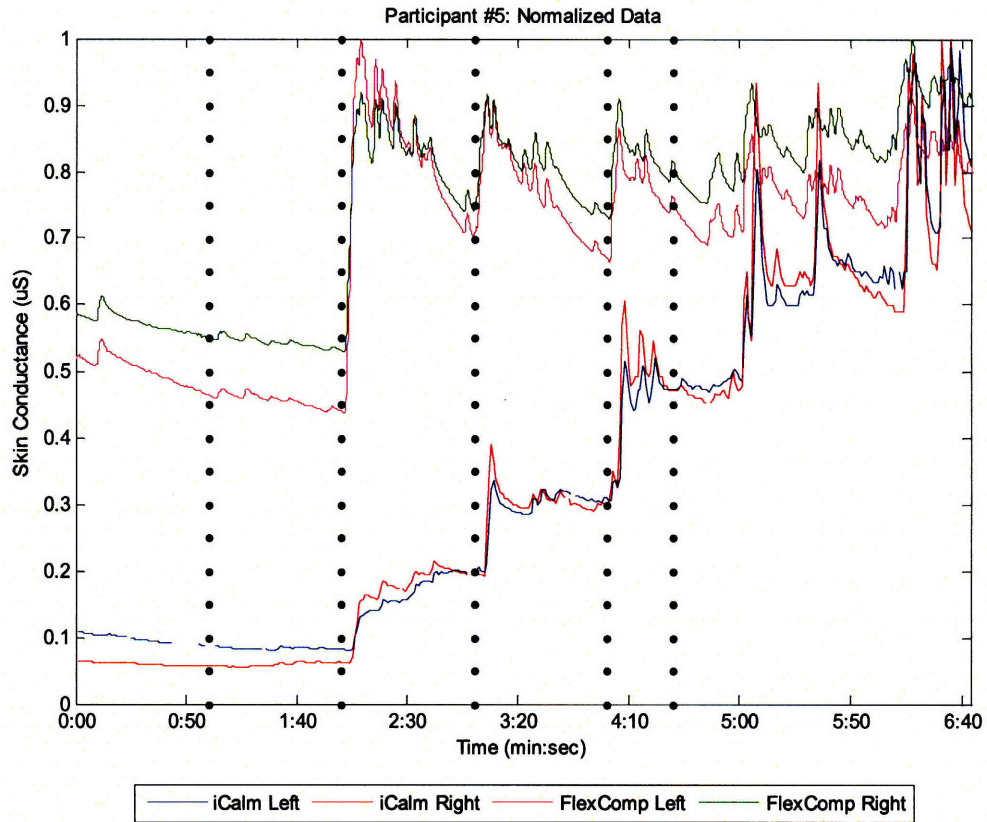
Figure B-15: Participant #5's normalized skin conductance data

B.6 Participant #6
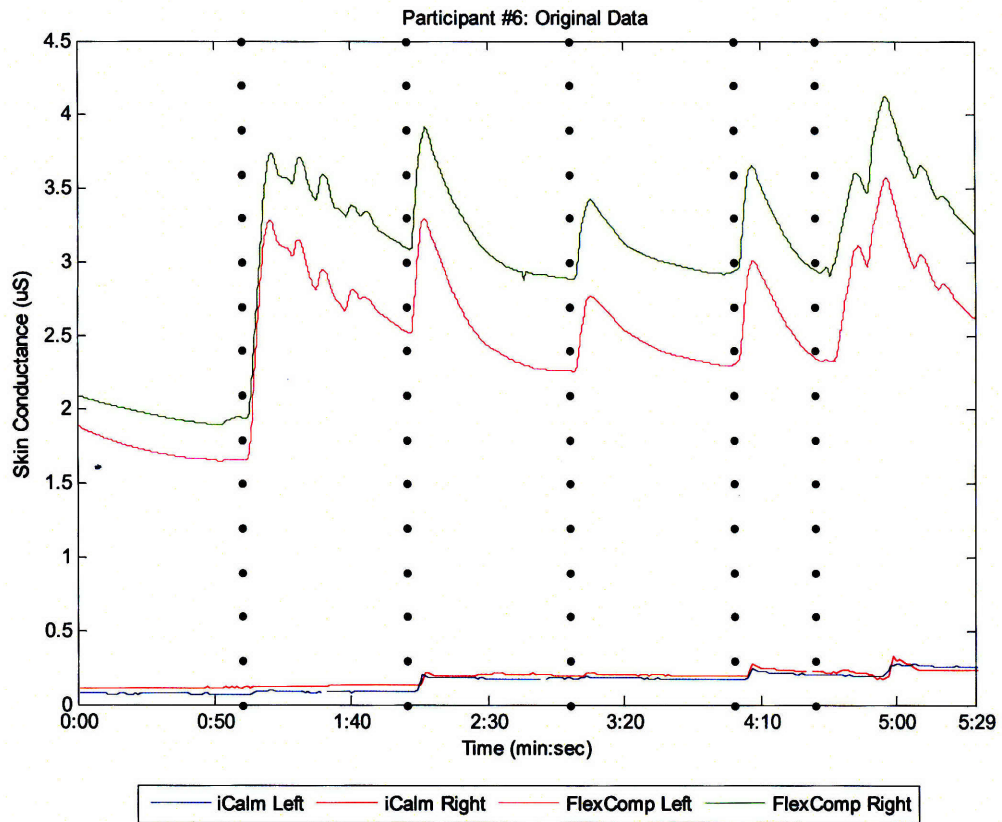
Figure B-16: Participant #6's original skin conductance data
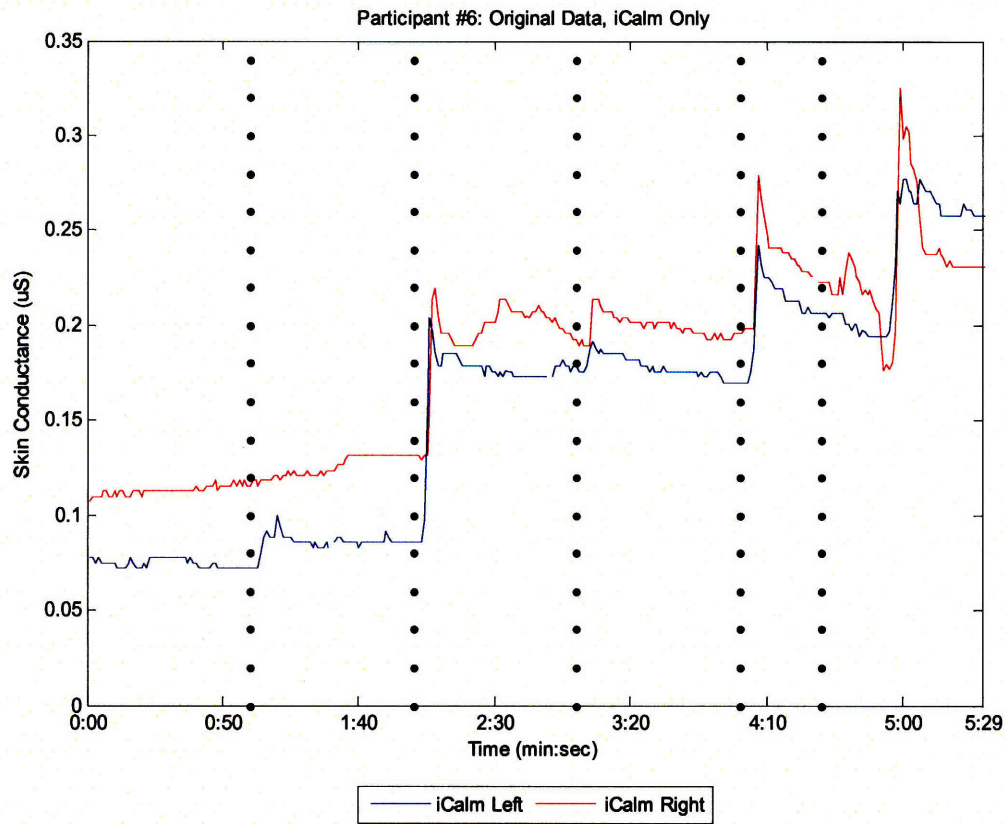
Figure B-17: Participant #6's original skin conductance data obtained with iCalm
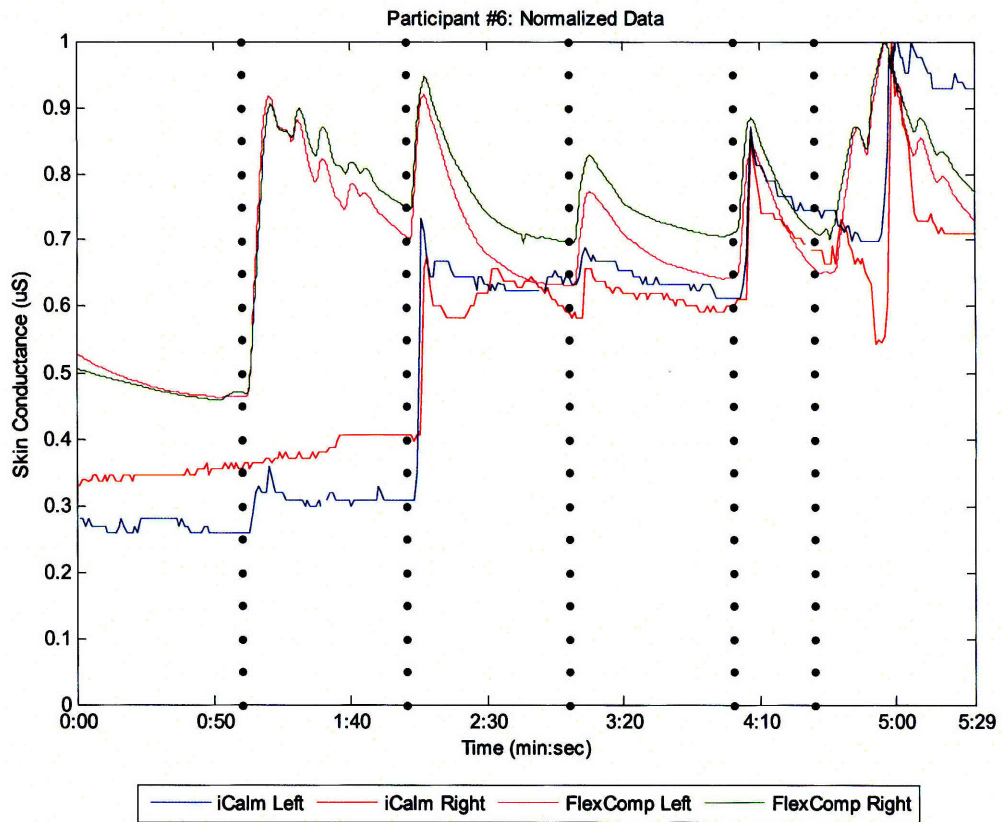
Figure B-18: Participant #6's normalized skin conductance data

B.7 Participant #7
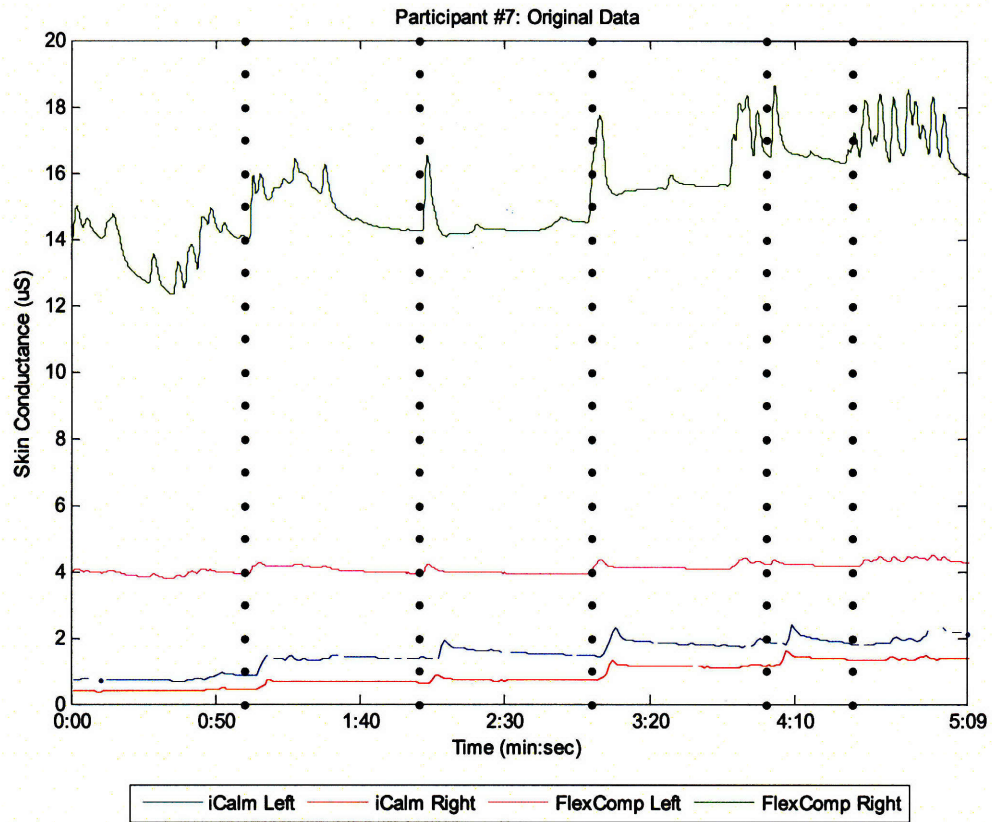
Figure B-19: Participant #7's original skin conductance data
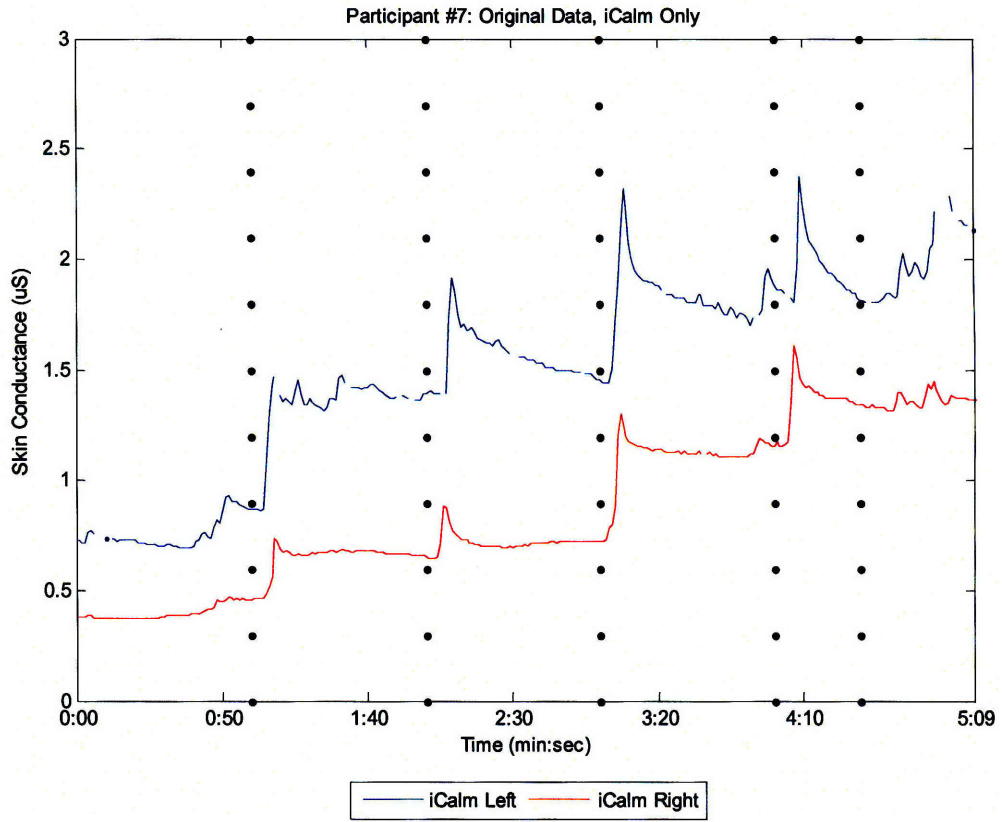
Figure B-20: Participant #7's original skin conductance data obtained with iCalm
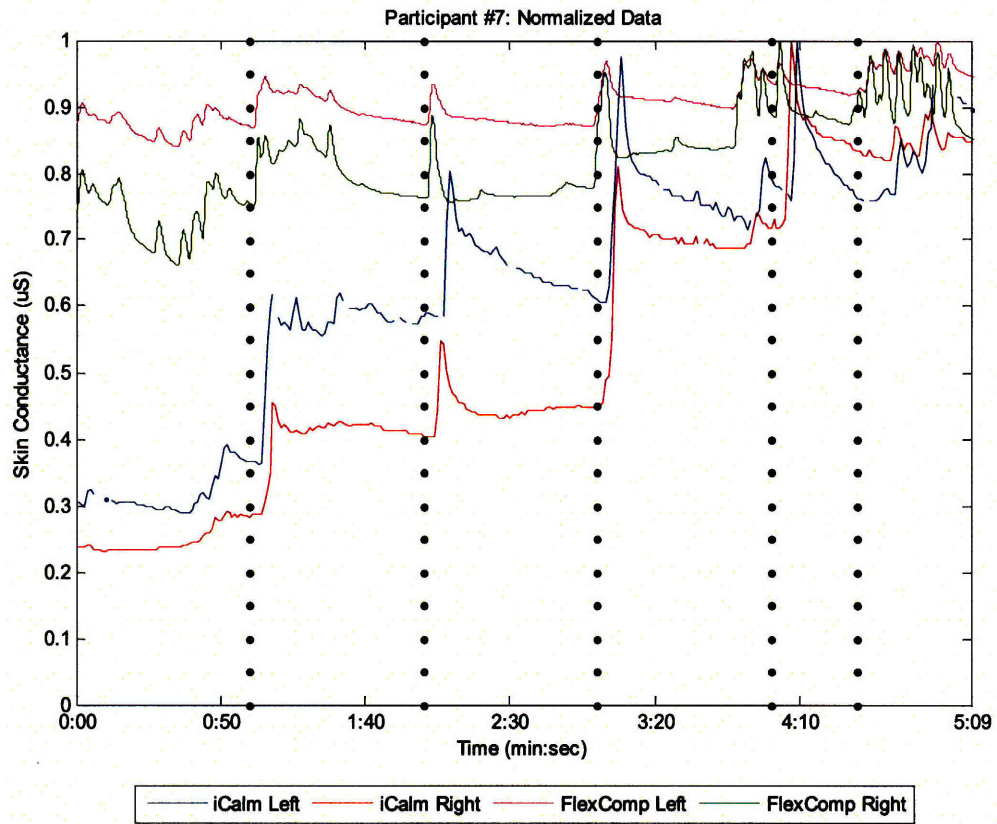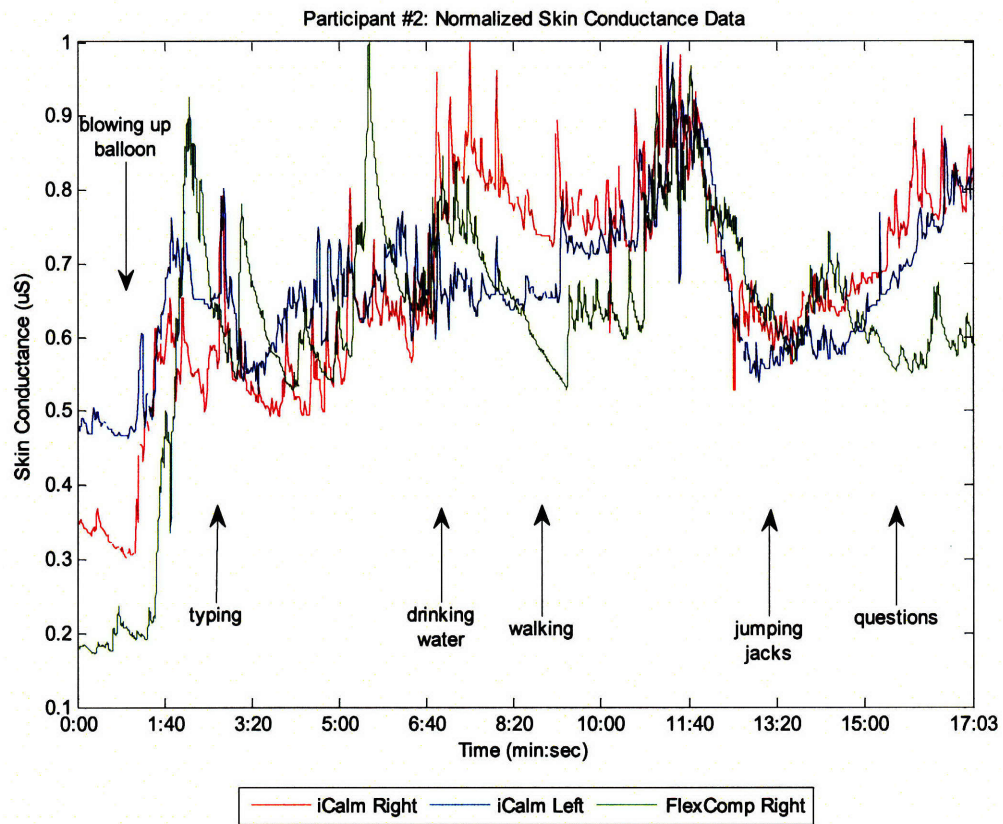
Figure B-21: Participant #7's normalized skin conductance data

B.8 Participant #8
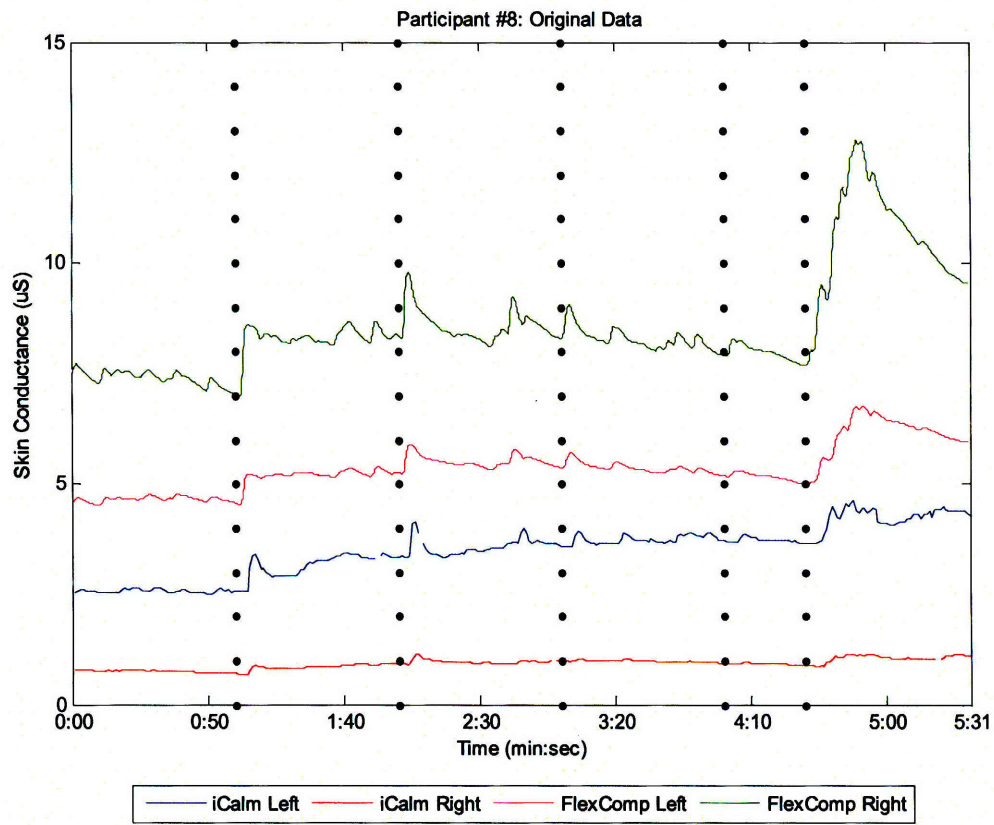
Figure B-22: Participant #8's original skin conductance data
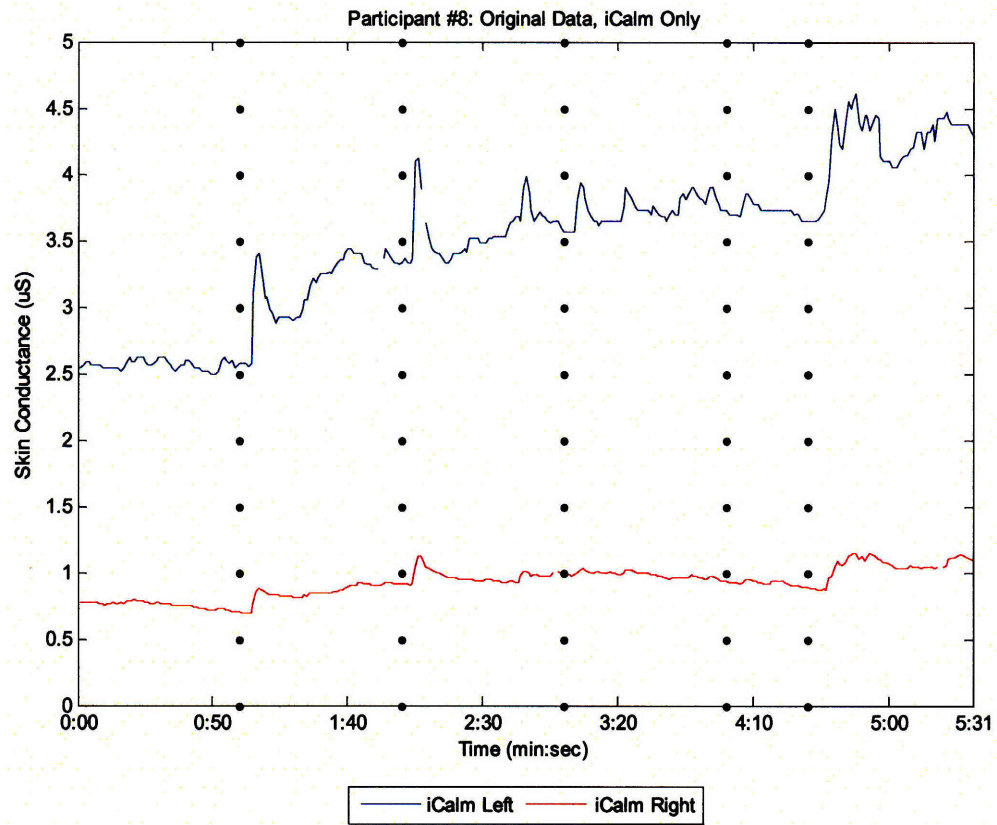
Figure B-23: Participant #8's original skin conductance data obtained with iCalm
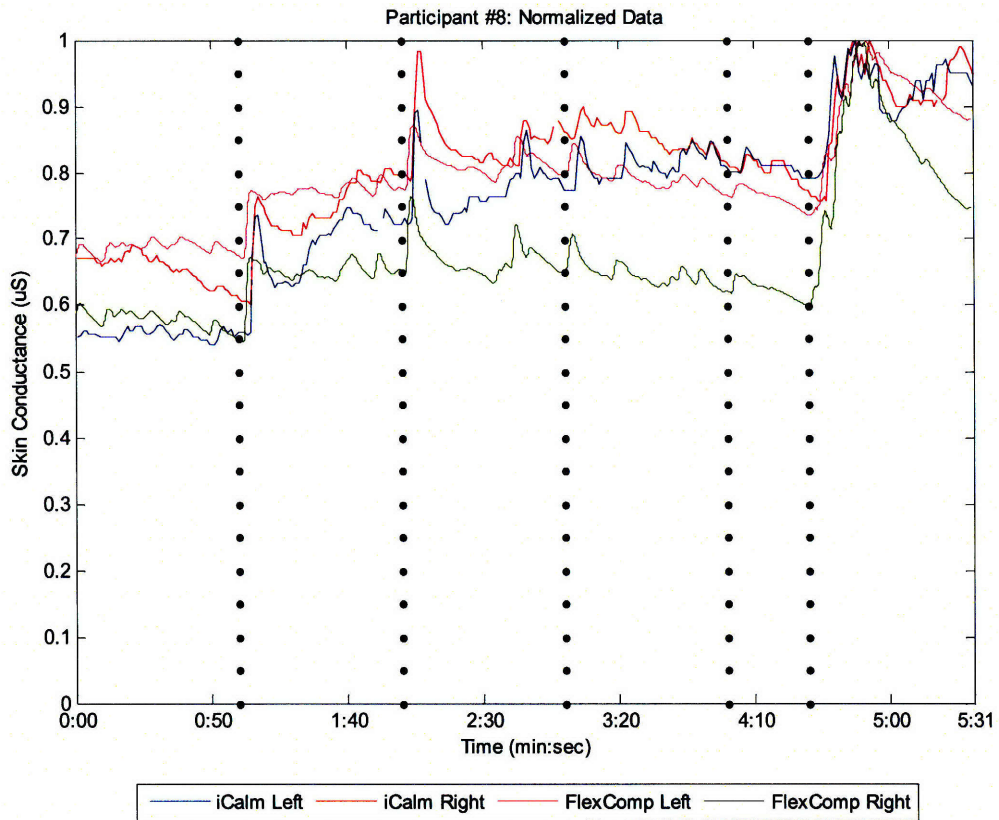
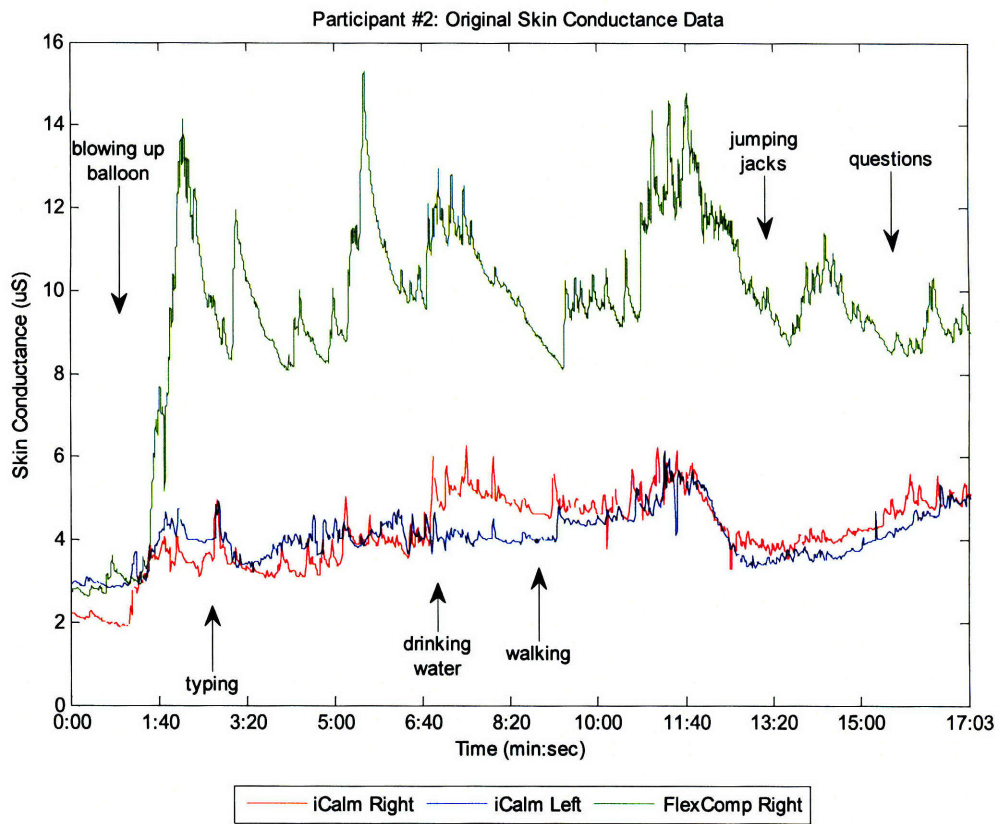Figure B-24: Participant #8's normalized skin conductance data

B.9 Participant #9
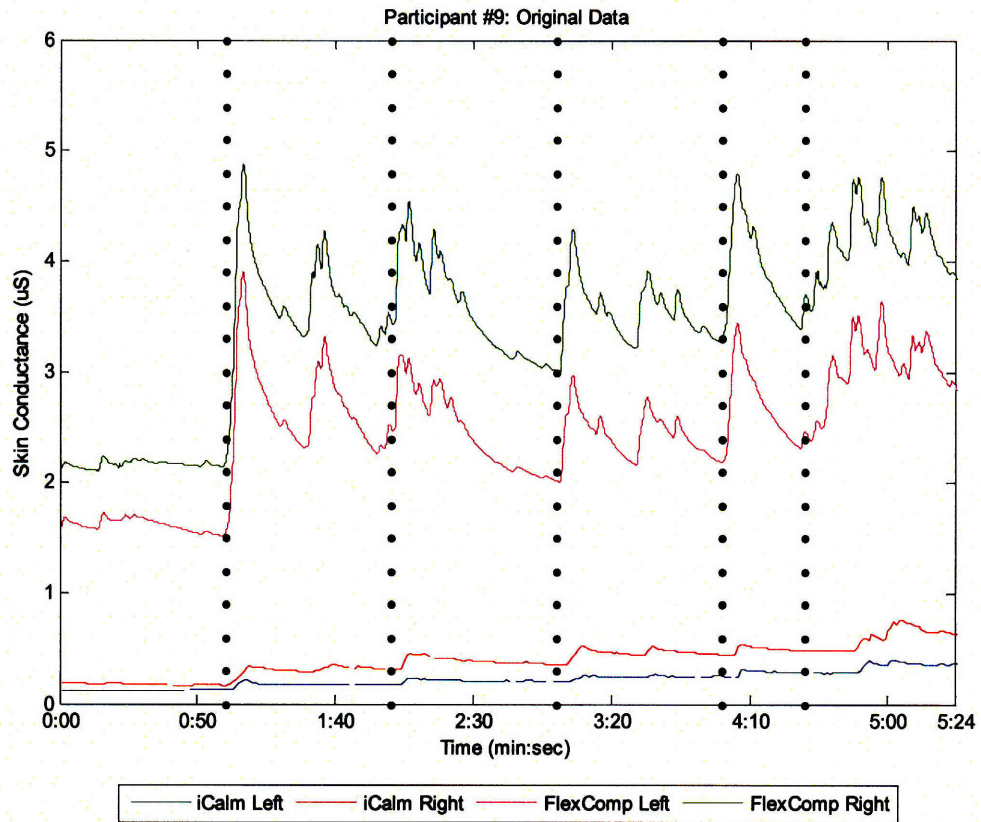
Figure B-25: Participant #9's original skin conductance data

Figure B-26: Participant #9's original skin conductance data obtained with iCalm

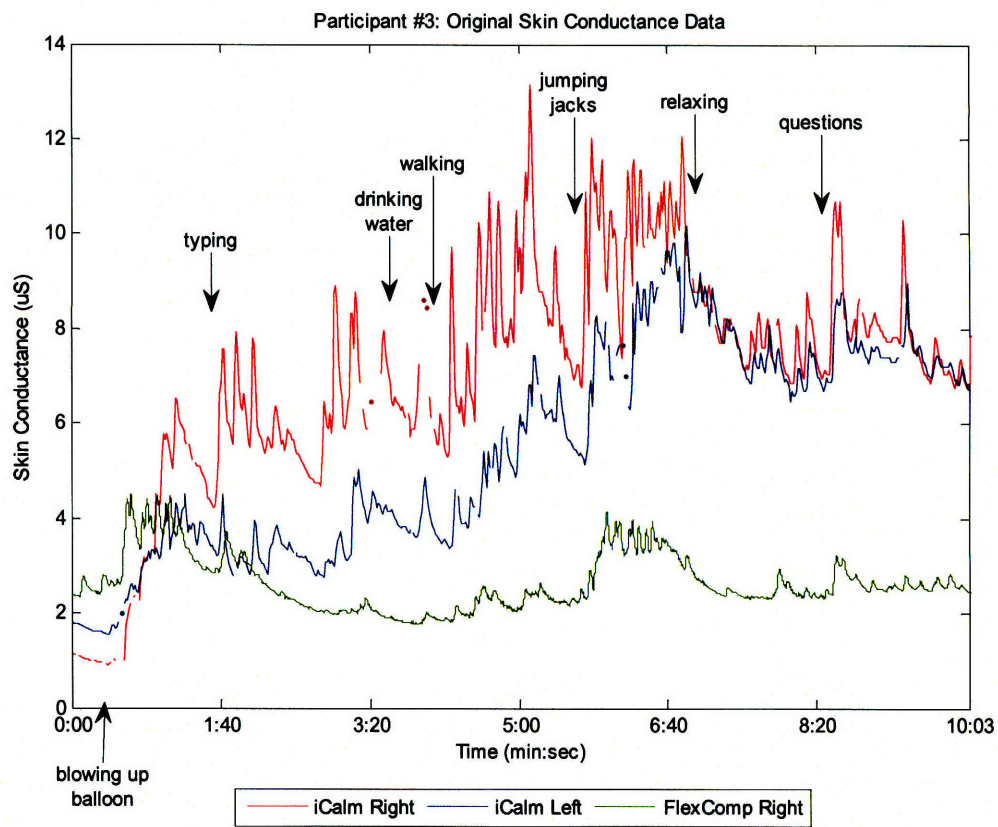Figure B-27: Participant #9's normalized skin conductance data

B.10 Participant #10

Figure B-28: Participant #10's original skin conductance data

Figure B-29: Participant #10's original skin conductance data obtained with iCalm

Figure B-30: Participant #10's normalized skin conductance data

B.11 Participant #11

Figure B-31: Participant #12's original skin conductance data

Figure B-32: Participant #11's original skin conductance data obtained with iCalm

Figure B-33: Participant #11's normalized skin conductance data

B.12 Participant #12

Figure B-34: Participant #12's original skin conductance data

Figure B-35: Participant #12's original skin conductance data obtained with iCalm
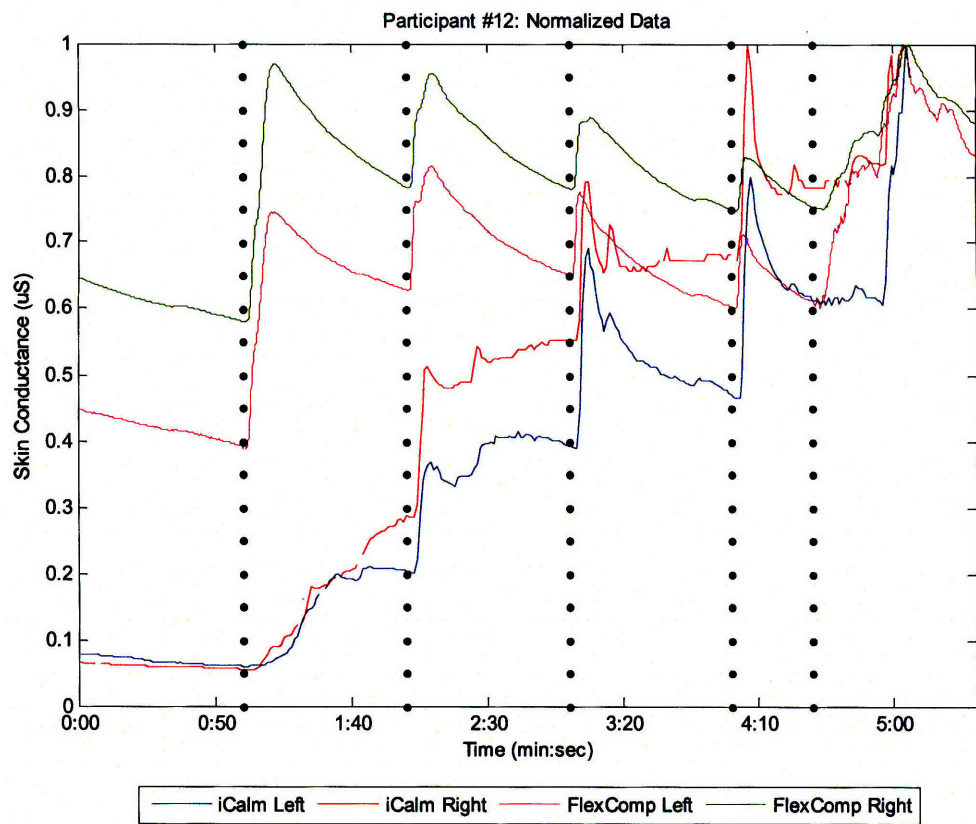
Figure B-36: Participant #12's normalized skin conductance data

Appendix C: Activities Experiment— Skin Conductance

C.1 Participant #1

Note: The experimental protocol for the first participant is different than that of other participants.
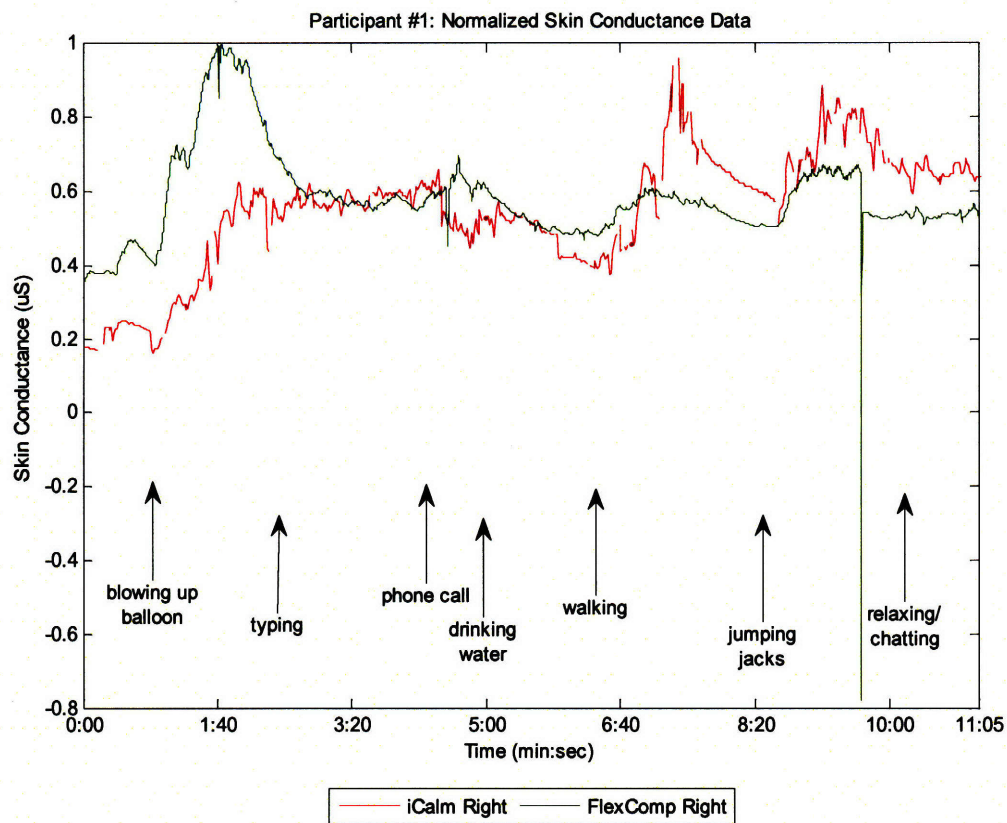
Figure C-1: Participant #1's normalized skin conductance data
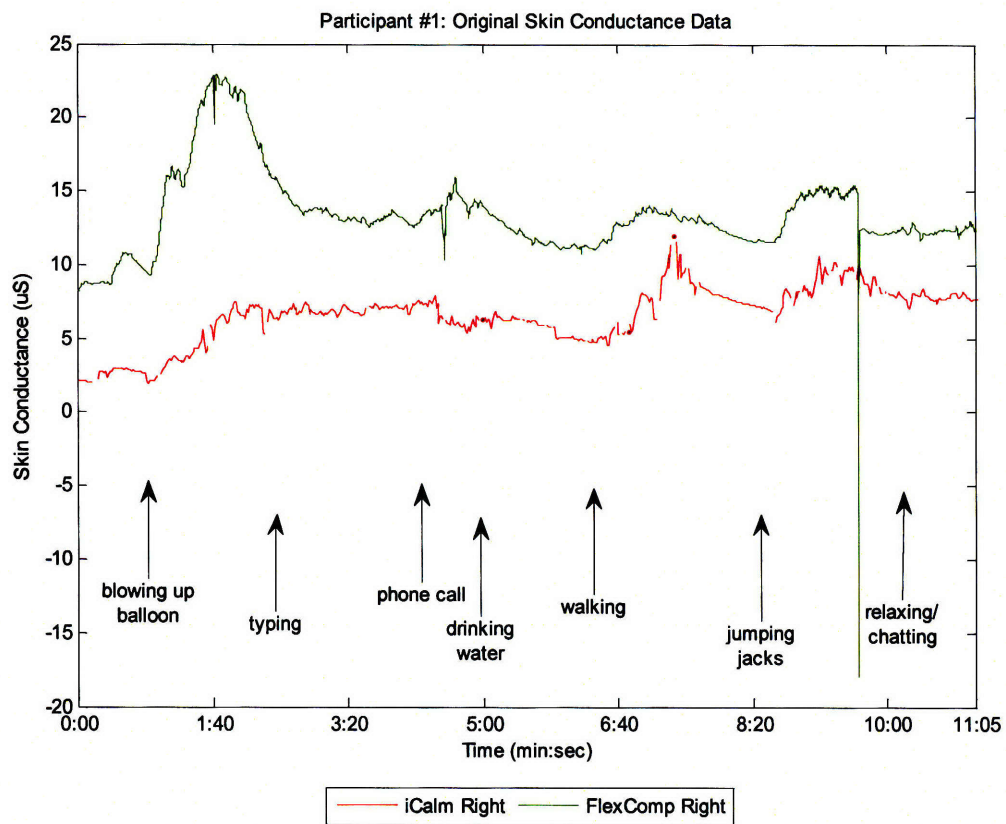
Figure C-2: Participant #1's original skin conductance data

C.2 Participant #2

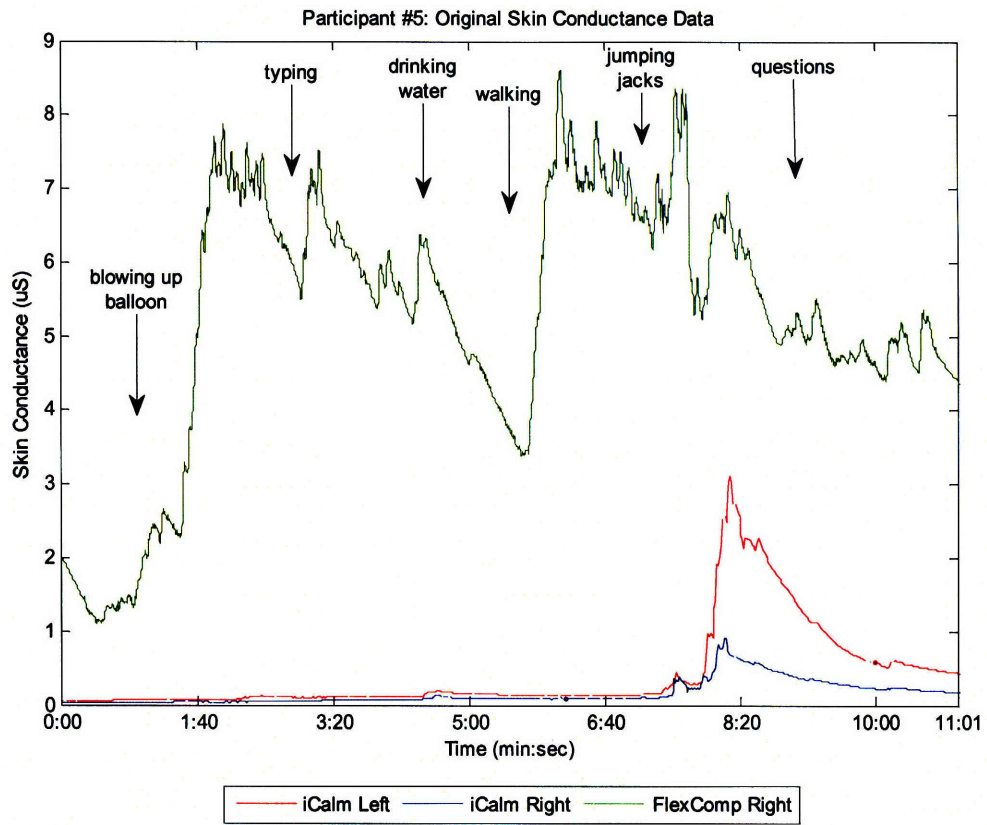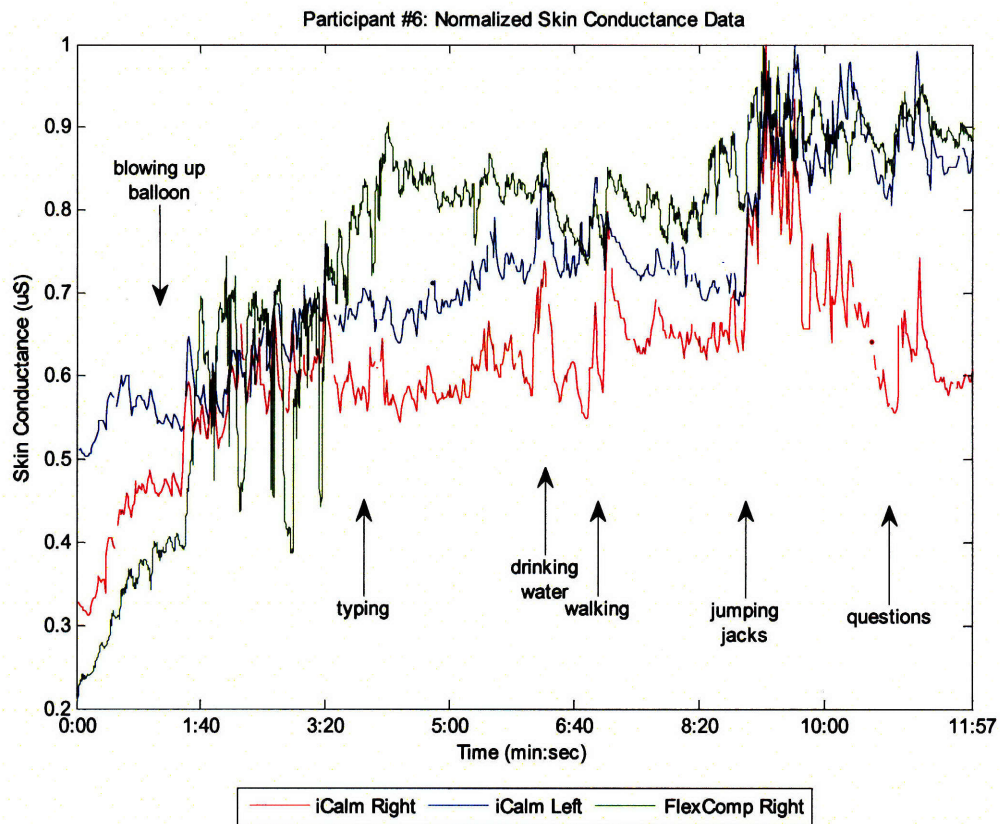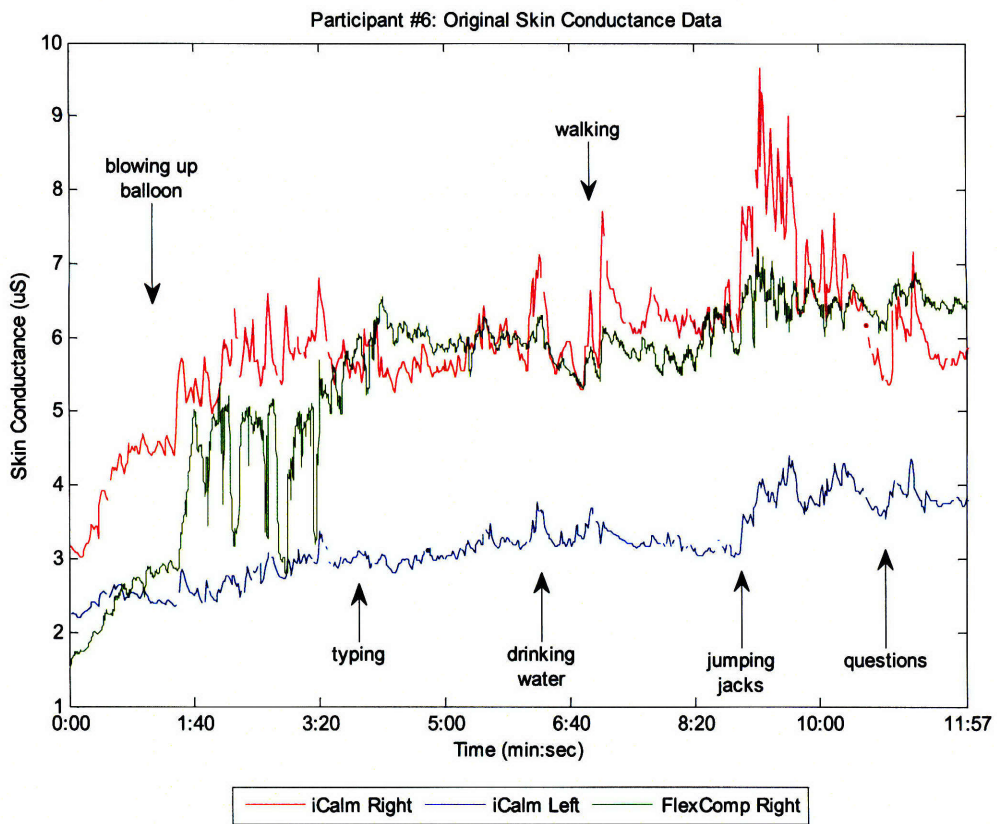Figure C-3: Participant #2's normalized skin conductance data

Figure C-4: Participant #2's original skin conductance data

C.3 Participant #3
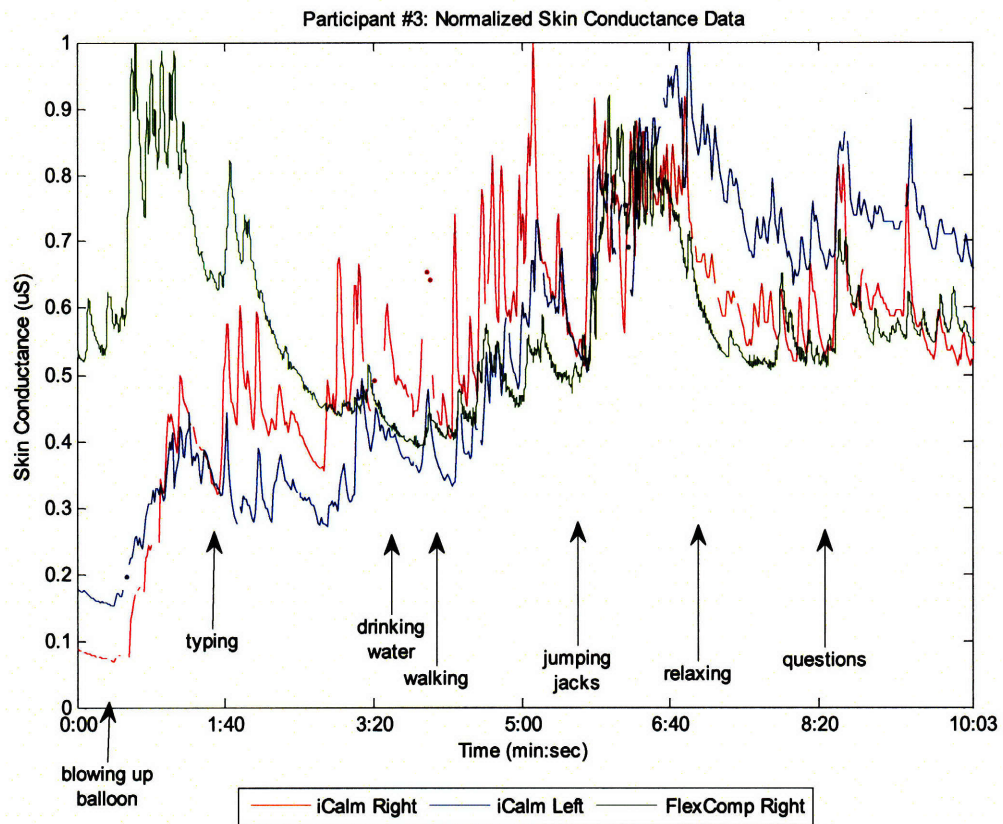
Figure C-5: Participant #3's normalized skin conductance data

Figure C-6: Participant #3's original skin conductance data
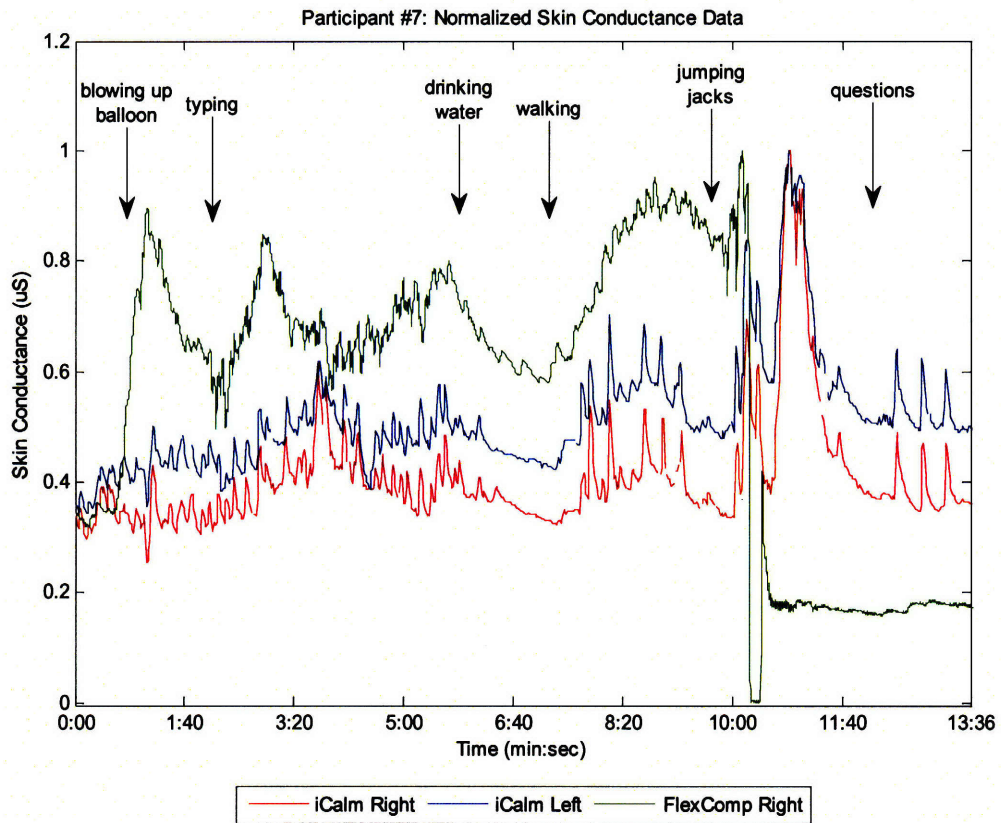
C.4 Participant #4
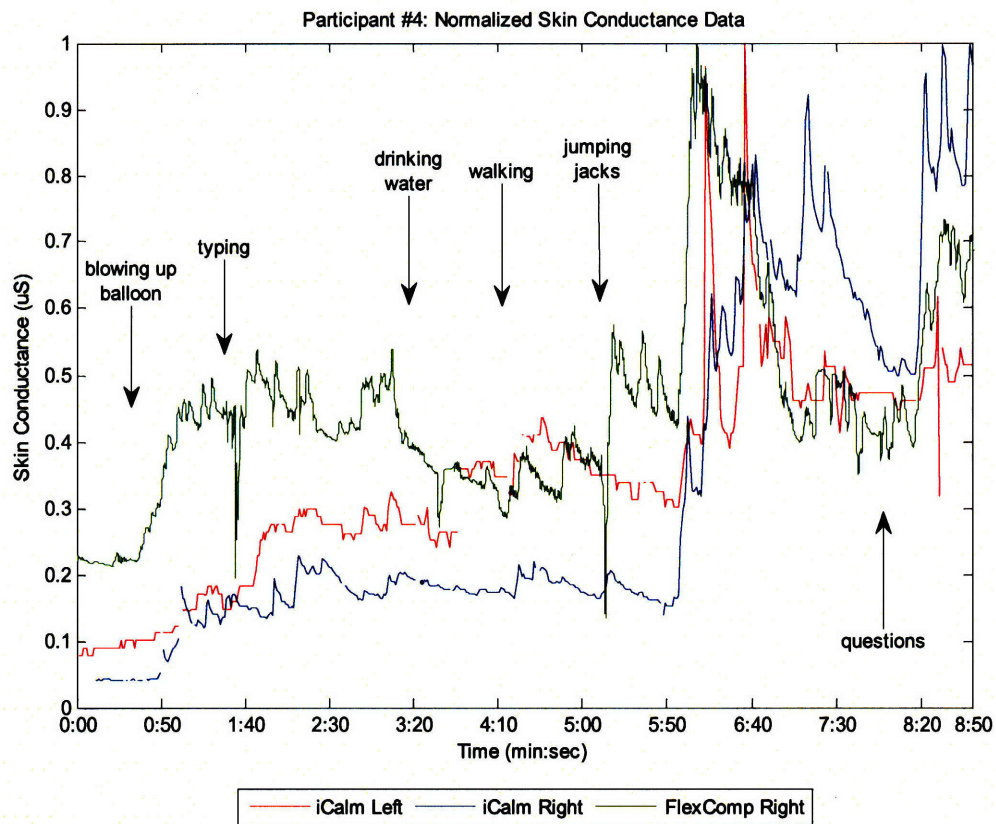
Figure C-7: Participant #4's normalized skin conductance data
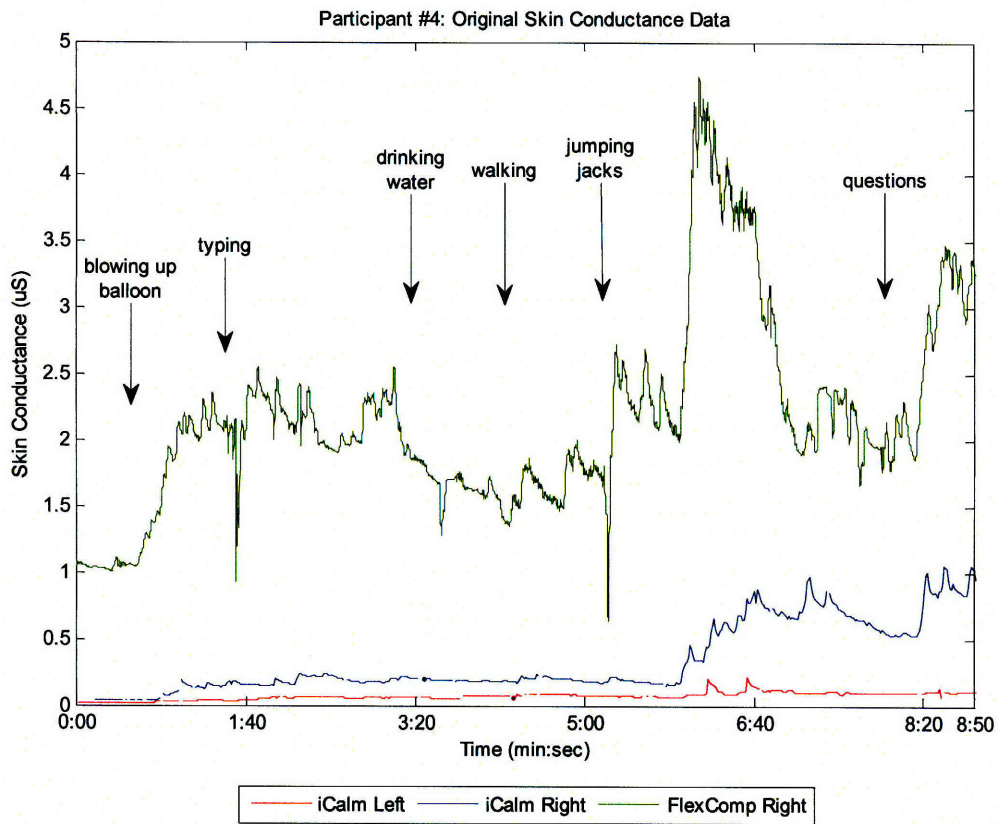
Figure C-8: Participant #4's original skin conductance data

C.5 Participant #5
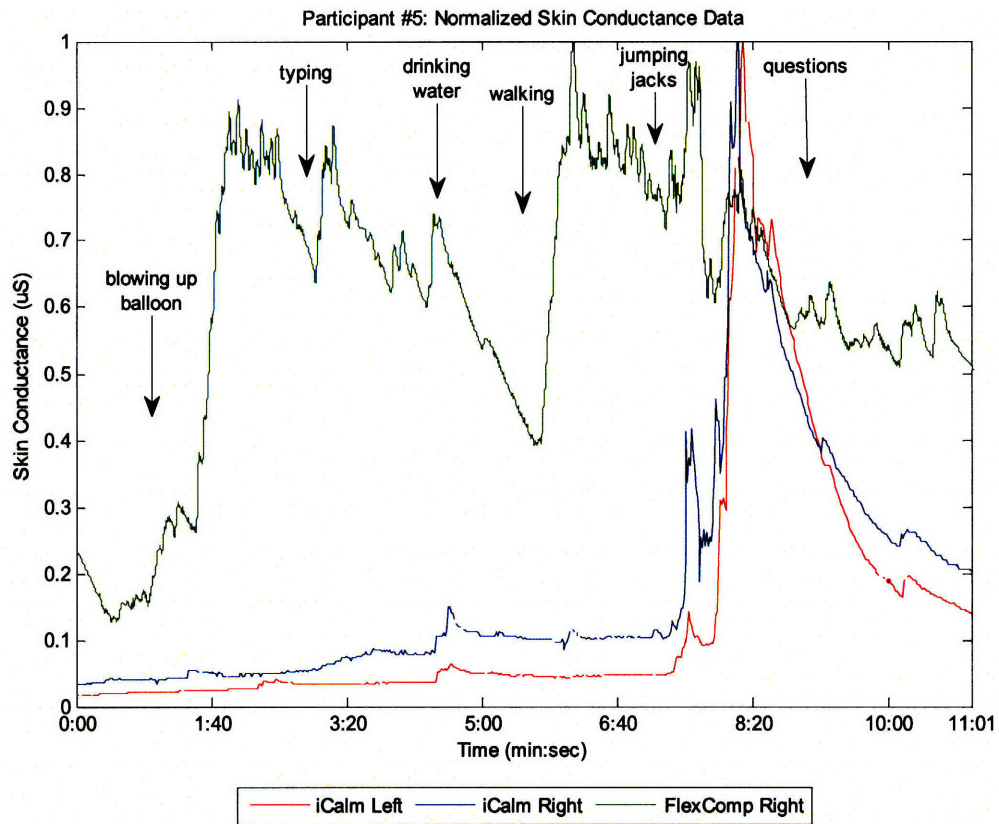
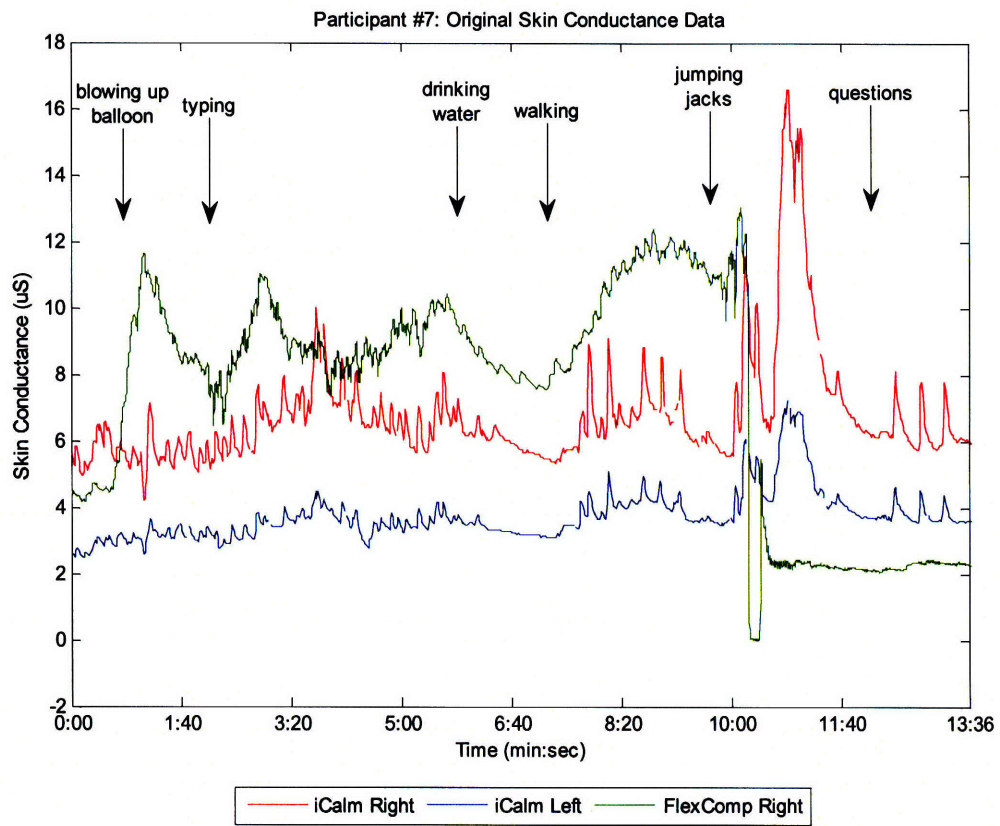Figure C-9: Participant #5's normalized skin conductance data

Figure C-10: Participant #5's original skin conductance data

C.6 Participant #6

Figure C-11: Participant #6's normalized skin conductance data

Figure C-12: Participant #6's original skin conductance data

C.7 Participant #7

Figure C-13: Participant #7's normalized skin conductance data

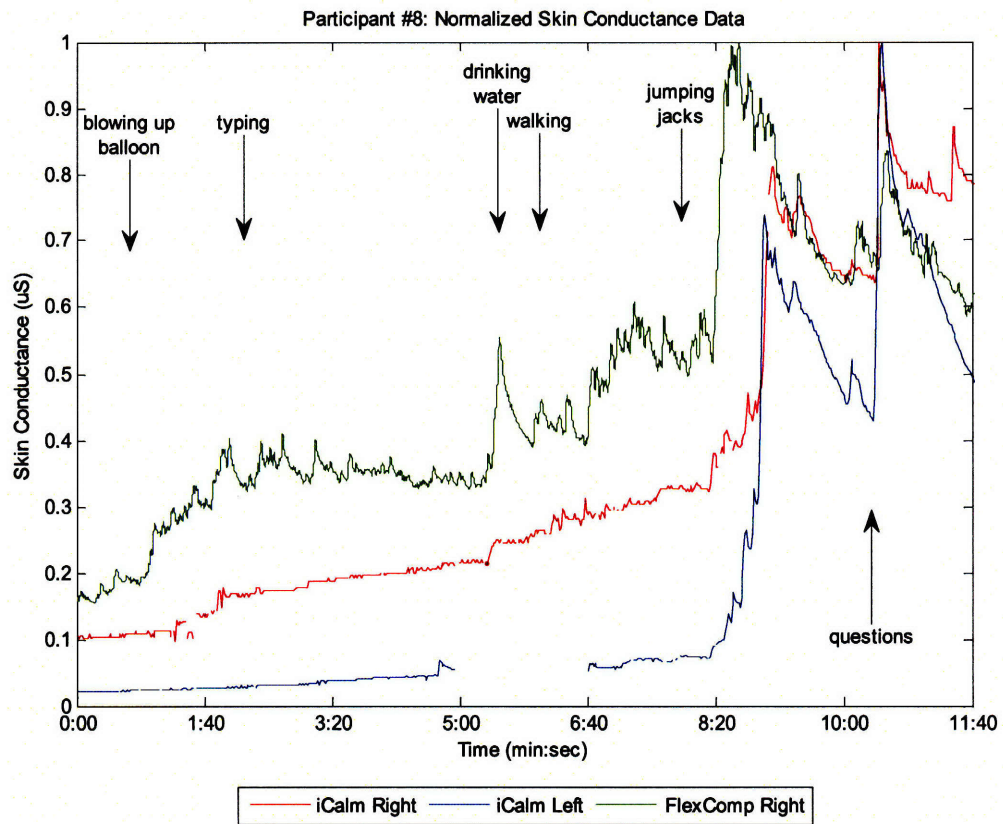Figure C-14: Participant #7's original skin conductance data

C.8 Participant #8

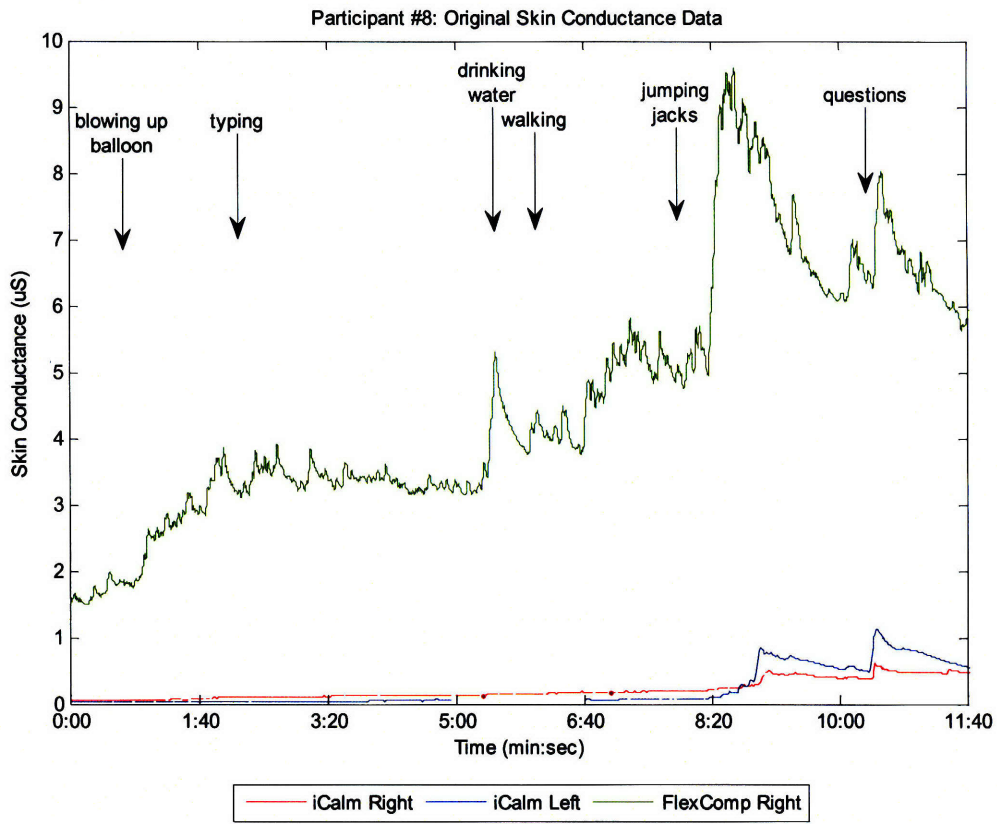Figure C-15: Participant #8's normalized skin conductance data

Figure C-16: Participant #8's original skin conductance data
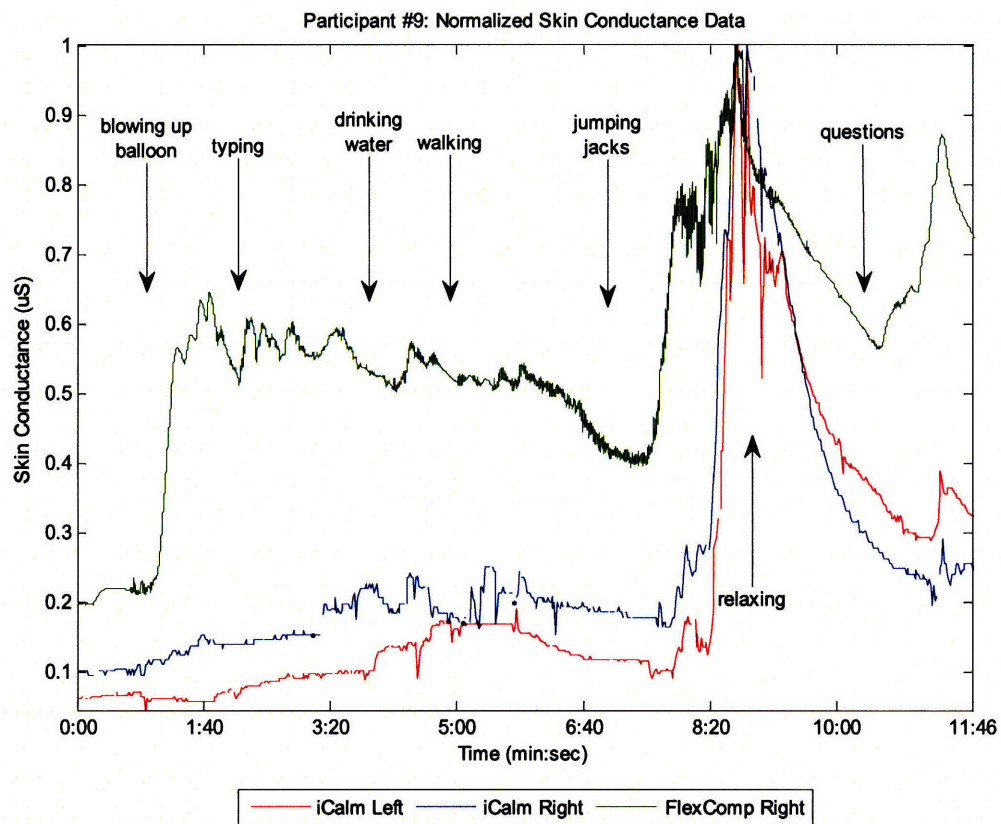
C.9 Participant #9

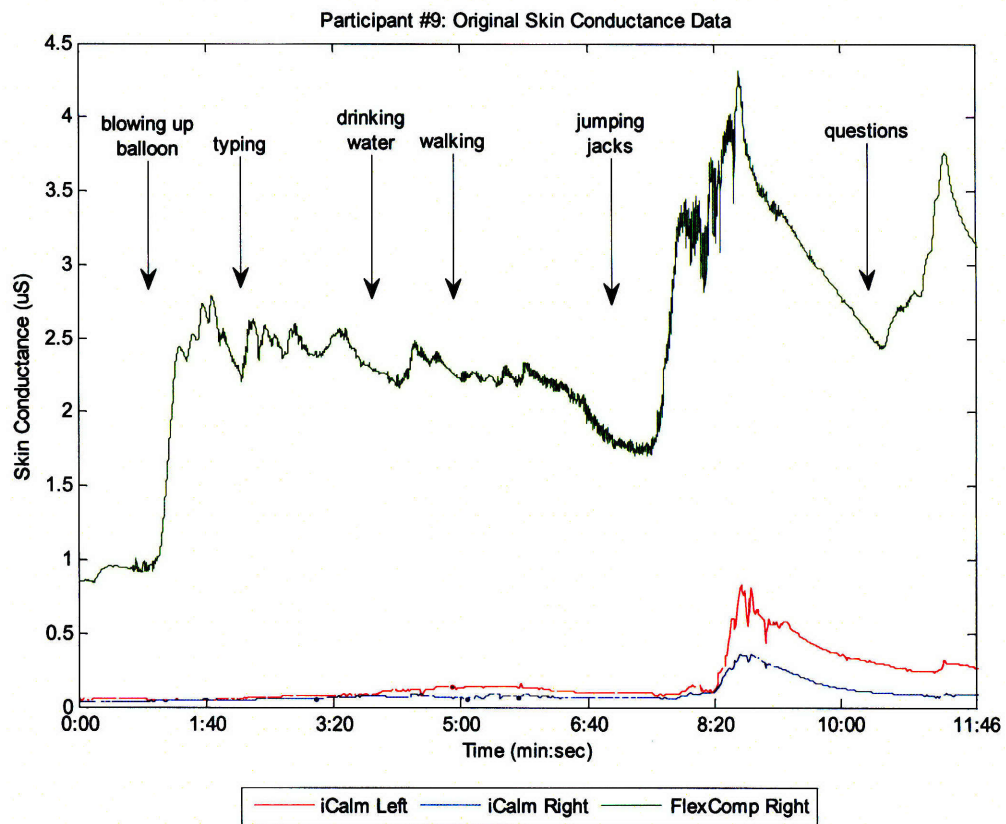Figure C-17: Participant #9's normalized skin conductance data

Figure C-18: Participant #9's original skin conductance data
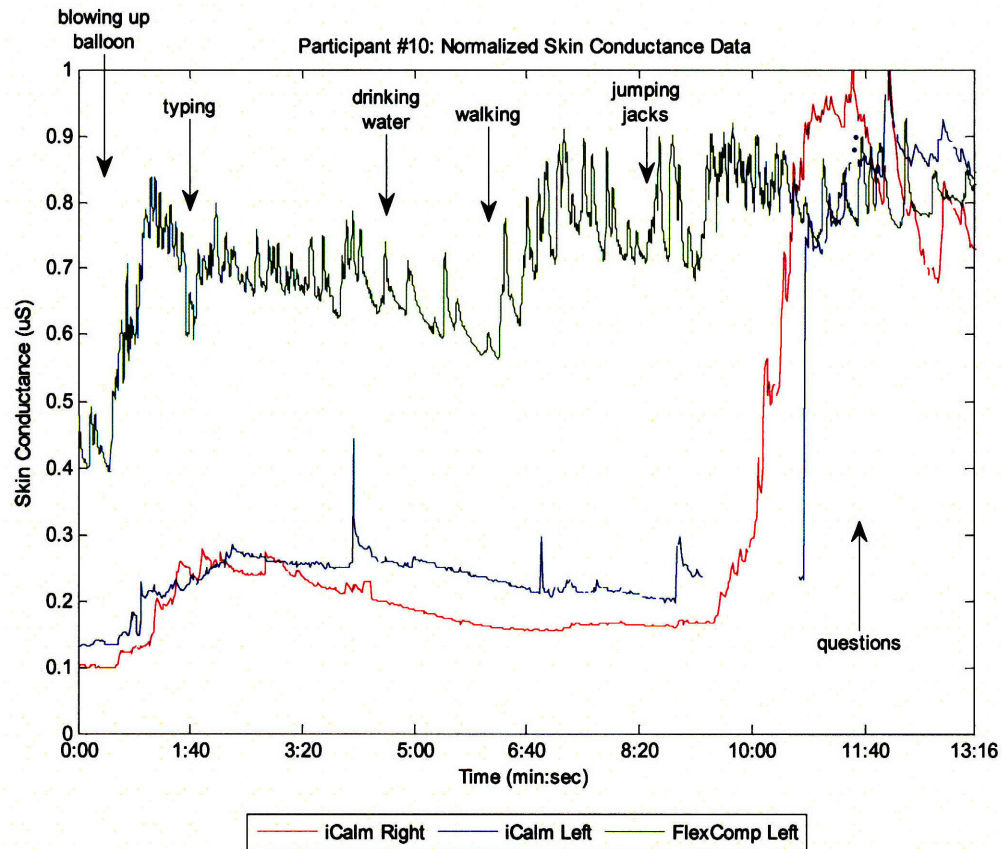
C.10 Participant #10

Figure C-19: Participant #10's normalized skin conductance data
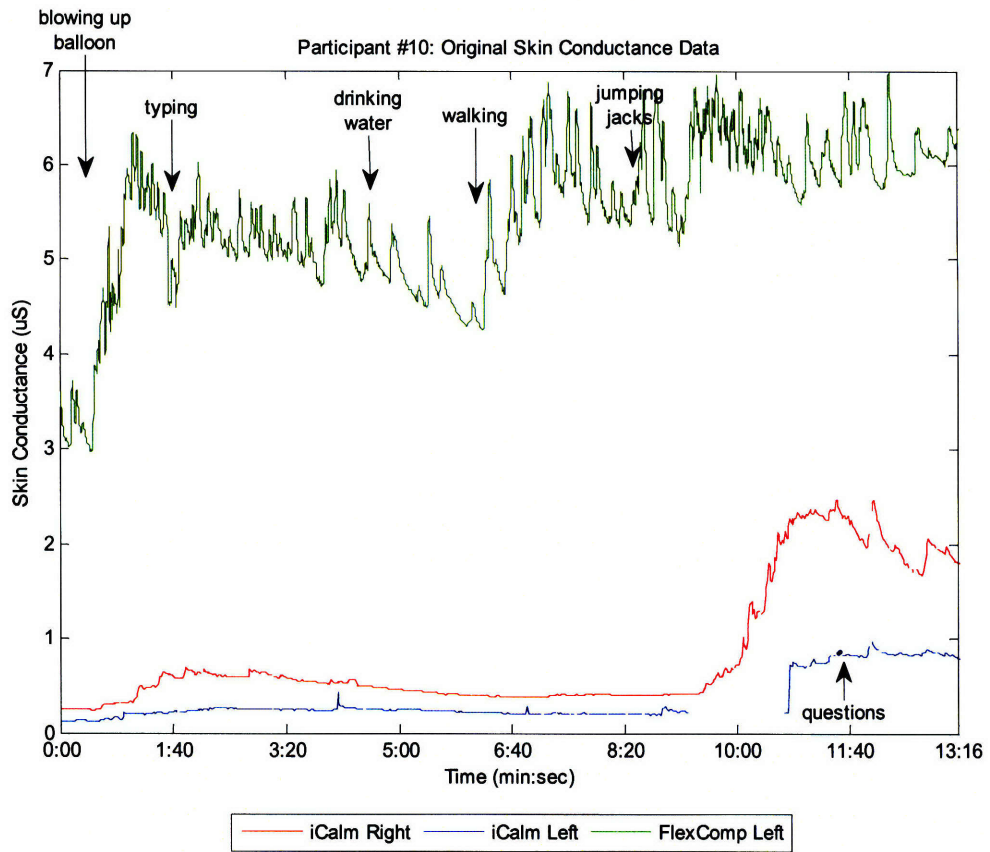
Figure C-20: Participant #10's original skin conductance data
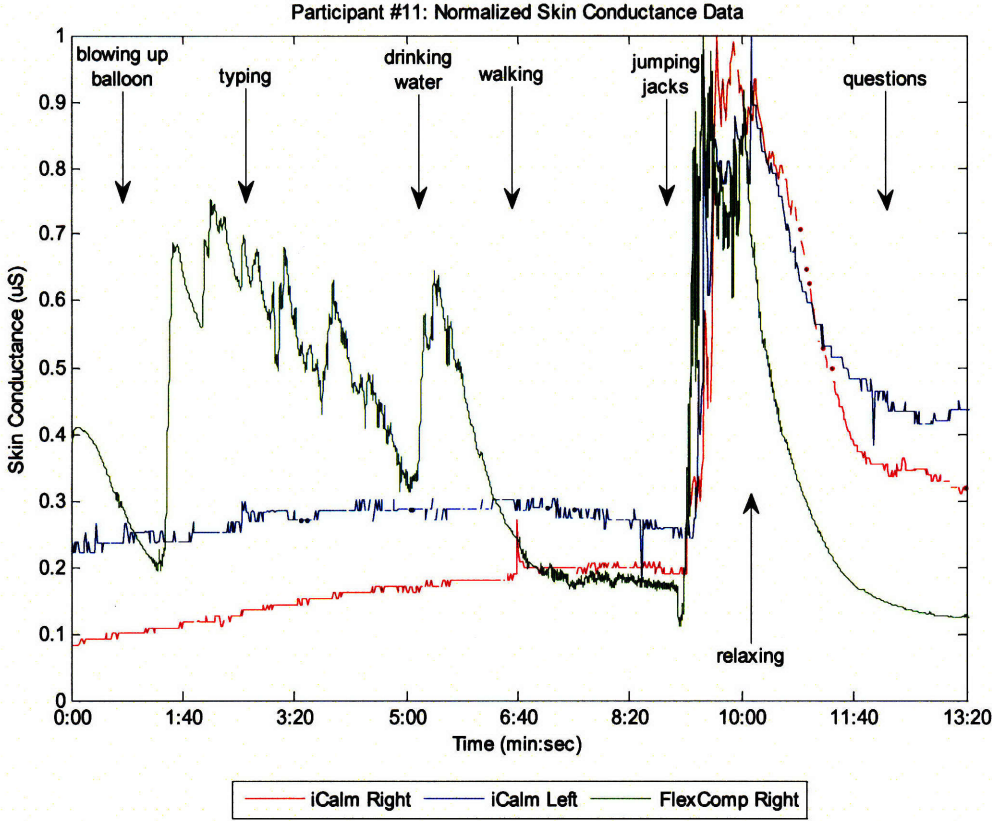
C.11 Participant #11

Figure C-21: Participant #11's normalized skin conductance data
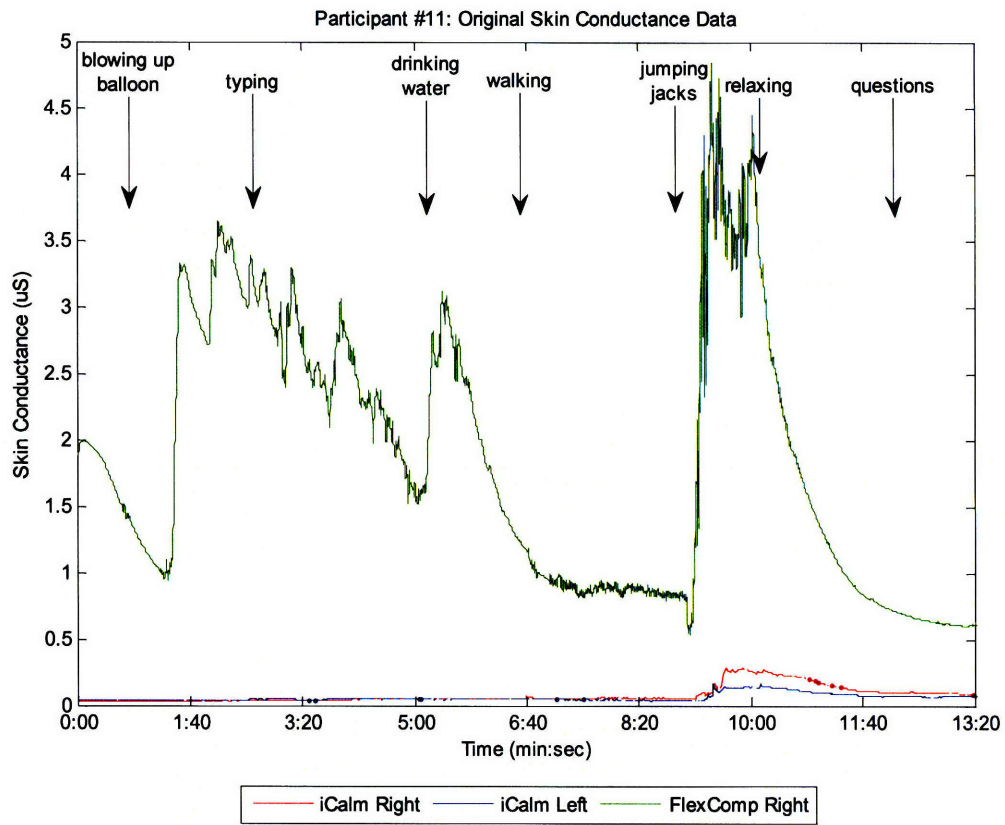
Figure C-22: Participant #11's original skin conductance data

C.12 Participant #12
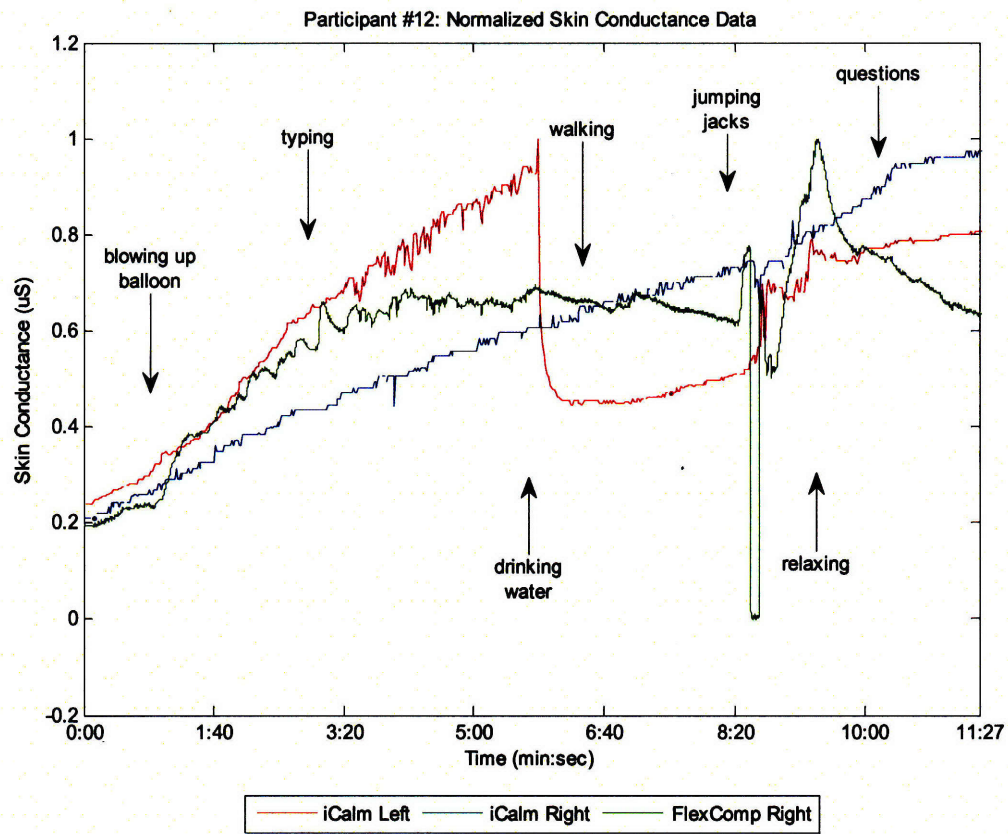
Figure C-23: Participant #12's normalized skin conductance data
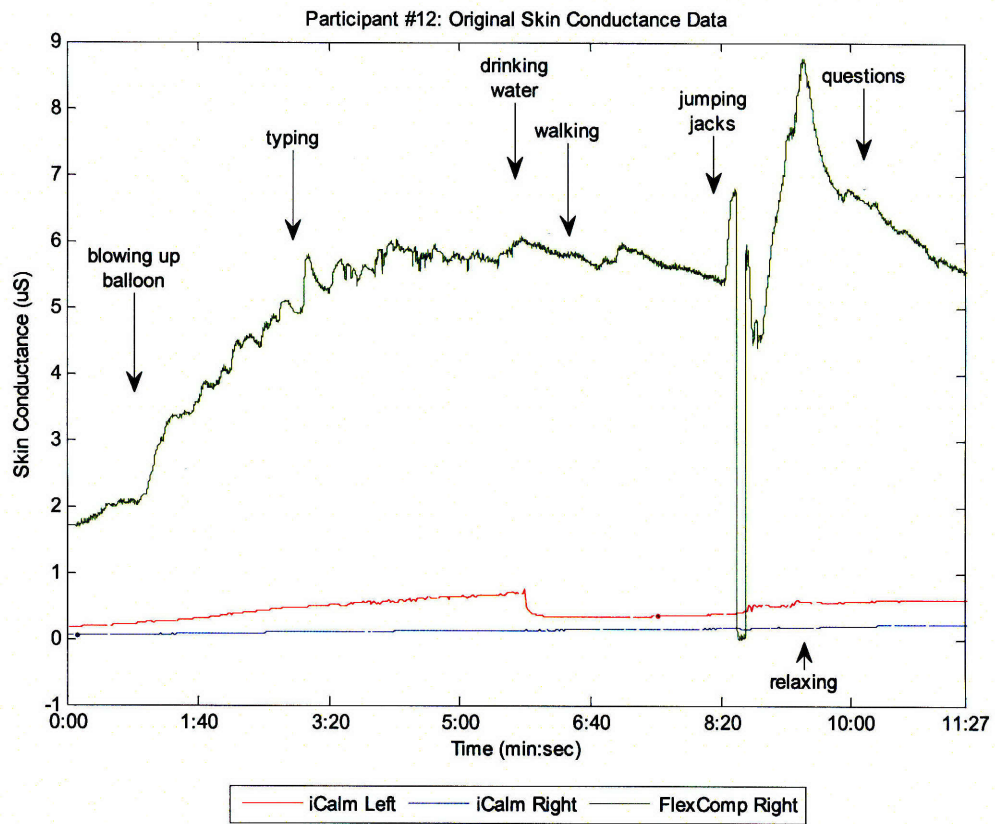
Figure C-24: Participant #12's original skin conductance data

Appendix D: Activities Experiment— Heart Rate

D.1 Participant #1

Note: Once again, the experimental protocol for the first participant is different than that of other participants.

Figure D-1: Participant #1's heart rate as determined by FlexComp (top) and iCalm (bottom)

D.2 Participant #2

Figure D-2: Participant #2's heart rate as determined by FlexComp (top) and iCalm (bottom)

D.3 Participant #3

Figure D-3: Participant #3's heart rate as determined by FlexComp (top) and iCalm (bottom)

D.4 Participant #4

Figure D-4: Participant #4's heart rate as determined by FlexComp (top) and iCalm (bottom)

D.5 Participant #5

Figure D-5: Participant #5's heart rate as determined by FlexComp (top) and iCalm (bottom)

D.6 Participant #6

Figure D-6: Participant #6's heart rate as determined by FlexComp (top) and iCalm (bottom)

D.7 Participant #7

Figure D-7: Participant #7's heart rate as determined by FlexComp (top) and iCalm (bottom)

D.8 Participant #8

Figure D-8: Participant #8's heart rate as determined by FlexComp (top) and iCalm (bottom)
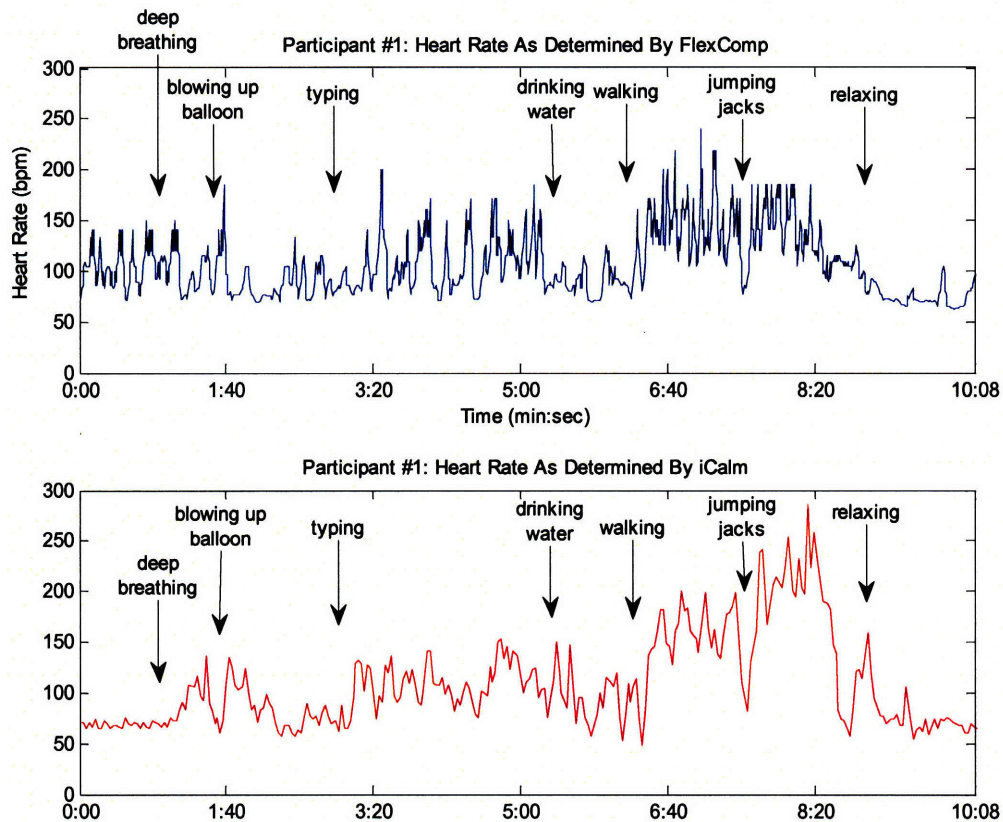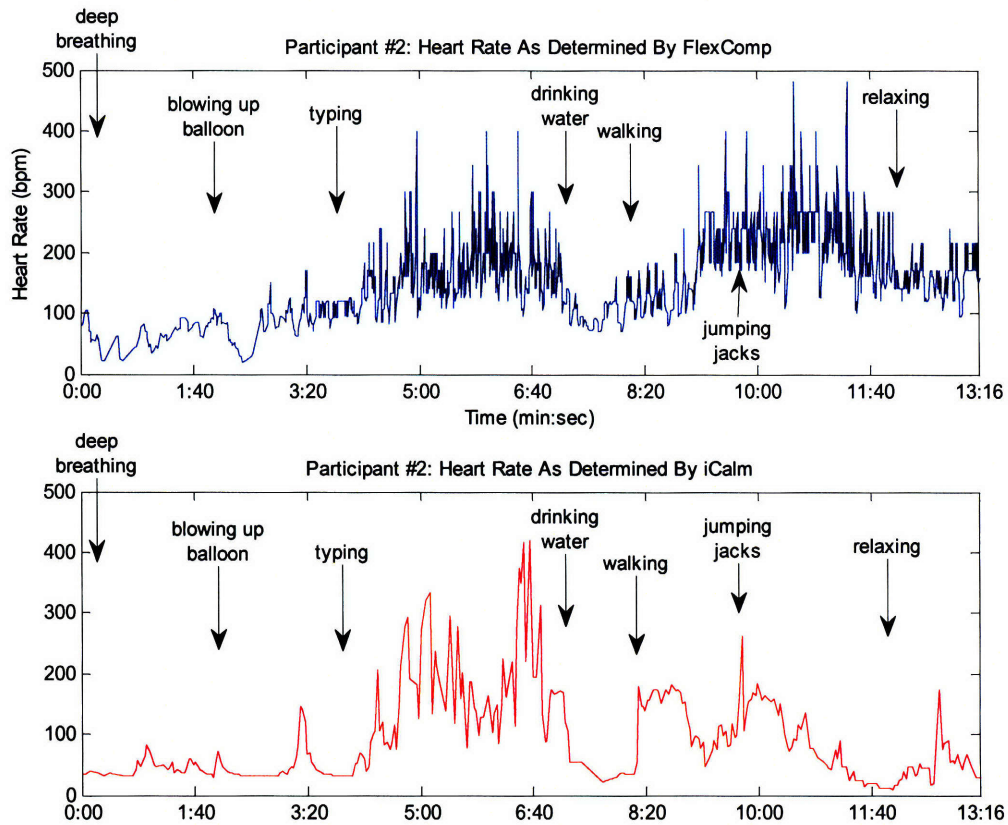
D.9 Participant #9

Figure D-9: Participant #9's heart rate as determined by FlexComp (top) and iCalm (bottom)

D.10 Participant #10
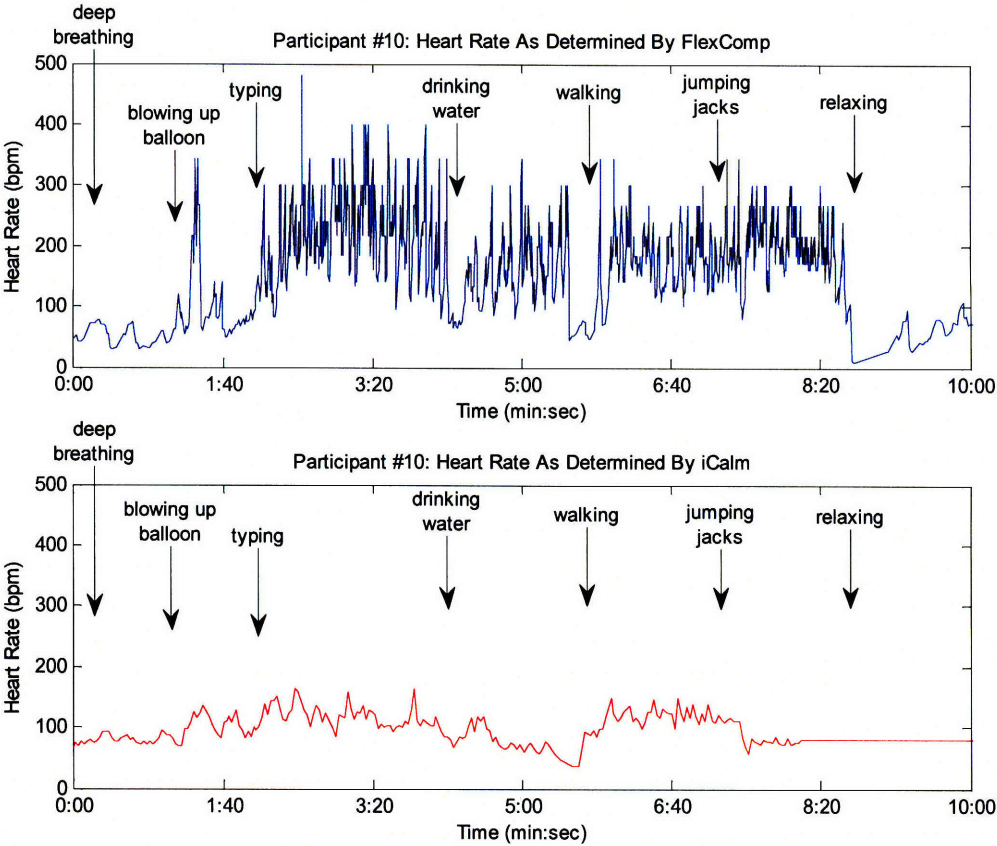
Figure D-10: Participant #10's heart rate as determined by FlexComp (top) and iCalm (bottom)
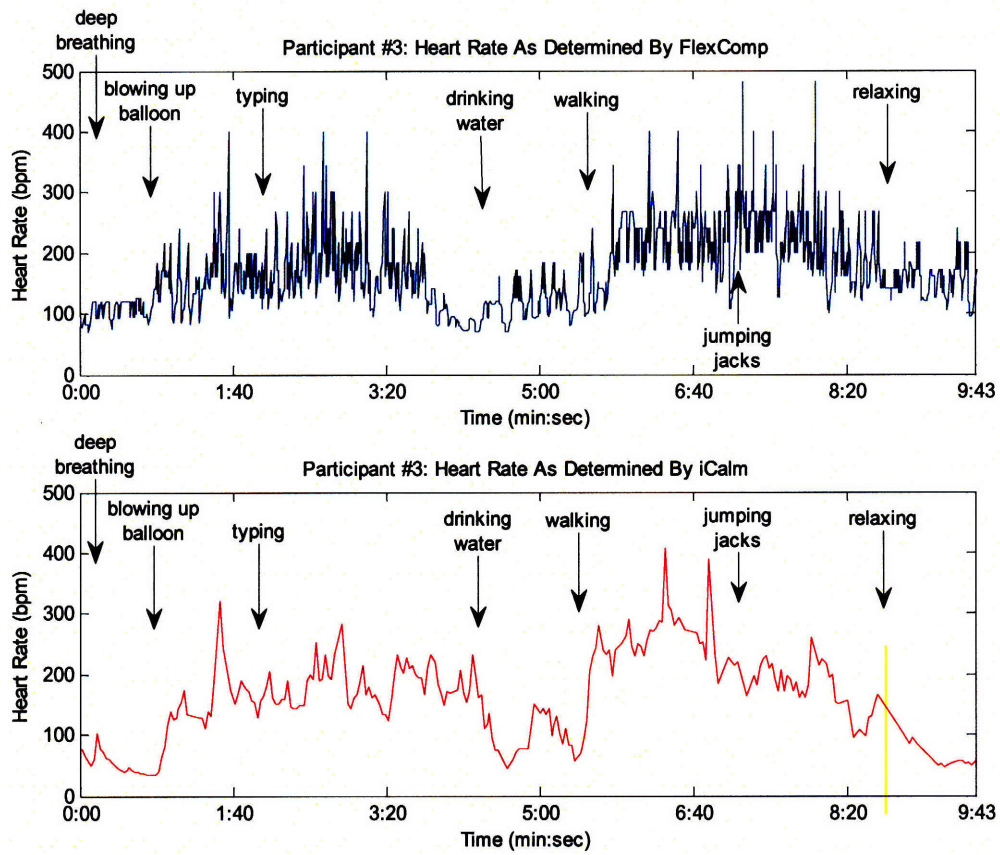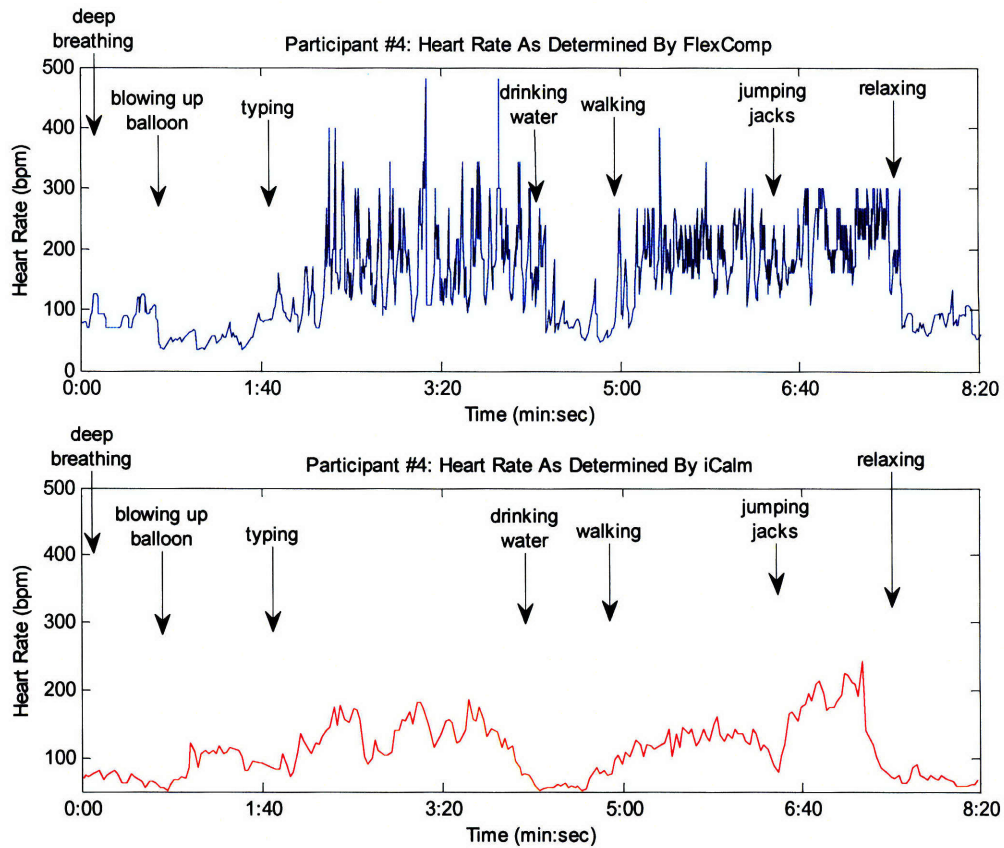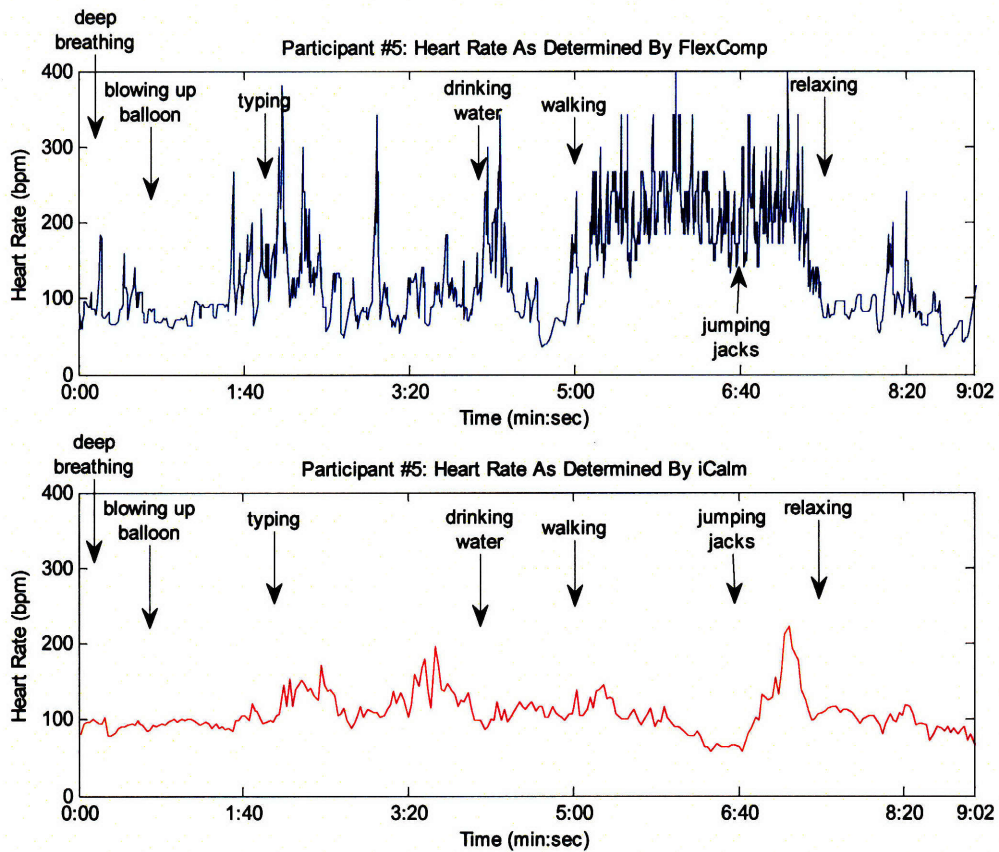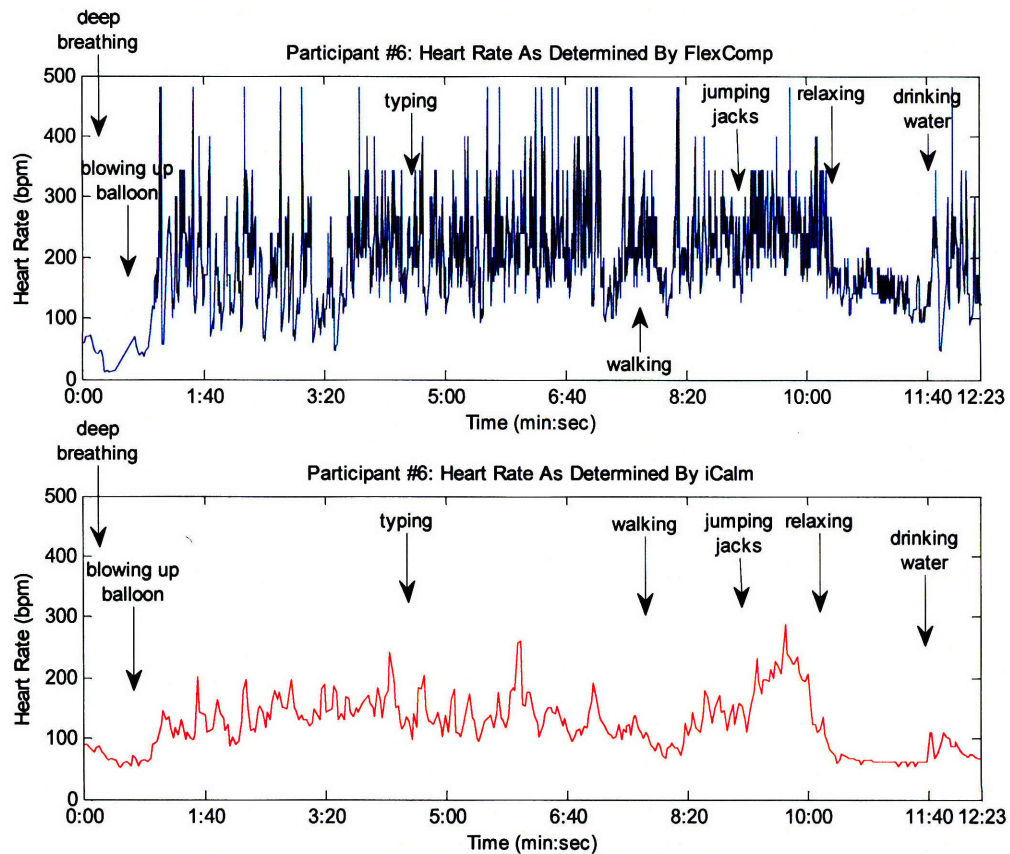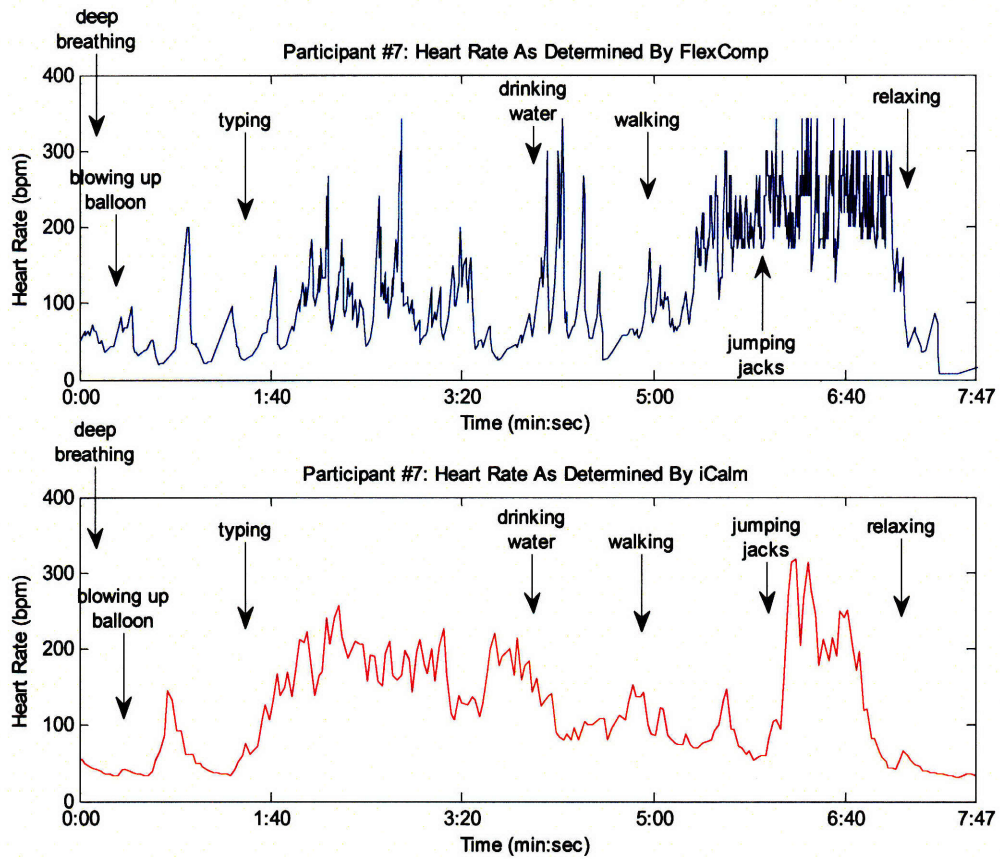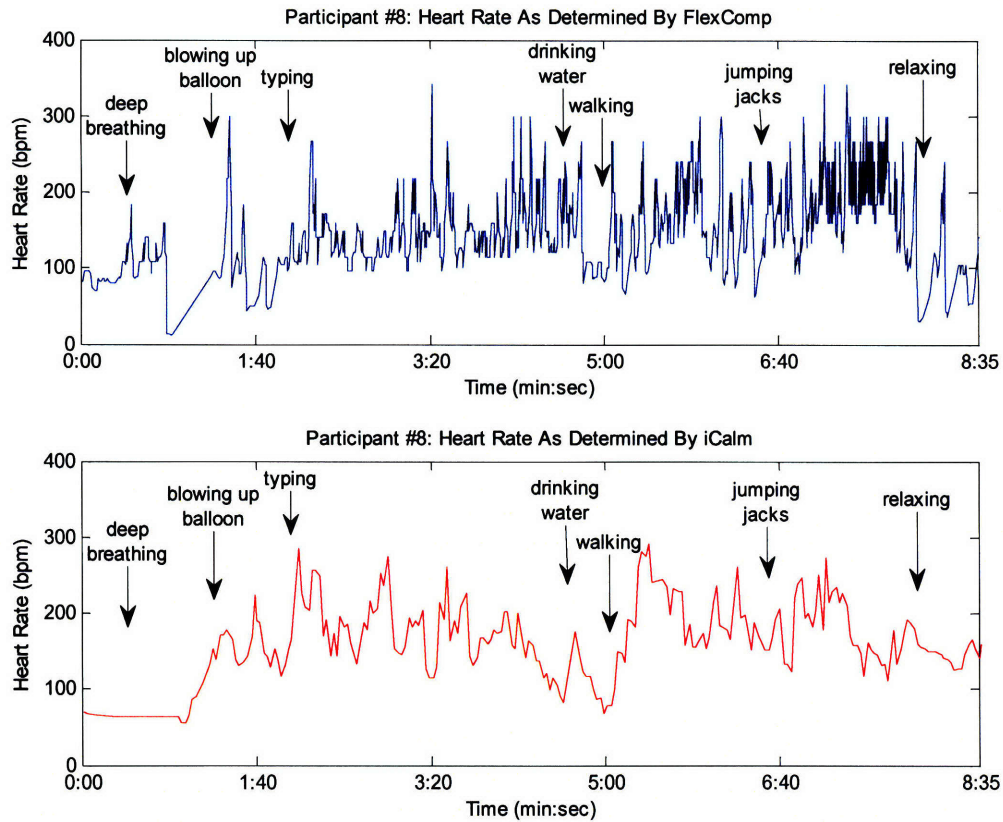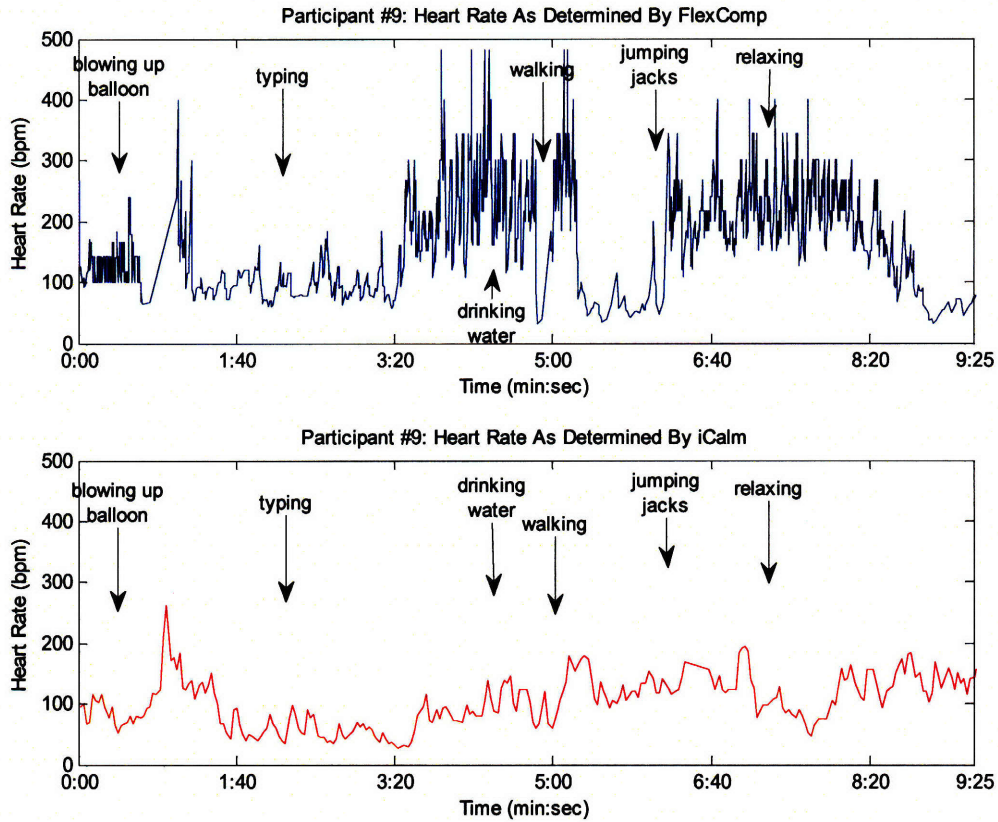
D.11 Participant #11
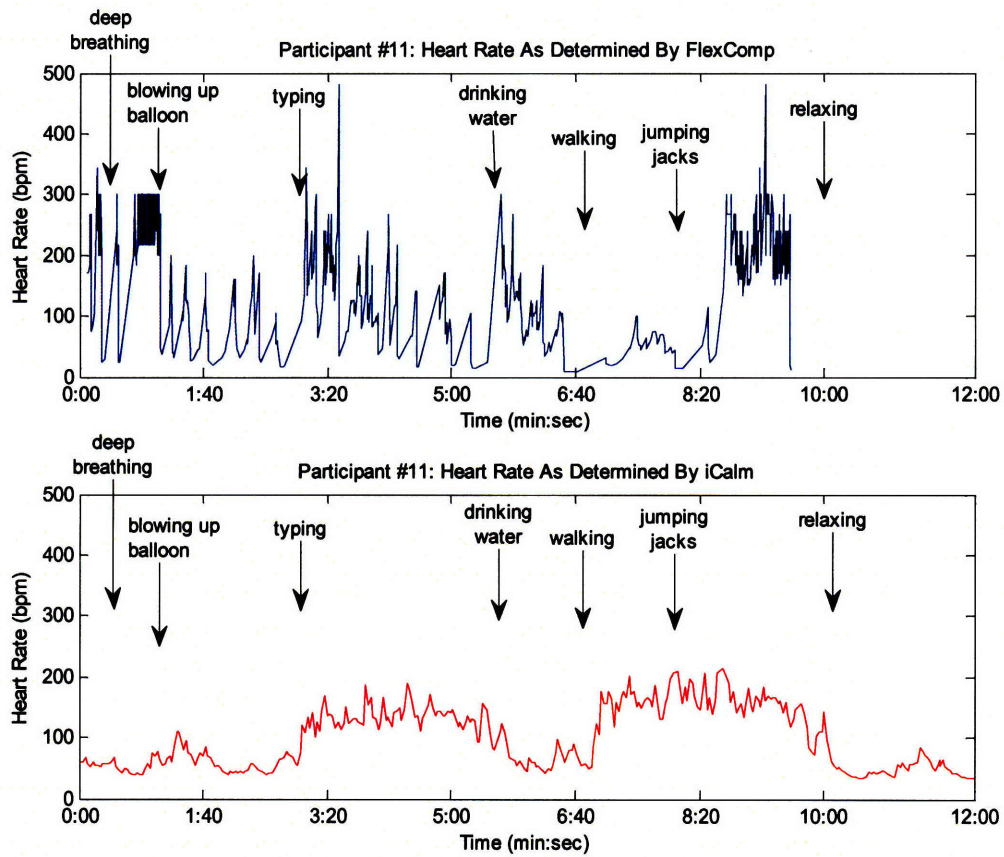
Figure D-11: Participant #11's heart rate as determined by FlexComp (top) and iCalm (bottom)

D.12 Participant #12
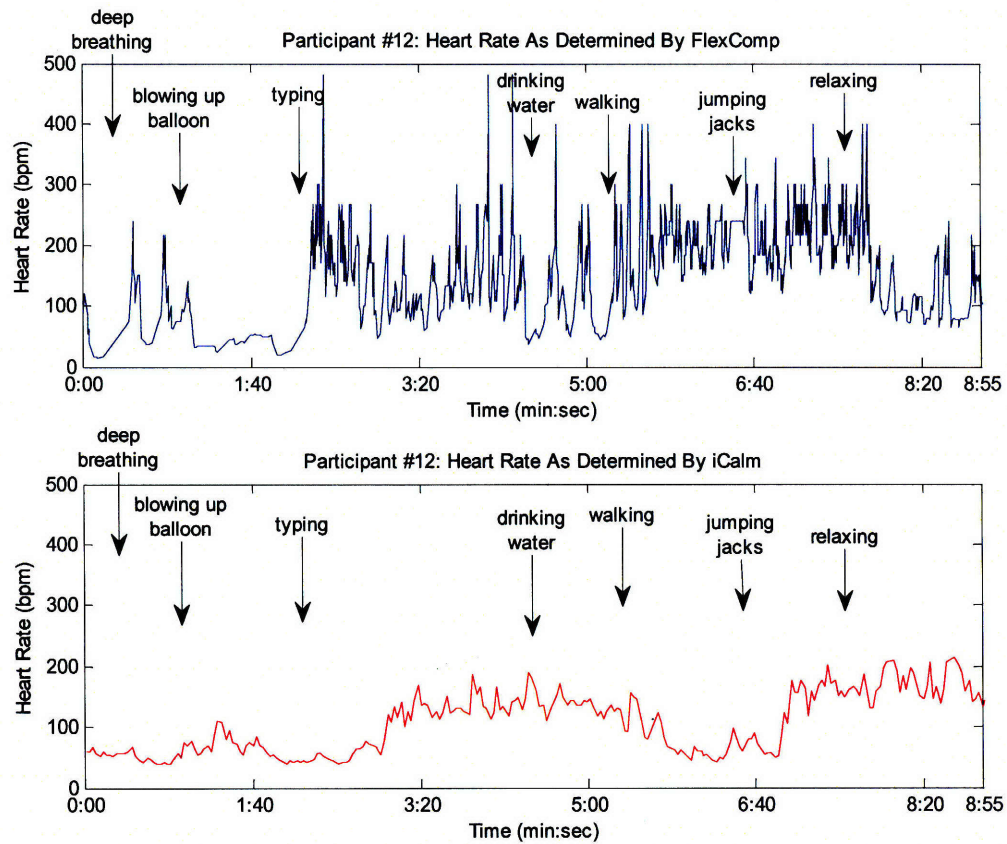
Figure D-12: Participant #12's heart rate as determined by FlexComp (top) and iCalm (bottom)

Bibliography

[1] C. Fere, "Note on changes in electrical resistance under the effect of sensory stimulation and emotion," *Comptes Rendus des Seances de la Societe de Biologie*, vol. 5, 1888, pp. 217–219.

[2] Vigouroux, R., "Sur le role de la resistance electrique des tissues dans le'electrodiagnostic.," *Comptes Rendus Societe de Biologie Series*, vol. 3, pp. 87-89.

[3] R. Vigouroux, "The electrical resistance considered as a clinical sign," *Progres Medicale*, vol. 3, 1888, pp. 87-89.

[4] W.D. Fenz and G.B. Jones, "The Effect of Uncertainty on Mastery of Stress: A Case Study," *Psychophysiology*, vol. 9, 1972, pp. 615-619.

[5] D.C. Raskin and R.D. Hare, "Psychopathy and Detection of Deception In a Prison Population," *Psychophysiology*, vol. 15, 1978, pp. 126-136.

[6] R.W. Picard and J. Scheirer, "The Galvactivator: A Glove that Senses and Communicates Skin Conductivity," *Proceedings from the 9th International Conference on Human-Computer Interaction*, 2001, pp. 1538–1542.

[7] M. Strauss et al., "The HandWave Bluetooth Skin Conductance Sensor," *The 1st International Conference on Affective Computing and Intelligent Interaction*, 2005.

[8] K. Ostertag and P. Derchak, "Continuous physiologic monitoring for athletes in training," 2005.

[9] Anonymous, *BodyMedia*, 2008; http://www.bodymedia.com.

[10] Anonymous, *Brainquiry*, 2008; http://www.brainquiry.nl/index.php?pId=52.

[11] Anonymous, *FitSense Technology, Inc.*, 2006; http://www.fitsense.com.

[12] Anonymous, *Institute of HeartMath*, 2008; http://www.heartmath.org.

[13] Anonymous, *PulseTracer*, 2008; http://www.pulsetracer.com.

[14] Anonymous, *Thought Technology Ltd.*, 2008;
http://www.thoughttechnology.com/hardware.htm.

[15] Anonymous, *TEMEC Instruments*, 2008;
http://www.temec.com/portal2/modules.php?name=products&cid=50.

[16] Anonymous, *Vivometrics*, 2008; http://www.vivometrics.com.

[17] J.D. Sackner et al., "Non-invasive measurement of ventilation during exercise using a respiratory inductive plethysmograph. I.," *Am Rev Respir Dis*, vol. 122, 1980, pp. 867-71.

[18] K. Konno and J. Mead, "Measurement of the separate volume changes of rib cage and abdomen during breathing," *Journal of Applied Physiology*, vol. 22, 1967, pp. 407-422.

[19] H.L. Watson, D.A. Poole, and M.A. Sackner, "Accuracy of respiratory inductive plethysmographic cross-sectional areas," *Journal of Applied Physiology*, vol. 65, 1988, pp. 306-308.

[20] K.J. Heilman and S.W. Porges, "Accuracy of the LifeShirt®(Vivometrics) in the detection of cardiac rhythms," *Biological Psychology*, vol. 75, 2007, pp. 300-305.

[21] F.H. Wilhelm, W.T. Roth, and M.A. Sackner, "The LifeShirt: An Advanced System for Ambulatory Measurement of Respiratory and Cardiac Function," *Behavior Modification*, vol. 27, 2003, p. 671.

[22] C.O. Prys-Picard, F. Kellett, and R.M. Niven, "Disproportionate Breathlessness Associated With Deep Sighing Breathing in a Patient Presenting With Difficult-To-Treat Asthma," *Chest*, vol. 130, 2006, p. 1723.

[23] K. Bogaerts et al., "Hyperventilation in patients with chronic fatigue syndrome: The role of coping strategies," *Behaviour Research and Therapy*, vol. 45, 2007, pp. 2679-2690.

[24] L.J. Myers and P.A. Derchak, "Effective method for quantifying respiratory instability during ambulatory recordings as a subsequent marker of anxiety."

[25] D.B. Keenan and P. Grossman, "Adaptive Filtering of Heart Rate Signals for an Improved Measure of Cardiac Autonomic Control," *International Journal of Signal Processing*, vol. 2, 2005, pp. 52-58.

[26] M.A. Coyle et al., "Evaluation of an ambulatory system for the quantification of cough frequency in patients with chronic obstructive pulmonary disease," *Cough*, vol. 1, 2005, pp. 1–7.

[27] C.F. Clarenbach et al., *Monitoring of Ventilation During Exercise by a Portable Respiratory Inductive Plethysmograph**, Am Coll Chest Phys, 2005.

[28] T.M. Nakra, "Inside the Conductor's Jacket: Analysis, Interpretation and Musical Synthesis of Expressive Gesture," 1999.

[29] T. Westeyn, P. Presti, and T. Starner, "ActionGSR: A combination galvanic skin response-accelerometer for physiological measurements in active environments," *Proc 10th IEEE Int Symp on Wearable Computers, Montreux, Switzerland*, 2006, pp. 129–130.

[30] K. Hiyamizu et al., "Development of human sensory sensor and application to massaging chairs," *Computational Intelligence in Robotics and Automation, 2003. Proceedings. 2003 IEEE International Symposium on*, vol. 1, 2003.

[31] Dong-Wan Ryoo, Young-Sung Kim, and Jeun-Woo Lee, "Wearable Systems for Service based on Physiological Signals," *Engineering in Medicine and Biology Society, 2005. IEEE-EMBS 2005. 27th Annual International Conference of the*, 2005, pp. 2437-2440.

[32] M. Makikawa et al., "Portable jogging monitor device and its application for health management," *Biomedical Engineering, 2003. IEEE EMBS Asian-Pacific Conference on*, 2003, pp. 40-41.

[33] D. David, P. Gopalakrishnan, and T. Teo, "Low-Power Low-Voltage Digital System for Wireless Heart Rate Monitoring Application," *Integrated Circuits, 2007. ISIC '07. International Symposium on*, 2007, pp. 212-215.

[34] J. Jacobs et al., "Characterization of a novel heart and respiratory rate sensor," *Engineering in Medicine and Biology Society, 2004. IEMBS '04. 26th Annual International Conference of the IEEE*, 2004, pp. 2223-2226 Vol.3.

[35] M. Yamashita, K. Shimizu, and G. Matsumoto, "Development of a Ring-Type Vital Sign Telemeter," *Biotelemetry XIII*, 1995.

[36] S. Rhee, "Design and Analysis of Artifact-Resistive Finger Photoplethysmographic Sensors for Vital Sign Monitoring."

[37] Sokwoo Rhee, Boo-Ho Yang, and H. Asada, "Artifact-resistant power-efficient design of finger-ring plethysmographic sensors," *Biomedical Engineering, IEEE Transactions on*, vol. 48, 2001, pp. 795-805.

[38] P. Shaltis et al., "Novel Design for a Wearable, Rapidly Deployable, Wireless Noninvasive Triage Sensor," *Engineering in Medicine and Biology Society, 2005. IEEE-EMBS 2005. 27th Annual International Conference of the*, 2005, pp. 3567-3570.

[39] E.A. López-Beltrán et al., "Non-invasive studies of peripheral vascular compliance using a non-occluding photoplethysmographic method," *Medical and Biological Engineering and Computing*, vol. 36, 1998, pp. 748-753.

[40] B.M. Pannier et al., "Methods and devices for measuring arterial compliance in humans."

[41] J.G. Webster, *Design of Pulse Oximeters*, Inst of Physics Pub Inc, 1997.

[42] J. Chang, S. McGrath, and G. Blike, "Investigating respiratory variation using a forehead reflectance pulse oximeter to identify airway obstruction for automated remote triage," *Bioengineering Conference, 2005. Proceedings of the IEEE 31st Annual Northeast*, 2005, pp. 244-245.

[43] K. Nakajima, T. Tamura, and H. Miike, "Monitoring of heart and respiratory rates by photoplethysmography using a digital filtering technique," *Medical Engineering and Physics*, vol. 18, 1996, pp. 365-372.

[44] C.C.Y. Poon and Y.T. Zhang, "Cuff-less and Noninvasive Measurements of Arterial Blood Pressure by Pulse Transit Time," *Engineering in Medicine and Biology Society, 2005. IEEE-EMBS 2005. 27th Annual International Conference of the*, 2005, pp. 5877-5880.

[45] W. Chen et al., "Continuous estimation of systolic blood pressure using the pulse arrival time and intermittent calibration," *Medical and Biological Engineering and Computing*, vol. 38, 2000, pp. 569-574.

[46] L.A. Geddes et al., "Pulse Transit Time as an Indicator of Arterial Blood Pressure," *Psychophysiology*, vol. 18, 1981, pp. 71-74.

[47] M. Maguire et al., "A comparative study in the use of brachial photoplethysmography and the QRS complex as timing references in determination of pulse transit time," *Engineering in Medicine and Biology Society, 2001. Proceedings of the 23rd Annual International Conference of the IEEE*, 2001, pp. 215-218 vol.1.

[48] D.B. McCombie, A.T. Reisner, and H.H. Asada, "Adaptive blood pressure estimation from wearable PPG sensors using peripheral artery pulse wave velocity measurements and multi-channel blind identification of local arterial dynamics," *Engineering in Medicine and Biology Society, 2006. EMBS'06. 28th Annual International Conference of the IEEE*, 2006, pp. 3521-3524.

[49] Strauss, Marc D, "HandWave: Design and Manufacture of a Wearable Wireless Skin Conductance Sensor and Housing," 2005.

[50] W. Boucsein, *Electrodermal Activity*, Springer, 1992.

[51] G. Uretzky and Y. Palti, "A method for comparing transmitted and reflected light photoelectric plethysmography," *Journal of Applied Physiology*, vol. 31, 1971, pp. 132-135.

[52] J.A. Nijboer, J.C. Dorlas, and H.F. Mahieu, "Photoelectric plethysmography-some fundamental aspects of the reflection and transmission methods," *Clinical Physics and Physiological Measurement*, vol. 2, 1981, pp. 205-215.

[53] K. Takazawa et al., *Assessment of Vasoactive Agents and Vascular Aging by the Second Derivative of Photoplethysmogram Waveform*, Am Heart Assoc, 1998.

[54] M.H. Sherebrin and R.Z. Sherebrin, "Frequency analysis of the peripheral pulse wave detected in thefinger with a photoplethysmograph," *Biomedical Engineering, IEEE Transactions on*, vol. 37, 1990, pp. 313-317.

[55] M. Hahn et al., "Local Cold Exposure Test with a New Arterial Photoplethysmographic Sensor in Healthy Controls and Patients with Secondary Raynaud's Phenomenon," *Microvascular Research*, vol. 57, 1999, pp. 187-198.

[56] K.W. Mun and K.S. Soh, "Radial artery pulse change during cold pressor test," *Engineering in Medicine and Biology Society, 2001. Proceedings of the 23rd Annual International Conference of the IEEE*, vol. 1, 2001.

[57] C.C.Y. Poon et al., "Changes in the photoplethysmogram waveform after exercise," *Medical Devices and Biosensors, 2004 2nd IEEE/EMBS International Summer School on*, pp. 115-118.

[58] D. Bersak et al., "Intelligent biofeedback using an immersive competitive environment," *Paper at the Designing Ubiquitous Computing Games Workshop at UbiComp*, 2001.

[59] R. Picard, "Helping Addicts: A Future Scenario," *Automating Addiction Treatment: Enhancing the Human Experience and Creating a Fix for the Future*, IOS Press, 2005.

[60] R.W. Picard and M. Goodwin,, "Developing Innnovative Technology for Future Personalized Autism Research and Treatment," *Autism Advocate*, vol. 50, 2008, pp. 32-39.

[61] Picard, R.W., Goodwin, M., Fletcher, R., Eydgahi, H., Williams, C., Marecki, A., Lee, C.H., Morris, R., Kim, K., Mota, S., and el Kaliouby, R. "Development of a New Toolkit Enabling Wearable Wireless Autonomic Nervous System Communication for Persons on the Autism Spectrum," *Poster at International Meeting for Autism Research*, 2008.